DOI:10.14753/SE.2020.2354

Investigation of the human ABCB6 transporter

PhD thesis

Zsófia Rakvács

Semmelweis University
Doctoral School of Molecular Medicine

Supervisor: Gergely Szakács MD., Ph.D.

Official reviewers: Miklós Geiszt, MD., DSc.
Péter Lőw Ph.D.

Chairman of the examination committee: János Réthelyi MD., Ph.D.
Members of the examination committee: Gergely Papp Ph.D.
Ákos Sveiczer Ph.D.

Budapest

2019

DOI:10.14753/SE.2020.2354

Table of Contents

DOI:10.14753/SE.2020.2354

DOI:10.14753/SE.2020.2354

List of Abbreviations

ABC	ATP binding cassette
AIF	Apoptosis inducing factor
ALA	δ-aminolevulinic acid
AO	Acridine-orange
BACE2	β-site APP-cleaving enzyme 2
CPIII	Coproporphyrin III
CYP	Cytochrome P450 oxygenase
DSB	Double strand brake
DUH	Dyschromatosis universalis hereditaria
EEA1	Early endosome antigen 1
EGFP	Enhanced green fluorescent protein
EM	Electron microscope
FACS	Fluorescence-activated cell sorting
FBS	Fetal bovine serum
Fech	Ferrochelatase
FISH	Fluorescent in situ hybridization
FP	Familial pseudohyperkalemia
GFAAS	Graphite furnace atomic absorption spectrometry
HDR	Homology drived recombination
HMT-1	Heavy Metal Transporter factor-1
KO	Knockout
LAMP1	Lysosomal-associated membrane protein 1
Lan	Langereis blood group
LRO	Lysosome-related organelle
MDR	Multidrug resistance
mtABC3	Mitochondrial ABC protein 3
NBD	Nucleotide binding domain
NHEJ	Non-homologous end-joining
Ntrg	Non-target
PC	Phytochelatin
PCS	Phytochelatin synthase
PMEL	Pre-melanosomal protein
PPIX	Protoporphyrin IX
PRP	P-glycoprotein related protein
Rab	Ras-associated binding proteins
RCAS1	Receptor-binding cancer-associated surface antigen
ROS	Reactiv oxigene species
RPE	Retinal pigment epithelium
RUSH	Retention Using Selective Hooks
Sa	Streptavidin
SA	Succinyl-acetone
SBP	Strepavidine-binding protein
TMD	Trasmembrane domain
TRP-1	Tyrosinase-related protein-1
UMAT	Ubiquitously expressed mammalian ABC half-transporter
Vctr	Vector control

DOI:10.14753/SE.2020.2354

1. Introduction

1.1. ABC protein family

Transporter proteins relocate substances across biological membranes to provide the appropriate concentration of molecules. Active transport is catalyzed by one of three energy sources: electrochemical or osmotic gradients or the hydrolysis of ATP. ATP binding cassette (ABC) transporters use ATP to mediate the energy-dependent movement of structurally diverse compounds across membrane barriers. The ABC superfamily is one of the largest protein families, performing diverse functions in organisms such as bacteria, fungi, plants, and members of the animal kingdom. ABC genes are widely dispersed in eukaryotic genomes and are highly conserved between species. The human ABC transporter superfamily lists 48 members and based on sequence and structure homology they are distributed into seven subfamilies (A-G)[1].

1.1.1. Structural determinants of function

A functional ABC protein typically contains two nucleotide binding domains (NBD) and two transmembrane domains (TMD) (Fig. 1A,B). The protein is a full transporter if the two NBDs and two TMDs are encoded in one polypeptide chain, but in case of half-transporters such as ABCB6, two polypeptide chains form a functional unit through dimerization. TMDs have low homology and are responsible for substrate binding and translocation, while NBDs are highly conserved and participate in ATP binding and hydrolysis. The NBD can be further divided into a RecA-like domain and a helical domain. RecA contains two characteristic motifs found in all ATP-binding proteins. The Walker motifs (A and B) are separated by ~90–120 amino acids and are involved in nucleotide binding. Signature A (or P-loop: GXXGXFKS; X can represent any amino acid) is responsible for H-bond formation with the α, β and γ phosphates, while the aromatic residues of A-loop interact with the adenine ring of ATP. The A-loop is found about 25 amino acids upstream of the Walker A motif. In signature B (hhhhDE, h represents any hydrophobic amino acid) the aspartate residue coordinates magnesium ions, and the glutamate is essential for ATP hydrolysis. ABC transporters contain an extra element, the signature C motif (LSGGQ) is placed opposite to the walker A and B of the other NBD and helps in completing the ATP binding sites[2] (Fig. 1B). The TMD

contains 6–11 membrane-spanning α-helices and provides the substrate specificity. Contrary to the nucleotide binding domain, the transmembrane domain has significant sequential plasticity between different ABC proteins, but based on X-ray crystallization studies, the structures are remarkably similar. The two TMDs together form a cavity in the plane of the membrane, thus forming the translocation channel and the substrate binding pocket (Fig. 1). The crystal structures of full length ABC transporters have provided a plausible mechanism for coupling ATP hydrolysis to transport. Effective coupling requires the transmission of the molecular motion from the NBDs to the TMDs. At this interface, architecturally conserved α-helices, which are part of the TMDs, are present in all reported crystal structures. These 'coupling helices' interact with grooves formed at the boundaries of the two sub-domains of the NBDs[3].

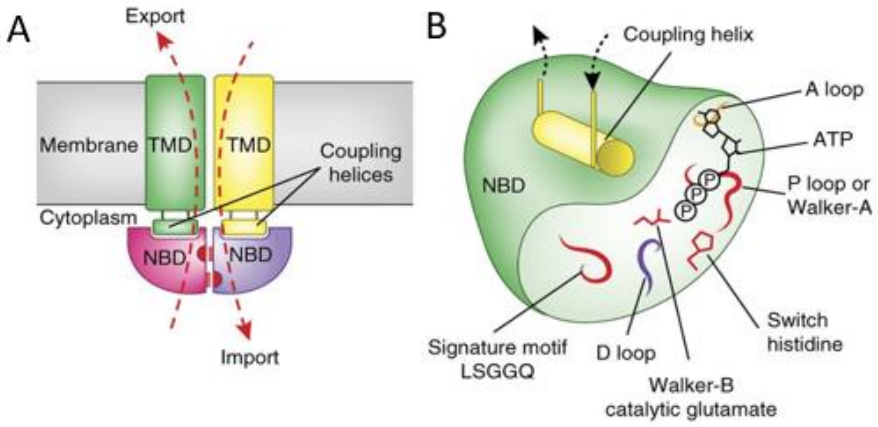

Figure 1. Architecture of ABC transporters A Domain arrangement of ABC transporters. Two NBDs and two TMDs form a functional transporter. **B** Conserved and functionally critical motifs of a single NBD: residues of the P loop are responsible for H-bond formation with the α, β and γ phosphates; the A loop interacts with the purine ring of adenine; a Walker-B motif provides the catalytic glutamate; a signature LSGGQ motif (Walker C) orients ATP during hydrolysis; and D loop has a role in coupling hydrolysis to transport. A groove in the NBD surface forms the contact interface with the coupling helix of the TMD. These helices are the only architecturally conserved contact among distinct TMD folds and provide the majority of contacts between TMD and NBD[4].

In some cases, the basic structure is supplemented with additional membrane and cytoplasmic sections. Based on the TMD layout, ABC proteins can be divided into three structural families: Type I and Type II importers and exporters (Fig. 2). Prokaryotes have all three types of ABC proteins, while in eukaryotes – like in humans - only exporters occur (Fig. 2 red underline). In bacteria ABC pumps are generally involved in the uptake of essential compounds, which cannot diffuse into the cell (e.g., sugars, vitamins, metal

ions, etc.). In eukaryotes, most ABC proteins move compounds from the cytoplasm to the outside of the cell or into an intracellular compartment. Most human ABC proteins are active transporters, meaning they work against the electrochemical potential, to translocate substances. However, we also find an example of an ABC transporter acting as an ion channel (ABCC7/CFTR) or a regulator protein that defines the operation of other transporters (ABCC8)[3,5,6].

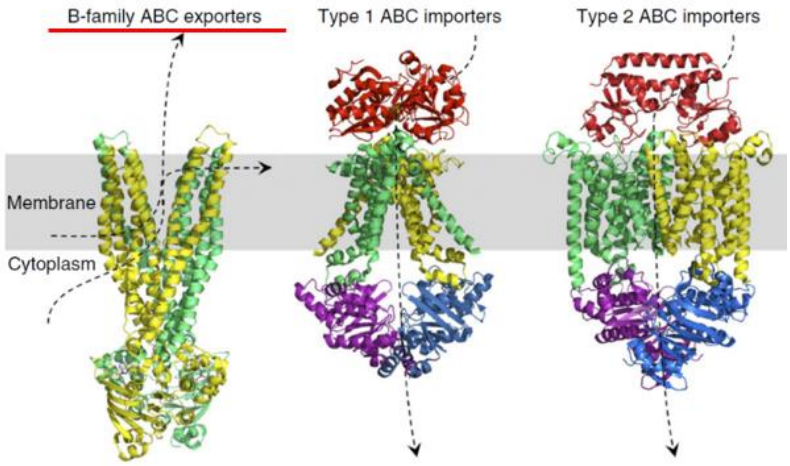

Figure 2. ABC-transporter structures. ABC importers TMDs are expressed as separate protein subunits that belong to either type I or type II. Yellow and green, TMDs; red, periplasmic substrate-binding proteins; purple and blue, NBDs. The TMDs and NBDs are fused in B-family exporters. In eukaryotes only exporters occur (red underline)[4].

Some ABC proteins exhibit a high degree of substrate specificity, while other ABC proteins can move a variety of significantly, even chemically different molecules (e.g. ABCB1)[7]. Presumably the functional difference is a consequence of the sequential variance of TMD, though the relationship between amino acid sequence and degree of specificity have not yet been fully understood[6].

Several ABC proteins are involved in detoxification (MDR1/ABCB1)[8], endo- and xenobiotic protection, oxidative stress reduction (MRP1/ABCC1)[9] Thus, ABC multidrug transporters are essential parts of an immune-like defense system, and their network is a major contributor to "chemoimmunity" in living organisms by transporting toxic molecules out of the cell[10]. They therefore can play a key role in development of multidrug resistance (MDR)[11]. MDR is a main cause of chemotherapy inefficacy. Some cancers exhibit significant primary resistance to cytostatic drugs, others acquire MDR phenotype after prolonged exposure to cytostatic drugs. The development of MDR makes

further treatment ineffectual[11–13]. Other ABC proteins play an important role in the lipid metabolism (ABCA1, ABCB4, ABCB11) [14,15] but also in the MHC I-type antigen presentation (TAP1/ABCB2, TAP2/ABCB3)[16] or the ionic balance of the epithelium (CFTR/ABCC7)[17]. Their mutation, malfunction, or potential deficiency is responsible for many diseases.

1.1.2. ABCB subfamily

In my doctoral research, I studied ABCB6, member of ABCB subfamily. Although results have been controversial in recent years, first studies identified ABCB6 as a mitochondrial transporter, importing an intermediate of heme synthesis into the mitochondrial lumen.

The ABCB subfamily contains four full transporters and seven half transporters. ABCB1 (MDR1/Pgp) was the first cloned human ABC transporter. It confers multidrug resistance phenotype to cancer cells. It has critical function in the blood–brain barrier and the liver[8]. ABCB11 (BSEP) exports bile salts from hepatocytes across the canalicular membrane. As a phospholipid translocator ABCB4 (MDR3), facilitates the incorporation of phosphatidylcholine into bile, so both proteins are involved in the secretion of bile acids[18]. ABCB2 and ABCB3 (TAP) are half transporters that form a heterodimer to transport peptides into the endoplasmic reticulum, which are presented as antigens by the Class I HLA molecules[16]. ABCB9/TAPL is a half transporter and shuttle cytosolic polypeptides into the lumen of lysosomes. Phylogenetic analysis suggests that TAPL was the common ancestor of the TAP family. TAPL orthologues are also found in *Caenorhabditis elegans* and in Agnates, as well in plants. None of these organisms has an adaptive immune system. Therefore, a more general function of TAPL can be assumed throughout multi-cellular organisms[19].

The remaining three half-transporters ABCB7, ABCB8 and ABCB10 localize to the mitochondria, and are involved in iron metabolism and transport of Fe/S protein precursors[20]. It is known that all three mitochondrial transporters contain a targeting signal[21]. The gene coding ABCB7 protein is considered to be the orthologue of the *atm1* gene found in yeast. The protein is responsible for mitochondrial iron homeostasis and plays a role in the maturation of iron-sulfur clusters. Its mutation causes X-linked sideroblastic anemia. Anemia is caused by the accumulation of a form of iron that cannot

be used to make heme molecules. The partial loss of the function of ABCB7 directly or indirectly inhibits hem biosynthesis thereby causing decreased amount of hemoglobin or red blood cells (RBCs) in the blood[22]. ABCB8 performs similar tasks in the body. Additionally, mitochondrial iron accumulation has been observed in the study of *abcb8*-deleted mouse myocardium tissue. Mitochondrial injury, increased levels of reactive oxygen radicals, and death of cells were also detectable. In vitro silencing of ABCB8 decreased iron excretion from mitochondria and overexpression of the protein resulted in an opposite effect[23]. Studies in mice also revealed that higher levels of oxidative stress occurred in heterozygous animals after ischemic/reperfusion. The amount of reactive radicals and damaged lipids increased, resulting in reduced mitochondrial respiration. Like ABCB7, ABCB8 is also essential for cytosolic maturation of the iron-sulfur cluster, its deletion in vivo and in vitro led to decreased activity of iron-sulfur-containing enzymes in the cell plasma[20]. ABCB10 is also localized in the inner membrane of the mitochondria, forming homodimers with its NBD orienting towards the mitochondrial matrix. During erythroid maturation, the protein is produced in large yields, which increases the hemoglobin synthesis in erythroid cells. ABCB10 is expressed not only in erythroid tissues but also in many other tissues, suggesting that its function is not directly related to hemoglobin synthesis. Although the dysfunction of the mitochondrial ABC transporters described above results in relatively well-detectable phenotypes, the specific mechanism of operation is not known in either case[22].

1.2. ABCB6

ABCB6 is a half ABC transporter of 842 amino acids, containing a unique N-terminal region followed by the ABC-core consisting of a transmembrane domain and a cytoplasmic nucleotide binding domain[24–26]. ABCB6 forms homodimers and is widely expressed in many tissues, especially in the heart, liver, skeletal muscles[27], red blood cells[28,29], and skin[30]. The first publications identified the protein under different names (PRP, MTABC3, UMAT) but finally the transporter was officially named ABCB6, based on ABC nomenclature.

1.2.1. Identification of a new protein

Pgp (P-glycoprotein/ABCB1) is an ATP-dependent drug efflux pump for xenobiotic compounds with broad substrate specificity. It is responsible for decreased drug accumulation in multidrug-resistant cells and often mediates the development of resistance to anticancer drugs[31]. ABCB6 was identified in 1997 and based on sequential similarity, it was named P-glycoprotein related protein (PRP). The authors screened a normal rat liver cDNA library with probes corresponding to the coding sequence of the NBD of Pgp protein. This new transcript was detected in many normal tissues and was overexpressed in rat hepatocarcinoma cells. Already the first sequence analysis pointed out that ABCB6 may be related to Heavy Metal Transporter factor-1 (HMT-1). BLAST search of the non-redundant databases revealed that a cDNA isolated from *Schizosaccharomyces pombe*, encoding a heavy metal tolerance gene, was the most similar to PRP, with 61% similarity and 44% identity over the nucleic acid and amino acid sequence[32]. The first hypothesis about the physiological role of ABCB6 was based on *Saccharomyces cerevisiae* studies. To identify the human ortholog of mitochondrial yeast Atm1p, researchers screened the GenBank data base, and found two ABC proteins: the already known ABCB7[33] and 'EST 45597'. Mitsuhashi and his colleagues showed that the transcript was expressed widely in rat tissues and in different cell lines. This new gene, named MTABC3 (mitochondrial ABC protein 3), encodes 842 amino acids of a protein that has 31.1% identity to Atm1p. The authors noticed that it has 47.5 and 42.9% similarity to *Schizosaccharomyces pombe* HMT-1[34] and human ABCB7, respectively. Based on this relation between ABCB6 and ABCB7, the authors hypothesized mitochondrial localization. For immunoblot and microscopic analysis, flag tagged MTABC3 was expressed in CHO cells. For functional analysis, an Atm1p-deficient *S. cerevisiae* strain was used that showed a 50-fold higher level of free iron accumulation then wild-type control cells. It was found that MTABC3 is mitochondrial and *atm1p* mutant cells can be rescued by the expression of MTABC3. The non-functional ABCB6 mutant variant surprisingly effectively rescued the mutant phenotype[27].

Meantime another group also identified the protein and because it was expressed universally in all tissue UMAT (Ubiquitously expressed Mammalian ABC half-Transporter) name was given to it. Using arsenic resistant hepatocarcinoma cells, the authors presumed association between arsenic tolerance and mRNA levels of multidrug

resistance-associated proteins (MRP1,2, or 3) or P-glycoprotein related protein (ABCB6) but alteration could not be detected[35].

As previously mentioned, Furuya and Schuetz identified rat *Abcb6* in 1997[32], then they reported the isolation of the human *ABCB6* gene in 2002[36]. The protein was identical to the previously cloned MTABC3 human ABC transporter[27]. Emadi-Konjin and his colleagues found that ABCB6 was overexpressed in human hepatocellular carcinomas compared to surrounding non-malignant tissue (there was no difference in ABCB6 copy number between tissues). Screening a human liver genomic DNA library, a 14 kb genomic DNA fragment was isolated which contained the *ABCB6* gene. Using luciferase assay the promoter region was predicted on the forward strand of ABCB6 beginning 3565 to 3315 bp from the translational start site. Based on bioinformatic analysis the 5'-flanking region contains a CpG island and a number of putative transcription factor binding sites. The predicted ABCB6 promoter region is GC-rich and contains six glucocorticoid response (GR) elements, three putative c-myc binding sites within the CpG island. In spite of different expression levels between normal and cancer liver cells, the function of ABCB6 remained unknown[36].

1.2.2. ABCB6 and porphyrins

In 2006, Krishnamurthy and colleagues established the classification of ABCB6 as mitochondrial transporter. In a seminal *Nature* article they claimed that ABCB6 imports porphyrins into the mitochondria[25]. Porphyrins are important intermediates of the highly conserved heme synthesis pathway. In humans, during erythroid maturation, cells have a high demand of heme molecules to produce hemoglobin. In other species, the pathway also produces similar substances such as cobalamin (vitamin B12). The heme synthesis starts and ends in the mitochondrial matrix, but the intermediate steps occur in the cytosol. The initial molecules are glycine and succinyl-CoA, they form δ-aminolevulinic acid (ALA) by ALA synthase, which is strictly regulated by intracellular iron levels and heme concentration. ALA is transformed into porphobilinogen in the cytoplasm, and four molecules of porphobilinogen form a linear tetrapyrrole, which is closed by enzymatic processes. The coproporphyrinogen III molecule (CPgenIII) enters the mitochondria and protoporphyrin IX (PPIX) is formed by oxidation steps. The closing step is made by ferrochelatase (Fech), the enzyme incorporates Fe^{2+} into the porphyrin ring in the

mitochondrial matrix (Fig 3). The heme synthetic pathway can be upregulated by ALA treatment and blocked by succinyl-acetone (SA)[37]. In 2006 Krishnamurthy and his colleagues observed elevated ABCB6 expression in human and murine fetal livers, which became upregulated during erythroid maturation. Treatment of MEL (myeloid erythroid leukemia) cells with ALA to induce heme biosynthesis caused a dose- and time-dependent increase in ABCB6 protein and mRNA levels. In contrast, blocking heme synthesis pathway by SA led to decreased intracellular PPIX levels and ABCB6 expression. Results from immunoblot and confocal microscopy experiments suggested that Flag-tagged ABCB6 is localized to the outer membrane of mitochondria. Using hemin-agarose affinity chromatography it was concluded that ABCB6 is a hemin binding protein and beside heme it could bind CPIII and PPIX molecules. Using isolated mitochondria, the ATPase activity of the ABCB6 protein seemed to be stimulated by CPIII. The authors found that PPIX fluorescence values were much greater in ABCB6-overexpressing K562, Saos-2 and MEL cells than in vector-control or ABCB6 non-functional mutant variant expressing cells (ABCB6-K629M). Every result therefore suggested that ABCB6 is located in the outer membrane of the mitochondria and it imports coproporphyrinogen III, thus acting as a main factor of heme biosynthesis[25,38].

Overexpression of ABCB6 significantly increased intracellular (but not intramitochondrial) heme concentrations in K562 myeloid leukemia cells. ABCB6 overexpression also positively influenced expression and activity of hemoproteins, catalase and cytochrome c oxidase. It was suggested that ABCB6 plays a primary role in regulating hemoproteins by modulating intracellular heme concentration. Interestingly it was found that ABCB6 overexpressing cells were more resistant to H_2O_2[39].

DOI:10.14753/SE.2020.2354

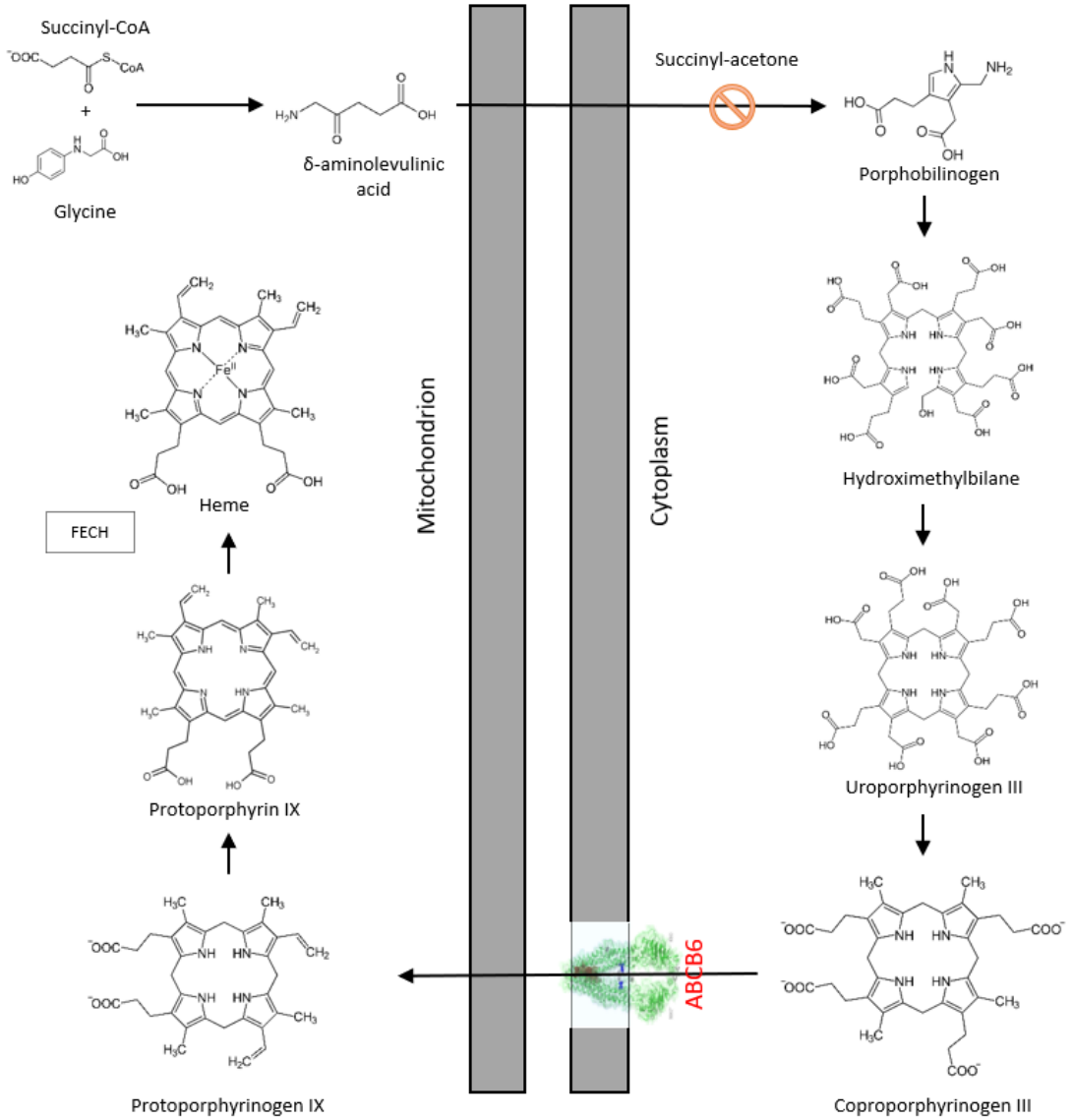

Figure 3. The putative role of ABCB6 in heme synthesis. The initial step is the condensation of a succinyl coenzyme-A and glycine molecule, resulting in the formation of δ-aminolevulinic acid in the mitochondrial matrix. The synthesis continues in the cytosol, where four molecules of porphobilinogen form a linear tetrapyrrole. This linear molecule is closed by enzymatic processes then protoporphyrin is produced by oxidation steps, to which the ferrochelatase enzyme incorporates the divalent iron ion. The putative role of ABCB6 in this pathway is the mitochondrial porphyrin uptake.

1.2.3. ABCB6 and resistance

Other early studies took a different approach and suggested that ABCB6 may be involved in multidrug resistance (MDR). It was found that increased ABCB6 expression correlated with different cancer types. Increased resistance was observed against chemotherapeutic drugs, such as camptothecin or cisplatin in A549 lung cancer cells[40]

and paclitaxel/FEC (5-fluorouracil, epirubicin and cyclophosphamide) in breast cancer cells[41]. Expression levels of 45 genes from the ABC superfamily were analyzed in different drug resistant (doxorubicin/methotrexate/topotecan/paclitaxel/vincristine) ovarian carcinoma cell lines. Three transporters were significantly upregulated: ABCB1, ABCB4 and ABCG2. ABCA8 gene was significantly downregulated. ABCB6 was slightly upregulated in every cell line and paclitaxel caused the biggest deviation in expression levels[42]. In 2007 an article was published in which high ABCB6 mRNA expression level was found in primary melanoma and also in metastatic melanoma cells[43]. In 2009 an antioxidant response element was identified at –7575 base pair up-stream of the ABCB6 transcription site in human small airway epithelial cells[44]. Moreover, in 2011 it was reported that ABCB6 protect cells from oxidative stress and conferred arsenite resistance to HepG2 and Hep3B hepatocellular carcinoma cells[45]. In another arsenite-resistant cell line, in KAS myeloma cells ABCB6 overexpression enhanced resistance to 5-fluorouracil (5-FU), SN-38 and vincristine (Vcr) but not to arsenite. However ATO (arsenic-trioxide) resistant human epidermoid carcinoma cell line had higher ABCB6 expression level and accumulated less arsenic then parental cells[46]. The cellular differences between epidermoid and hepatocarcinoma cells may have led to different results[47].

ABCB6 was also connected to drug resistance but not in a chemotherapeutic perspective: Gómez and colleagues found that increased intracellular survival of *Leishmania panamensis* in human macrophages treated with antimonial drug correlates with low expression of the transporter ABCB6. It seemed that antimony could induce ABCB6 expression in human macrophages. Furthermore, the protein was detected in the cell membrane and the phagolysosomal membrane surrounding the intracellular pathogen. Based on these results the authors speculated that ABCB6 acts as an efflux pump in the cell membrane and as an importer when localized to intracellular membranes[48].

In the last few years several papers have been published about the diverse pharmacological relevance of ABCB6. A study showed that women younger than age 50 had significantly higher levels of mRNA expression for several drug transporters, including ABCB6[49]. Analyzing Taxol resistant cells, ABCB6 was identified as an androgen receptor target gene[50]. Investigating patients with prostate cancer, it seemed that

expression levels of ABCB6, ABCC3 and ABCC10 can be valuable predictors of prostate cancer progression[51]. Strong correlation was also detected between ABCB6 expression levels and progression of human gliomas[52]. Another prostate cancer study showed elevated PPIX levels in dormant PC3 cells and upregulated ABCB6 expression[53]. Interestingly, in acute myeloid leukemia mRNA expression of ABCC3 and ABCB6 were significantly higher in daunorubicin resistant samples compared to sensitive ones[54]. Another observation occurred in *D. melanogaster*, where authors found that suppression of ABCB6 increased mortality when animals were treated with malathion insecticide[55].

Researchers hypothesized several times that ABCB6 can mediate protection against cytosolic ROS[45,56–58]. It was mentioned above that Hübner and his colleagues identified an antioxidant response element in ABCB6 promoter region examining epithelial cells[44]. Association between ABCB6 and resistance to these diverse therapeutic compounds required explanation. The putative protective mechanism was to eliminate ROS by producing more heme to increase catalase activity[38]. Catalase enzyme converts toxic hydrogen peroxide to water using heme as a co-factor. In the recent years three studies supposed positive correlation between ABCB6 expression level and smoking[59–61]. In the latest article an in vitro model of oral keratinocyte cell line was developed by exposing them with different concentrations of cigarette smoke extract (CSE). CSE treatment increased cytotoxicity and cell death through ROS generation in keratinocyte cells. Cigarette smoke exposure was associated with elevated ABCB6, while smoking cessation was associated with lower expression of ABCB6. In addition to toxic components, cadmium and arsenic can be found in tobacco products[61].

In 2018 another puzzling result emerged about the connection of ABCB6 and a parasite. It was observed that erythrocytes from Lan null individuals are resistant to invasion by *Plasmodium falciparum* parasites. Cells from six unrelated donors with null alleles were examined and it was found that parasite invasion was impaired in all cases when ABCB6 was absent. But other Plasmodium species could invade Lan null erythrocytes, so this genetic background does not provide defense against all *Plasmodium* parasites. This suggests that *P. falciparum* may have special connection with ABCB6 as a host factor during invasion. Based on this observation, Lan null blood group can be considered as evolutionary advantage[62].

1.2.4. ABCB6 – contrasting results on intracellular localization

Contrary to the suggested mitochondrial function[25], in 2007 researchers observed extramitochondrial localization of ABCB6. Paterson and co-workers found that two distinct molecular weight forms of ABCB6 protein exist in SNB-19, U251 glioblastoma and KB-3-1 epidermoid carcinoma cells. Using novel antibodies, it seemed that the low weight form (79 kDa) was located to the mitochondria while high weight form (104 kDa) was located to the plasma membrane of the cells[63]. Tsuchida and his colleagues suggested other extramitochondrial localization for ABCB6. It was found that the transporter is located mainly in the Golgi system, and they presented confocal pictures of Cos-7 cells and proposed that the N-terminal extension of ABCB6 acts as an ER-targeting signal owing to its special hydrophobic nature[64]. A human colon adenocarcinoma line (LoVo) cell line was found devoid of endogenous ABCB6 mRNA. LoVo cells were used for heterologous expression of rat Abcb6. Performed distinct methods (subcellular fractionation, indirect immunofluorescence analyses, and determination of fluorescent rAbcb6-GFP distribution) authors concluded that rAbcb6 was localized to endolysosomal structures. Primary rat hepatocytes and liver tissue sections also corroborated this intracellular localization. Moreover, expression of rAbcb6 in LoVo cells increased the tolerance toward copper. The authors suggested that rAbcb6 may play a role in transition metal homeostasis[56].

In our laboratory during her PhD work, Katalin Kiss tried to prove the mitochondrial localization of ABCB6. It was difficult to reconcile mitochondrial localization with studies suggesting that ABCB6 may play a role in increased resistance to chemotherapeutic agents in tumor cells. After years of thorough work our results[24] questioned the reigning concept linking ABCB6 to mitochondrial porphyrin import[25,65]. During the study more approaches were used, first, we examined the intracellular location of ABCB6 in K562 human erythroleukemia and in HeLa cells. Intracellular organelles were separated from HeLa cells by differential centrifugation. Different membrane fractions were analyzed by immunoblot to characterize the localization of endogenous ABCB6. Because mitochondrial contamination was detected in the fractions, in further experiments, immunomagnetic separation was used. With the organelle markers we proved that lysosomes are devoid of mitochondrial contamination. The experiments unanimously demonstrated that ABCB6 is located in the lysosomal compartments and is

absent from the mitochondrial fractions. In the next step, it was shown that ABCB6 is expressed in human erythrocytes. The glycosylation of the protein was studied on erythrocyte ghosts. Glycosidase treatment resulted in a marked shift in molecular weight of the protein. This meant that B6 was indeed produced in the N-glycosylated form and was located to the plasma membrane of mature erythrocytes. Note, that mature red blood cells no longer contain other membrane structures (intracellular organelles), including mitochondria. Fukuda and his colleagues also observed that the protein undergoes glycosylation in the cells[66]. This posttranslational modification is predominantly specific for proteins in the plasma membrane and the endolysosomal continuum. The hypothesis proposed by the laboratory of J. Schuetz suggested that ABCB6 caused elevated mitochondrial uptake of porphyrin which led increased PPIX fluorescence in the cells. The following experiments showed that however the level of ABCB6 increased during erythroid maturation of K562 cells, the attenuation of ABCB6 did not affect hemoglobin synthesis or erythroid maturation of the cells. We concluded that ABCB6 is not required for the synthesis of porphyrins. Fluorescently labeled ABCB6 was expressed and analyzed by confocal microscopy in K562 and HeLa cells. Results showed that endogenous protein clearly colocalized with lysosomal markers, which were in line with data from membrane fractionation. These results fundamentally call into question the mitochondrial localization and the role of ABCB6 in heme biosynthesis.[24].

1.2.5. Structure – Function relation

Although ABCB6 was thought to be a mitochondrial protein, it is important to note that it does not contain a target signal like the other mtABCs[24]. Generally, the mitochondrial targeting signal is a 10-70 amino acid sequence forming an amphipathic helix at the N-terminal. Cleavable pre-sequences are the classical type of mitochondrial targeting signals. However, numerous types of non-cleavable targeting and sorting signals, which are located in the mature regions of mitochondrial proteins, have also been described[21]. Half-transporters in the B subfamily contain additional, relatively long and unique sequences, which have been implicated in protein–protein interactions and targeting. Topology prediction programs for transmembrane proteins (i.e., CCTOP, or HMMTOP) suggested that ABCB6 contains 11 transmembrane (TM) helices, of which five helices are not found on the basic ABC structure. This N-terminal extra domain

(TMD_0) does not show sequence homology to any other protein. Kiss investigated the function of the TMD_0 domain and created N-terminal truncated variants of ABCB6 in Sf9 (*Spodoptera frugiperda*) model cell lines. The expression level of ABCB6-core in Sf9 insect cells was comparable to full-length ABCB6, suggesting that it could fold properly and integrate into the membrane. After checking the expression of the truncated protein, functional assays were performed. Being an ABC transporter, ABCB6 cleaves ATP generating ADP and inorganic phosphate (Pi) which is linked to substrate translocation. This can be tested in an ATPase assay where Pi can be measured by a simple colorimetric reaction. The amount of released Pi is directly proportional to the activity of the transporter and transported substrates can increase baseline ATPase activity. On Sf9 vesicles containing ABCB6, basal or substrate-stimulated ATPase activity could not be detected. However, implementing azido-ATP and trapping assays, we showed that ABCB6-core variant was able to bind ATP and cleave the bound ATP molecule. The non-functional K629M mutant allowed ATP binding, but prevented ATP hydrolysis. For further experiments, ABCB6 protein variants were successfully expressed in human cell lines (HeLa and K562). Co-immunoprecipitation assay revealed that the TMD_0 is not required for protein dimerization but it contains a glycosylation site[67]. This predicted glycosylation site was in agreement with the literature[66]. In the next step intracellular localization of the truncated variant was examined by confocal microscopy. While the wild-type protein co-localized with lysosomal markers, ABCB6-core variant was detected in the plasma membrane. In contrast, the TMD_0 fragment showed lysosomal localization similar to the wild-type protein. These results suggested that the N-terminal extension of the transporter is an independent folding domain with sufficient information for lysosomal targeting (Fig. 4). Electron microscopy analysis showed that ABCB6 was localized to the membranes of multivesicular bodies, multilamellar lysosomes and dense lysosomes[67]. Fukuda and co-workers studied intramolecular disulfide bonds and glycosylation of ABCB6. They showed that during maturation, ABCB6 is glycosylated at a conserved single atypical amino-terminal site (Cys-8). Results showed that mutation of highly conserved cysteines destroyed the disulfide bonds, leading ER retention of the protein. The data suggested that these cysteines are important for proper folding and stability of ABCB6[66].

DOI:10.14753/SE.2020.2354

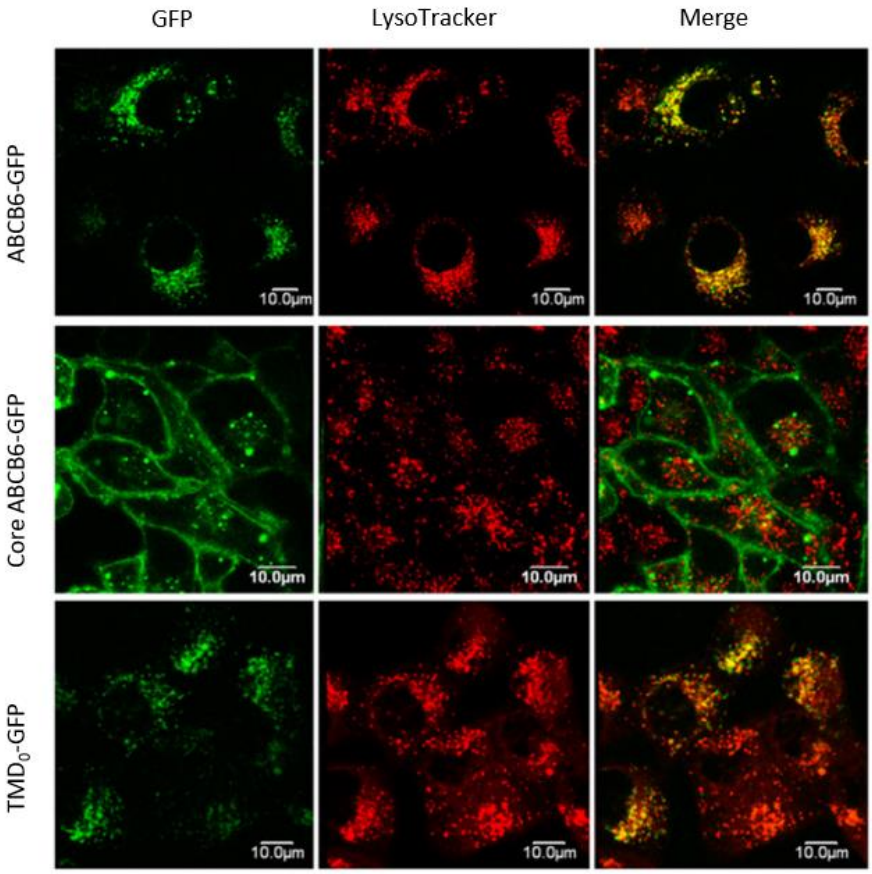

Figure 4. Intracellular targeting of GFP-tagged ABCB6 variants in HeLa cells. Cells were transfected by GFP-fusion proteins. Localization of ABCB6–GFP, core–ABCB6–GFP and TMD_0–GFP was revealed by GFP (green) in the context of the lysosomal marker LysoTracker (red)[67].

In case of transporters a functional assay greatly facilitates the examination of the structure-function relation. Chavan and his colleagues developed an in vitro system with pure and active protein, where they could investigate the function of ABCB6. In the first step of the essay, the FLAG tagged protein was overexpressed in HEK293 cells. The tagged ABCB6 was purified from the mitochondrial fraction of the cells. In binding assay, they saw that ABCB6 retained its ability to bind ATP through the purification process. In ATPase assay the non-functional mutant (ABCB6-K629M) showed only background activity, while the purified ABCB6 was active in ATP hydrolysis. To analyze ABCB6 in its membrane-embedded state, purified mitochondrial ABCB6 (both WT and K629M) was reconstituted into preformed detergent-destabilized liposomes. Performing hemin-agarose affinity chromatography authors found that CPIII was able to displace liposome-reconstituted ABCB6 from hemin-agarose in a dose-dependent manner. In ATPase assay

lipid-reconstituted ABCB6 demonstrated basal ATPase activity that was comparable to the ATPase activity of the purified detergent-solubilized protein. Activity was strongly stimulated in the presence of CPIII, hemin, and protoporphyrin IX. CPIII uptake of WT-ABCB6 and transport incompetent ABCB6-KM liposomes were also measured, which authors concluded as an ATP-dependent substrate transport of ABCB6[26].

1.2.6. ABCB6 knockout mice

In spite of the putative essential mitochondrial porphyrin transport, *Abcb6* knockout mice appeared phenotypically normal. However, evaluation of their hematological parameters revealed mild anemia. Phenylhydrazine (Phz) is a generally used molecule to induce acute hemolytic anemia in animal models. When *Abcb6* KO mice were chemically stressed with Phz greater mortality and a more sustained anemia was observed. The authors concluded that ABCB6 is the sole mammalian ATP-dependent mitochondrial porphyrin importer, while they suggested that ABCB6 only mean benefit in stressful situations[58]. Next, Krishnamurthy and his co-workers also studied the physiological function of Abcb6 in knockout mice. It was found that deficiency of the protein in vivo does not have a significant impact on basal hepatic porphyrin or heme levels. Based on earlier results of the research group[68] cytochrome P450 oxygenase (CYP) enzymes were investigated in *Abcb6+/+* and *Abcb6-/-* mice. CYPs are hemoproteins, they use heme molecule as a cofactor. Mammalian hepatic CYPs are involved in the metabolism of endogenous compounds and xenobiotics[69]. *Abcb6−/−* liver microsomes showed significant decrease in midazolam biotransformation, suggesting decreased Cyp3a11 activity in *Abcb6* KO mice. Several CYP enzymes were tested and results showed that Abcb6 deficiency in mice modified the activity of a specific set of hepatic P450s. Measuring mRNA and protein levels of CYPs, it was found that altered P450 activity in *Abcb6−/−* mice is due to decreased expression of P450s. Though *Abcb6−/−* mice did not show any observable gross or histological alteration in liver, nor did they demonstrate any increase in serum biomarkers of liver injury. *ABCB6* was attenuated in human hepatoma cell lines (Hep3B and Huh7) and expression of CYPs were monitored. Results showed decreased level of CYP1A2, CYP2B6, and CYP3A4 transcript. After accurate experiments with CYP enzymes authors concluded that ABCB6 deficiency could involve repression of P450 promoter activity[70].

1.2.7. ABCB6 and pathology

In each specific porphyria the activity of specific enzymes in the heme biosynthetic pathway is defective. Porphyrias may also be classified as either erythropoietic or hepatic, depending on the principal site of accumulation of pathway intermediates[71]. In 2016 it was found that severely affected porphyria patients were heterozygous for ABCB6 alleles. In experiments using a mouse model, genetic deficiency of ABCB6 coupled with a Fech deficiency (a classic porphyria model) produced greater porphyrin elevation in red blood cells, hepatocytes, and increased liver damage[72]. Despite these results, in the well-controlled laboratory environment, *Abcb6* KO mice have no pathological phenotype[70]. While researchers were hunting for a connection between ABCB6 and drug resistance[45,58] or cell cycle regulatory components that are involved in carcinogenesis[73,74], the first disease linked to a mutation in the *ABCB6* gene was described. In ocular coloboma, which is an eye development disorder, two missense mutations were identified (L811V and A57T) in *ABCB6* in Chinese population. Comparative analyses of *ABCB6* genes in different species showed that both amino acids are highly conserved, presumably essential to normal biological function. In RPE cells wild type and L811V mutant ABCB6 showed colocalization with ER and Golgi markers. *ABCB6* attenuation by morpholino oligos caused coloboma-like phenotype in zebra fish. Normal phenotype could be restored by the co-injection of wild type, but not by the mutant ABCB6 mRNA. In these experiments there was no detectable porphyrin accumulation that would suggest a role for ABCB6 in tetrapyrrole transport[75].

The Langereis (Lan) blood group was first described in 1961[76] but scientists identified ABCB6 as the Lan blood group antigen only in 2012. First monoclonal antibody with Lan specificity (OSK43; IgG1κ) was generated from immortalized lymphocytes of a healthy Japanese Lan (-) woman who had developed anti-Lan antibody during pregnancy. This antibody proved that the protein is located at plasma membrane of RBC (which are devoid of mitochondria) and also hepatocellular carcinoma cells. 10 patients bearing *ABCB6* null mutations were analyzed and they seemed asymptomatic, they did not show anemia or abnormal erythropoiesis[28]. Lan-negativity is believed to be very rare[77,78] but recent population and genetic studies show that missense polymorphisms in *ABCB6* gene can be more common than previously expected[29].

While reports published continuously about porphyrin transport[68,79,52] other clinically important mutations of ABCB6 appeared in the literature[30,30,80–82]. Genetic studies reveal that mutations in ABCB6 can cause two other phenotypes, familial pseudohyperkalemia (FP)[81] and dyschromatosis universalis hereditaria (DUH)[83]. FP is a dominant red cell trait characterized by increased serum potassium concentration in whole blood stored below room temperature, without additional hematological abnormalities. DUH is a pigmentary genodermatosis characterized by a mixture of hyperpigmented and hypopigmented macules distributed randomly over the body. I shall return to this in more detail below. Through the years new heterozygous mutations were described: healthy Lan (-) individuals[84,85,86], DUH[87 88–91], FP[92,93] and coloboma patients[94].

We are not aware yet of the factor when ABCB6 protein expression provides obvious benefits to a cell or organism but it is clear that mutations in the *ABCB6* gene can lead to hereditary forms of eye dysfunction, pigmentary defect and pseudohyperkalemia (Fig. 5).

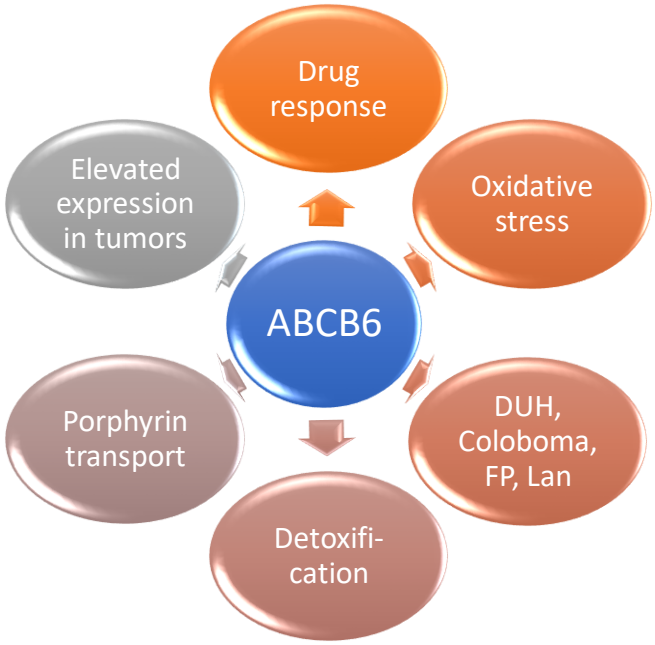

Figure 5. Diverse observations about ABCB6

1.2.8. ABCB6 and cadmium

Observation that ABCB6 exhibits topological and sequential similarities with a heavy metal transporter protein family has appeared earlier in several places in the literature[32,65,95].

Detoxification capacity of organisms is extremely important, as heavy metals such as cadmium (Cd), mercury (Hg), lead (Pb), and arsenic (As), are constantly present in our environment. Contamination in the drinking water and food can cause serious damage to living organisms. Research summarizing statistical data suggests that the risk of developing cancer can increase in areas exposed to high Cd levels[96]. By using chelators, the intracellular concentration of free metal ions can be reduced, thereby lower their toxic effect. The natural defense is based on similar principle, meaning animals and fungi produce cysteine-rich proteins that bind heavy metals to form thiolate bonds[97]. On the other hand, plants and certain species of fungi, (i.e. *Schizosaccharomyces pombe*) produce small peptides, phytochelatins (PCs). *Caenorhabditis elegans*, which is an exception in the animal kingdom also use PCs in its detoxification pathways. PCs are characterized by the repetition of glutamic acid-cysteine amino acid residues followed by glycine. The formation is catalyzed by phytochelatin synthase (PCS) from glutathione[98,99]. Importance of PCs is proven by the fact that PCS-deleted fission yeast (*S. pombe*) strains become more sensitive to heavy metals[100]. After finding PC-mediated Cd tolerance, the goal was to identify the proteins involved in the transport process. As a first step, the genomic library of *S. pombe* was created, and then a coding region was identified, which could restore the Cd-tolerant phenotype. The identified gene was named Heavy metal tolerance factor-1 *(hmt-1*). The gene is located on chromosome 3 and it encodes a protein containing 830 amino acids with a molecular weight of 90.5 kDa. Homologues were identified in fission yeast (*Schizosaccharomyces pombe*), nematode (*Caenorhabditis elegans*) and the fruit fly (*Drosophila melanogaster*) fulfill a conserved role in conferring resistance to heavy metals, specially cadmium[34,101].

In *S. pombe* HMT-1 localizes to the vacuolar membrane and catalyzes the sequestration of cadmium complexes to this intracellular compartment[102]. Experiments with *C. elegans* surprisingly revealed that, unlike SpHMT-1, CeHMT1 is able to provide tolerance to cadmium, arsenic and copper as well. The Vatamaniuk Lab showed that CeHMT-1 is expressed in liver-like cells, the coelomocytes, head neurons and intestinal

cells[103,104]. In 2018 they identified the intracellular localization of CeHMT-1 in the intestinal cells. The transporter is located to the apical recycling endosomes and partly to early and late endosomes. Similar to ABCB6[67], CeHMT-1 lacking the NTE domain was targeted to the plasma membrane[95]. A deficiency in Ce-HMT-1 does not interfere with the phenotype associated with CePCS-1 deficiency and vice versa. It became clear that HMT1-deficient worms are more sensitive to Cd than PCS-deficient ones. It was concluded that although CeHMT-1 is required for Cd detoxification, it is not only PC-dependent[105]. This is important because, following the evolution of HMT-1, neither *D. melanogaster* cells nor the human cells carry out the detoxification of heavy metals by conjugation with phytochelatins. Since *D. melanogaster* is devoid of PCs, further experiments were needed to determine whether Cd-PC complex is transported in yeast cells. Heterologously expressed DmHMT-1 suppressed the Cd hypersensitivity of *S. pombe hmt-1* mutants and localized to the vacuolar membrane. Despite this the vacuolar level of PCs were similar to the vacuoles from *hmt-1*-deleted cells. The authors assumed that SpHMT-1 is not the only Cd-PC carrier in the system. Several heavy metals were also tested in this rescue system. PCS-deficient *S. pombe* cells were hypersensitive to Cd, Hg and As, but SpHMT-1 does not cause tolerance to additional (heavy) metals Pb, Ag, As(III), Cu or Hg[101]. Experiments with *C. elegans* have revealed that, unlike SpHMT-1, CeHMT-1 can provide tolerance to cadmium, arsenic and copper[106]. These results indicated that the HMT-1-mediated detoxification of heavy metals is preserved during evolution, extending to some invertebrate species lacking the ability to synthesize PC[101].

1.2.9. ABCB6 and pigmentation

Dyschromatosis universalis hereditaria (DUH) is a pigmentary genodermatosis characterized by diffuse symmetrically distributed hypopigmented macules mixed with hyperpigmentation. The molecular basis of DUH was unknown until Zhang and his colleagues reported ABCB6 as a causative gene[30]. Since then, more mutations of ABCB6 were identified relating to DUH phenotype[30,83,87,88,91,107]. Interesting fact, that Lan (-) individuals[28] and ABCB6 knockout mice show no abnormal pigmentation phenotype[70,72].

Melanin is a natural pigment widespread in most organisms. Specialized pigment cells, including melanocytes and retinal pigment epithelium, synthesize melanin. Melanocytes are found in the basal layer of the epidermis. There are three basic types of

melanin: eumelanin, pheomelanin, and neuromelanin. Eumelanin is generally black or dark brown, pheomelanin is a yellow to reddish brown pigment[108]. Both pigments are polymeric and are derived via a series of redox reactions from a common precursor, dopaquinone, which is formed by the action of the enzyme tyrosinase on Tyr residue. Pheomelanin synthesis starts from tyrosine and cystine and contains polybenzothiazine portions[109,110]. Melanosomes are specialized intracellular organelles of pigment cells in which melanin pigments are synthesized and stored. They are members of a family of cell-type-specific lysosome-related organelles (LROs) that coexist with traditional endosomes and lysosomes and are generated from them through a progressive series of membrane sorting steps[87,111]. Lysosomal-like organelles carry a number of common characteristics with lysosomes, while requiring special proteins, other additional elements, cellular organelles for their construction and function[112,113]. Lysosomes and LROs are involved in a number of processes, including cholesterol homeostasis, maintenance and repair of plasma membranes, bone and tissue regeneration, protection against pathogens, regulation of cell death and signaling processes (Fig. 6). There are four steps in the maturation of the melanosome (Fig. 7A). Melanosomes originate from endosomal precursors (pre-melanosomes). The best known of the structural components is the pre-melanosomal protein (PMEL), which is a fibrillar component of melanosomes.

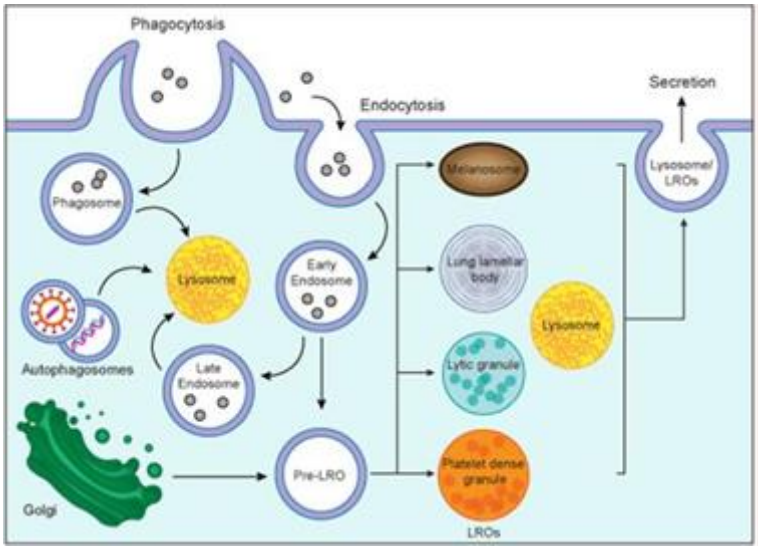

Figure 6. Biogenesis of lysosomes and lysosome-related organelles (LROs) (https://mynotebook.labarchives.com) LROs comprise a group of functionally diverse compartments that share features with lysosomes but are distinct and harbor specific cargoes that confer their unique properties. There are four well-studied LROs: pigment cell melanosomes, endothelial lamellar bodies, platelet α-granules and natural killer cell lytic granules[114].

PMEL is processed into amyloid fibrils forming the intraluminal matrix of stage II melanosomes. PMEL-derived amyloid structures belong to the emerging category of physiological amyloids that have beneficial cellular functions[115]. During maturation, PMEL is cleaved by several proteases to release luminal amyloidogenic fragments[116–118] (Fig 7). After translation, the full length peptide chain reaches the endosomal membrane where β-site APP-cleaving enzyme 2 (BACE2) generates the transmembrane M-β fragment[118]. This C-terminal polypeptide is processed by the gamma-secretase complex containing presenillin-2 in the lysosomes of pigment cells[119]. BACE2-mediated cleavage releases the M-α fragment, the amyloidogenic luminal domain of PMEL, into the melanosome lumen[118]. The M-α fragment is proteolytically processed to produce the amyloidogenic peptides that finally assemble into detergent insoluble protofibrils and fibrils recognized by the HMB45 and NKI-beteb antibodies (Fig. 7B,C)[116]. Melanin starts to be produced in stage III melanosomes by Tyrosinase (TRP-1) and stage IV melanosomes correspond to fully-melanized mature organelles. At the final step, melanin-filled, mature melanosomes enter the extracellular space, similar to exosomes and are passed on to the keratinocytes around the pigment cell. Stage I melanosomes are tyrosinase negative, whereas stage II melanosomes, including fibrillary elongated structures, are tyrosinase positive[43,111,120,121].

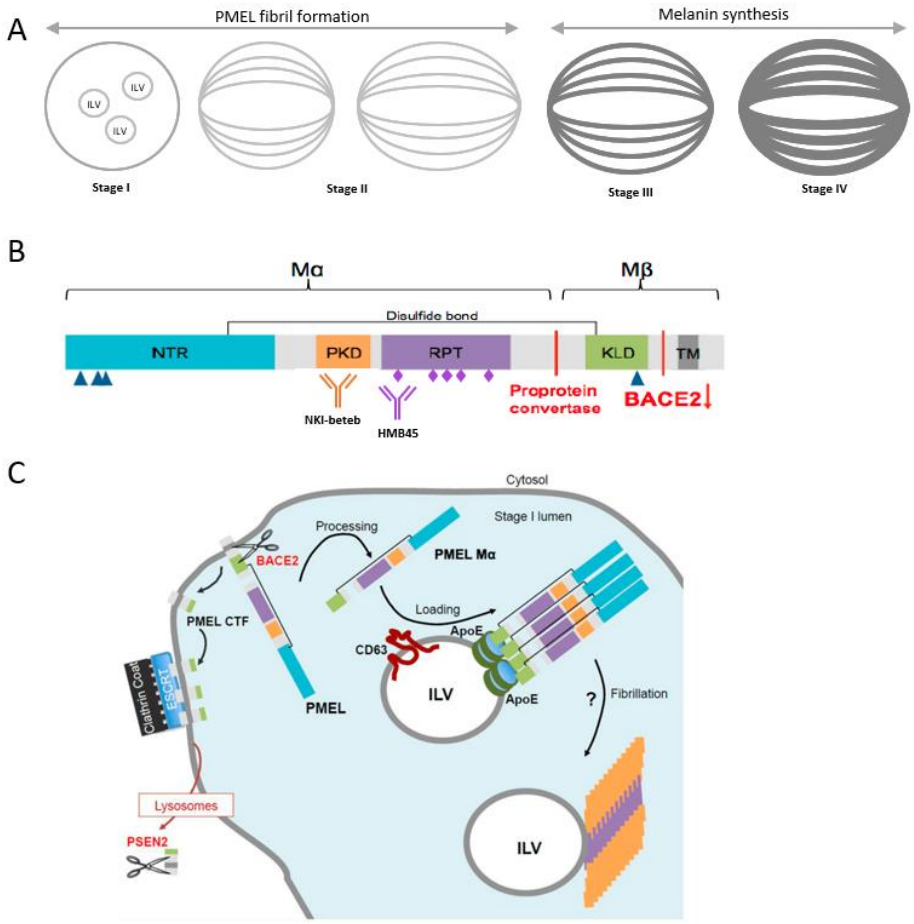

Figure 7. Schematic picture of PMEL isoforms melanosomes and in different compartments. A Biogenesis of melanosomes. Stage I melanosomes, where PMEL fibrils start to assemble. In stage II melanosomes, PMEL fibrils give the melanosomes their characteristic ellipsoidal shape and striated appearance. Melanin starts to be produced in stage III melanosomes, to which melanin synthesizing enzymes, such as Tyrosinase (TRP-1), are transported. Melanin is sequestered on PMEL fibrils, which become completely masked by melanin in stage IV melanosomes. **B** Schematic representation of pre-melanosomal protein (PMEL) domain structure. Triangles, pentagons and rhombuses represent N- and O-linked glycosylation. PMEL cleavage sites and the involved proteases are indicated in red. **C** Model for pre-melanosomal protein (PMEL) fibril formation in stage I melanosomes. The Mα fragment of PMEL is released into the lumen of stage I melanosomes by action of BACE2 (beta-site APP cleaving enzyme 2) protease. This cleavage also produces a C-Terminal Fragment (CTF) that is sequestered at the limiting membrane of stage I melanosomes by the endosomal sorting complexes required for transport (ESCRT) machinery, to be further cleaved by the presenilin 2 (PSEN2) of the γ-secretase complex in lysosomes. The Mα fragment is then loaded onto intraluminal vesicles (ILVs). ILVs have been proposed to act as nucleators for PMEL fibril formation[115].

Amyloid PMEL fragments can be cytotoxic, so mutations distracting PMEL trafficking or processing can be associated with melanocyte survival or melanin defects[115,117,122]. However, melanocytes devoid of PMEL expression still have normal pigment levels[123].

Whereas melanosomes and lysosomes are distinct organelles in melanocytes[124], recent studies have proposed that lysosomes are required for correct PMEL amyloid matrix formation[125–127], suggesting a potential role for lysosomal proteins such as ABCB6 in early steps of melanosome biogenesis.

Genetic pigmentation disorders give new insights into the understanding of the pigmentation process, including melanosome biogenesis, melanin synthesis[111]. Mutations in the ABCB6 gene manifest in DUH, which is characterized by hyper- and hypopigmented areas over the body. Skin histological examination of a DUH proband showed a normal number of melanocytes in the basal layer in both hyper- and hypo pigmented areas. However, the number of mature melanosomes in normal control and hyperpigmented skin areas was considerably higher than in hypopigmented area. Additionally, many immature melanosomes were observed in hypopigmented skin region. However, the influence of ABCB6 on the above described process of melanogenesis is not known and its intracellular localization and function are also not clear.

We can see that conflicting observations were described about ABCB6 in the last two decades. Based on healthy Lan (-) patients, healthy ABCB6-KO mice and studies about the extramitochondrial localization we supposed that the protein is not an essential mitochondrial porphyrin importer. In summary, the pathophysiological function of ABCB6 in the endo-lysosomal continuum remains to be clarified. Therefore, we thought that the answer must be sought in another direction.

DOI:10.14753/SE.2020.2354

2. Aims

ABCB6 is usually discussed in the context of mitochondrial ABC transporters based on early studies suggesting that it catalyzes the mitochondrial import of a heme synthesis intermediate. Recent studies have evidenced alternative localizations, but the physiological function of ABCB6 in these extramitochondrial compartments has remained elusive. My overall aim was to establish in vitro assays for the study of the function and intracellular localization of ABCB6. ABCB6 shows high amino acid sequence similarity to HMT-1, which is involved in the heavy metal tolerance of *Schizosaccharomyces pombe, Caenorhabditis elegans* and *Drosophila melanogaster*. HMT-1 (heavy metal tolerance factor-1) localizes to the vacuolar/endosomal membrane of *S. pombe* and *C. elegans* where it catalyzes the sequestration of cadmium complexes. To analyze the relation of ABCB6 function to the HMT-1 proteins, I pursued the following aims:

1. Investigation of the localization of heterologously expressed human ABCB6 in *S. pombe* and *C. elegans.*
2. Pending successful expression in these model systems, the second aim was to analyze the function of ABCB6 in wild-type and knock-out strains.
3. Relevance of Cd detoxification in human cells

An additional aim was to use cellular models to decipher the role of ABCB6 in melanogenesis, and to suggest a functional model explaining the DUH phenotype.

4. The third aim was to set up an in vitro model system to study the localization of ABCB6 in a melanocytic cell line.
5. Given the link of *ABCB6* mutation to aberrant pigmentation, the final aim was to set up an in vitro model system to characterize the role of ABCB6 variants melanogenesis in a human cell line.

DOI:10.14753/SE.2020.2354

3. Methods

3.1. Cell culturing

S. pombe culture conditions and strains — The *S. pombe* strains BG_00008 (*ade6-M216, ura4-D18, leu1-32*) and the *hmt1*-deleted mutant strain BG_H4691 (*ade6-M216, ura4-D18, leu1-32*) were a kind gift from R. Lill (Philipps-Universität Marburg). A common feature of these laboratory strains is adenine, uracil and leucine autotrophy. EMM Broth, EMM agar and EMM without dextrose were purchased from Formedium (Hunstanton, UK). Depending on the experiment, medium was supplemented with 225 mg/l adenine-HCl, 225 mg/l L-leucine and 225 mg/l uracil.

C. elegans culture conditions and strains — *C. elegans* experiments were performed together with János Barna and Dániel Kovács (Department of Genetics, Eötvös Loránd University). The strains were grown on solid Nematode Growth Medium (NGM) at 20 °C containing a lawn of the bacterium *Escherichia coli* OP50[128]. The following strains were used: N2 *C. elegans* wild-type, var. Bristol; DP38 *unc-119(ed3)III*; VC287 *hmt-1(gk161)III*; VF31 *gfIs1[phmt-1::hmt-1::gfp, unc-119(+)*; VF12 *hmt-1(gk161)III; gfIs1[phmt-1::hmt-1::GFP, unc-119(+)]*. For microscopic studies we used the following strains (generous gift from Dr. Xiaochen Wang (Institute of Biophysics, Chinese Academy of Sciences)): *XW1957: qxIs110 (pges-1::mCHERRY::RAB-5); XW1962: qxIs111 (pges-1::mCHERRY::RAB-7); XW9119: qxIs213 (pges-1::mCHERRY::RAB-10).*

Cell lines — HeLa cells were purchased from ATCC, the glioblastoma SNB-19 cells were from DSMZ (Germany), and the melanoma MNT-1 cell line was a kind gift of Guillaume van Neil. HeLa and SNB-19 cells were grown in high glucose DMEM (Gibco 521000-47) supplemented with 10% FBS, 2 mmol/l glutamine, and 100 units/ml penicillin and streptomycin (Life Technologies) at 37 °C in 5% CO_2. MNT-1 cells were grown in DMEM high glucose medium (4.5 mg/ml Gibco, Grand Island, NY, USA) supplemented with 10% v/v AIM-V, 20% v/v FBS, 1% v/v sodium pyruvate, 1% v/v non-essential amino acids, 100 U/ml penicillin and 100 μg/ml streptomycin. MNT-1 cells were incubated at 37 °C with 5% CO_2 and regularly passaged at a density of 80% (1:8 ratio). Cells were periodically tested for mycoplasma contamination with the MycoAlert mycoplasma detection Kit (Lonza, Basel, Switzerland).

3.2. Molecular cloning of ABCB6 and HMT-1 constructs

Plasmid constructs were amplified in *E. coli* strain Top10 (Invitrogen, Carlsbad, CA, USA), grown at 37 °C in liquid Luria-Bertani (LB) medium supplemented with appropriate antibiotics.

S. pombe — The hemagglutinin-tagged *S. pombe* hmt-1 cDNA (Z14055) was ordered from GenScript (Piscataway, NJ, USA). Human ABCB6 (NM_005689) cDNA was provided by Jill Paterson in pcDNA3.1-Flag vector[63]. My former colleague, Katalin Kiss generated the Walker-A region lysine mutant ABCB6 variant (K629M) by overlap extension PCR mutagenesis[24]. Melinda Gera generated various mutants of ABCB6 (Table S1). *Hmt-1* and *ABCB6* variants encoding cDNAs were subcloned into the pREP1 fission yeast expression vector. pEGFP-N1 (BD Biosciences, Franklin Lakes, NJ, USA) plasmid was used for the N-terminal GFP-tagging of the transporters by exchanging the ABCB6-GFP construct from a respective pAcUW plasmid[129] HMT-1-GFP was assembled by PCR (Polymerase Chain Reaction) using a primer pair generating a new restriction site at the 3'end of the cDNA. First, HMT-1 C-terminal was cloned to pEGFP-N1, then the pREP1-HMT-1-GFP expression plasmid was created by exchanging the C-terminal region of HMT-1.

C. elegans — For experiments in *C. elegans*, codon-optimized ABCB6 cDNA was synthetized by GenScritpt (Piscataway, NJ, USA). To generate the p*hmt-1::ABCB6::gfp* and p*hmt-1::ABCB6::mCherry* reporter for localization studies, *ABCB6* was subcloned in frame with the *GFP* sequence of the pPD95.75-GFP vector. The 5' regulatory region of *hmt-1* (2.8 kb immediately upstream of the start of the *hmt-1* coding sequence) was PCR-amplified using primer pairs as previously[104] and with another primer pair we introduced the appropriate restriction enzyme recognition sites at the 5′ and 3′ends (Table S1). The PCR-amplified *hmt-1* promoter was subcloned into the pPD95.75-ABCB6-GFP vector. In the case of p*hmt-1*::*ABCB6::mCherry*, the GFP reporter sequence of pPD95.75-ABCB6-EGFP was changed to the sequence encoding mCherry from plasmid pRH21.

Human cell lines — The lysine mutant ABCB6 variant of the Walker-A region (K629M) and DUH mutation G579E[83] were generated by overlap extension PCR mutagenesis[24,130]. Constructs were cloned into lentiviral plasmid obtained via the Addgene Plasmid Repository. (Table S2).

3.3. Generation of transgenic lines

S. pombe *transgenic strains* — Transformation of fission yeast cells was performed by Clontech Yeastmaker™ protocol[131]. Cells were grown to the appropriate density (A_{600nm} of 0.5) in 50 ml of low glucose EMM medium (5 g/L glucose and adenine, leucine, uracil) then pelleted and washed with 50 ml of sterile water (700 g, 5 min) and suspended in 1 ml water. Cells were then washed with 1 ml of LiAc-TE (1.1 ml 10x TE, 1.1 ml of 1 M LiAc 7.8 ml water) (700 g, 5 minutes). The pellet was resuspended in 250 µl LiAc-TE ($2x10^9$ cells/ml). To 100 µl cell suspension, 2 µl of 10 mg/ml carrier DNA was added. 1.5 µg of DNA was added to the cells, and the mixture was incubated for 10 min at room temperature then 50 min at 30 °C. Thereafter, 43 µl preheated (40 °C) of DMSO was added, and cells were heat-shocked (42 °C, 5 min). The transformed yeast was washed with 1 ml water (700 g, 5 min), and cells were plated in 100 µl water on EMM plate. EMM Broth and EMM Agar products were used for the growth of transformed cells, which were supplemented with adenine and uracil (225 mg/L), because S. pombe transformants were selected for leucine prototrophy (*LEU2* gene is encoded on pREP1 expression plasmid).

C. elegans *transgenic strains* — Applying Biolistic PDS-1000/He particle delivery system (BioRad, Hercules, CA, USA) transgenic strains were generated according to standard protocol by J. Barna and D. Kovács. 50 µl of a 60 mg/mL gold grain was coupled with 10-10 µg of pre-linearized ABCB6:GFP or ABCB6::mCherry construct or co-transformation marker (unc-119(+)). Transgenic animals can be easily identified on immobile *Unc* phenotype background, because the wild allele of the co-transformed *unc-119* gene rescues the motionless unc-119(ed3) mutant adult hermaphrodites. Non-Unc transgenic animals exhibiting GFP or mCherry-mediated fluorescence were selected, and the stable integrated strains TTV634: *eluIs310 [phmt-1::ABCB6::gfp + unc-119(+)]; unc-119(ed3)* and TTV677: *eluEx383[phmt-1::ABCB6::mCherry + unc-119(+)]; unc-119(ed3)* carrying the array extrachromosomally were selected for further analysis. TTV 634 was crossed with *hmt-1(gk161)* to generate TTV 635: *hmt-1(gk161); eluIs310 [phmt-1::ABCB6::gfp + unc-119(+)]*.

DOI:10.14753/SE.2020.2354

Table 1. List of worm strains used in the publication[132].

Strains	Relevant genotype	Source/Reference
N2	Wild-type var. Bristol	Caenorhabditis Genetics Center (CGC)
DP38	*unc-119(ed3)III*	Caenorhabditis Genetics Center (CGC)
VC287	*hmt-1(gk161)II*	Caenorhabditis Genetics Center (CGC)
VF31	*gfIs1[phmt-1::hmt-1::gfp, unc-119(+)*	Dr. Olena Vatamaniuk (Cornell University)
VF12	*hmt-1(gk161)III; gfIs1[phmt-1::hmt-1::GFP, unc-119(+)]*	Dr. Olena Vatamaniuk (Cornell University)
XW1957	*qxIs110 (pges-1::mCHERRY::RAB-5)*	Dr. Xiaochen Wang (Institute of Biophysics, CAS)
XW1962	*qxIs111 (pges-1::mCHERRY::RAB-7)*	Dr. Xiaochen Wang (Institute of Biophysics, CAS)
XW9119:	*qxIs213 (pges-1::mCHERRY::RAB-10)*	Dr. Xiaochen Wang (Institute of Biophysics, CAS)
TTV634	*eluIs310 [phmt-1::ABCB6::gfp + unc-119(+)]; unc-119(ed3)*	[132]
TTV 635	*hmt-1(gk161); eluIs310 [phmt-1::ABCB6::gfp + unc-119(+)]*	[132]
TTV701	*unc-119(ed3)III; eluIs310[phmt-1::ABCB6::gfp + unc-119(+)]qxIs110(Pges-1mCHERRY::RAB-5)*	[132]
TTV702	*unc-119(ed3)III; eluIs310[phmt-1::ABCB6::gfp + unc-119(+)];* qxIs111*(Pges-1mCHERRY::RAB-7)*	[132]
TTV703	*unc-119(ed3)III; eluIs310[phmt-1::ABCB6::gfp + unc-119(+)]; qxIs213(Pges-1mCHERRY::RAB-10)*	[132]
TTV705	*unc-119(ed3)III; gfIs1[phmt-1::hmt-1::gfp, unc-119(+)]; qxIs110(Pges-1mCHERRY::RAB-5)*	[132]
TTV706	*unc-119(ed3)III; gfIs1[phmt-1::hmt-1::gfp, unc-119(+)];* qxIs111*(Pges-1mCHERRY::RAB-7)*	[132]
TTV707	*unc-119(ed3)III; gfIs1[phmt-1::hmt-1::gfp, unc-119(+)]; qxIs213(Pges-1mCHERRY::RAB-10)*	[132]

Human cell lines with enhanced or silenced ABCB6 expression — Lentiviral expression plasmids were made by K. Kiss and the cell lines were generated by N. Kucsma as described previously[24]. To induce the expression of the shRNA constructs, IPTG (1 mM) was added to the cells for 6 days before additional treatments.

Transduction of MNT-1 cells with ABCB6 variants was carried out by the laboratory of G. van Niel using lentiviral transduction. For downregulation of ABCB6 cells were transfected with siRNA using oligofectamine (Invitrogen). siRNA transfections were performed twice at 48 h interval and experiments were performed 96 h after the first siRNA transfection. Predesigned siRNA obtained from Qiagen. siRNA non-targeting control: 5'- AAT TCT CCG AAC GTG TCA CGT -3', siRNA ABCB6#1 (Cat no.SI00080353), siRNA ABCB6#2 (Cat no.SI00080360), siRNA ABCB6#3 (Cat no.SI00080374), siRNA ABCB6#4 (Cat no.SI00083731), siRNA ABCB6#5 (Cat no.SI00080873), siRNA ABCB6#6 (Cat no.SI00080880).

3.4. Immunoblotting

S. pombe — Heterologous expression of the transporters in the fission yeast strains was verified by Western blotting. Before the Lowry protein concentration measurements (OD=600), we had to disrupt the cell wall of yeast cells. Cells were collected at 3000 g 2 min and diluted in 1 ml of sterile water. 150 µl of 1.85 M NaOH and 7.5% β-mercaptoethanol were added and the cells were incubated for 10 minutes at RT. 150 µl of 50% TCA was added and the samples were centrifuged at 2000 g for 5 min. The protein extract was washed in sterile water and suspended in DB buffer. Samples were homogenized by sonication.

Human cell lines — Immunoblotting of HeLa and SNB-19 cell line were performed according to standard protocols. In the case of MNT-1 cells a Triton X-soluble lysate was prepared in 20 mM Tris-HCl pH 7.4, 150 mM NaCl, 1% TX-100, 1 mM EDTA, protease inhibitors. The Triton X-insoluble fraction was resuspended in 1% SDS, 1% β-mercaptoethanol in PBS containing protease inhibitors, incubated for 10 min at RT and then heated for 10 min at 100 °C. Light and dense melanosomal fractions and exosome isolation were performed as already described[121,133]. Lysates, fractions and exosomes were incubated in sample buffer with or without 350 mM 2-mercapthethanol (Sigma), incubated at 60 °C for 5 min, and fractionated by SDS-PAGE using Nupage (4-

12%) Bis-Tris gels (Invitrogen) and transferred onto nitrocellulose membranes (Millipore). The membranes were blocked in PBS/Tween 0.1% (PBS/T) with 5% non-fat dried milk, incubated with the indicated primary antibody diluted in PBS/T, washed four times in blocking solution, and finally incubated with HRP-conjugated secondary antibody followed by washing in PBS/T. Blots were developed using the ECL Plus Western blotting detection system (GE Healthcare) according to the manufacturer's instruction. Signal intensities were quantified with the Image J software (National Institute of Health).

3.5. Cytotoxicity assays

S. pombe — Transformed cells were grown in EMM complemented with appropriate supplements. To characterize the chemosensitivity of yeast strains in liquid medium, 100 µl overnight cultures (A_{600nm} of 0.8) were diluted into 2 ml EMM containing different concentrations of metal compounds (Cd(II) As(III) As(V), Sb(III), Sb(V), Hg(II), Cu(II) or Zn(II)). In case of Sb(III) and Cu(II) we could not detect toxic concentrations in EMM medium. Cells were then grown at 30 °C, 200 rpm. After 72 h the extent of growth was determined by measuring absorbance at 600 nm (A_{600nm}). Viability curves were fitted with Graph Pad Prism 5 software using the sigmoidal dose–response model. To characterize chemosensitivity on agar plates, overnight cultures were diluted in EMM (A_{600nm} of 0.7). Colonies were spotted onto plates containing different concentrations of metal compounds and incubated for 6-7 days at 30 °C.

C. elegans —Experiments were performed by J. Barna and D. Kovács as described by Schwartz et al[104]. Adult worms were allowed to lay eggs for 2 hours at 20 °C on a medium containing 0, 5 µM and 10 µM $CdCl_2$. Then the adults were removed from the plates, thus synchronized populations grew. Animals were allowed to grow for 4 days at 20 °C. After 4 days, samples were taken from each plate, 20-20 animals/category were counted how many animals have reached adulthood or larval stages by light microscopy in 3 independent trials.

Human cell lines — Living, proliferating cells maintain reducing environment within their cytosol. The PrestoBlue reagent contains a blue, nonfluorescent, cell-permeant compound which can be modified by the reducing environment of the viable cell and turns red in color and becomes highly fluorescent. This change can be detected

by using a plate reader such as Perkin-Elmer EnSpire. In cytotoxicity experiments the cells were seeded in 100 µl DMEM medium at a density of 4000 cells/well in 96-well plates, and serially diluted drugs were added the following day in 100 µl medium to give the indicated final concentration. Cells were then incubated for 72 h at 37 °C in 5% CO_2. Cell survival was assessed by the PrestoBlue assay, according to the manufacturer's instructions. Viability curves were fitted with Graph Pad Prism 7 software using the sigmoidal dose–response model.

Cytotoxicity assays were performed in triplicates

3.6. Determination of the vacuolar cadmium content

Vacuole isolation — *S. pombe* cultures were treated overnight with 20 µM $CdCl_2$, then vacuoles were isolated with the valuable help of N. Kucsma as described earlier[134], with some modifications. Briefly, 5 ml stationary phase cultures diluted in 25 ml of EMM were grown for 4-6 h at 30 °C. Next, 25 ml cultures were diluted in 200 ml EMM medium containing 20 µM $CdCl_2$, and the cultures were grown for 18 h at 30 °C to an A_{600nm} (OD600) of 1.5. Cells were pelleted by centrifugation at 3000 g for 5 min and were washed in 50 ml distilled water. After resuspension in 50 ml buffer (20 mM β-mercaptoethanol, 100 mM Tris-HCl (pH 9.4)), cells were incubated for 20 min at 30 °C with gentle shaking. Spheroplasts were created by pelleting and suspending the cells in 20 ml of digestion medium (DM: 1.2 M sorbitol (pH 7.5), 10 mM β-mercaptoethanol, 20 mM potassium phosphate, 50 mg of Zymolyase 20T (ICN) and 100 mg of lysing enzymes from *Trichoderma harzianum* (Sigma-Aldrich) to disrupt cell wall). The suspension was incubated for 2 h at 30 °C with gentle shaking, followed by centrifugation at 3000 g for 5 min. The spheroplasts were washed in 20 ml ice-cold homogenization medium (HM: 1.6 M sorbitol, 10 mM MES-Tris (pH 6.9), 0.5 mM $MgCl_2$, 5 mM β-mercaptoethanol, and to avoid protein degradation 1 mM phenylmethylsulfonyl fluoride, and 1 µg/ml each of leupeptin, aprotinin, and pepstatin (protease inhibitor cocktail, Sigma P8340 in 500×dilution) were added). Pelleted spheroplasts were lysed in the same medium by homogenization in a 5-ml glass Dounce homogenizer. The crude lysate was cleared of cell debris and unbroken cells by centrifugation at 3000 g for 8 min. The supernatants were collected, and the pellet was resuspended in 3.5 ml HM, homogenized again (30X), and centrifuged at 3000 g for 8 min. Supernatants were centrifuged at 13000 g at 4 °C for

35 min. The pellet, containing the partially purified vacuolar fraction was suspended in 1.5 ml HM, layered onto 1 ml Sucrose step gradient (40%/50% (v/v)), and pelleted at 40000 rpm using a Beckman Coulter 70.1 Ti rotor at 4 °C for 1 h. Purified vacuoles were suspended in 3 ml suspension medium (SM: 1.6 M sorbitol, 100 mM KCl, 10 mM MES-Tris, pH 6.9, 5 mM $MgCl_2$, and protease inhibitors) and were centrifuged at 4 °C at 13000 g for 12 min in Eppendorf microcentrifuge. The final vacuolar pellet was stored at -80 °C.

Assessment of Integrity of Vacuole Preparations — The success of the measurement depended on intact vacuoles. With the help of Nóra Kucsma, the integrity of the vacuoles was assessed by measuring fluorescence as described[135] based on that Acridin-Orange (AO, Sigma-Aldrich) indicates acidic compartments. In control experiments vacuoles were lysed with detergent destroying their lipid bilayer, so acidic pH was no longer sustainable. The decreased fluorescent signal of AO was measured using an Attune Acoustic Focusing cytometer (Applied Biosystems, Life Technologies, Carlsbad, CA, US).

Determination of vacuolar Cd contents — Vacuolar Cd content was determined by graphite furnace atomic absorption spectrometry (GFAAS) performed by László Bencs and Norbert Szoboszlai. All GFAAS measurements were performed at Wigner Research Centre for Physics of HAS on an Analytik Jena Model ContrAA-700 tandem high-resolution AAS (Analytik Jena AG, Jena, Germany), equipped with an autosampler. Each final vacuolar pellet after the isolation was digested in 200 µl cc. (65% v/v) HNO_3 for 24 h at room temperature. After appropriate dilution, an aliquot of 20 µl of each sample was directly dispensed by the autosampler into the graphite tube (fitted with a graphite platform) to determine the concentration of Cd in the isolated vacuoles. The Cd 228.8018 nm spectral line was selected for the determinations, with a 3-pixel evaluation of the CCD camera, which corresponds to a resolution of 3.78 pm at this wavelength. The GF heating program consisted of smooth drying (at 100 °C for 20 s, 110 °C for 5 s, 130 °C for 10 s), pyrolysis (350 °C for 15 s, 450 °C for 10 s), atomization/measurement (at 1200 °C for 3 s), and clean-out (2450 °C for 4 s) steps. In these steps, maximum flow (2 dm^3/min) of the GF sheath gas (5N Ar) was applied, except the atomization step under stopped air flow. Integrated absorbance signals were measured with signal integration time of 3 s and using iterative background correction approach. Each measurement data

corresponds to an average of three replicate determinations. For quantitative determinations, external standardization was applied by means of setting up five-point calibration curves (range: 1-50 ng/ml Cd, preserved in 2.6% HNO_3). Recovery was checked by spiking selected samples with 5 µl of a Cd standard solution at a concentration of 500 ng/l and 50 ng/l. The precision of the determinations, expressed as relative standard deviation (RSD) was typically below 2.1%, but not worse than 5.3%. All Cd concentration data were normalized to the protein content of the samples.

3.7. Measurement of melanin content

Cells were seeded in 6-well plates at a density of 1×10^5 cells per well and were allowed to grow 48 hours. MNT-1 cells were washed with phosphate-buffered saline (PBS) and dissolved in 250 µl of 1 N NaOH for 1 hour at 80 °C. 100 µl sample was transferred to 96-well plates. Melanin contents were determined by measuring absorbance at a wavelength of 405 nm using a plate reader such as Perkin-Elmer EnSpire.

3.8. Confocal microscopy

Localization of ABCB6 in S. pombe — For the evaluation of intracellular localization of the transporters, *hmt-1*-deleted *S. pombe* was transformed with pREP1-HMT-1-GFP or ABCB6-GFP. Cells were grown to mid-log phase (A_{600nm} of 0.5-0.8) and stained with FM 4-64 (T3166 ThermoFischer Scientific Waltham, MA, USA) as described with the following modifications. FM4-64 dye was dissolved in DMSO at a concentration of 1.64 mM. Cells were harvested and incubated with 1 µl FM4-64 in 50 µl EMM medium at 30 °C for 20 min to internalize the dye (on ice endocytosis is inhibited and the dye stains the plasma membrane). Excess dye was washed with 1 ml EMM, cells were centrifuged at 5000 g for 5 min at RT. The cell pellet was resuspended in 5 ml EMM, and the suspension was shaken at 30 °C for 90 min for enrichment of the dye in the vacuolar membrane. The total volume was transferred to a centrifuge tube and spun for 5 min at 5000 g at room temperature (RT). The cell pellet was resuspended in 1 ml sterile water and centrifuged at 5000 g for 5 min at RT. Cells were resuspended in 25 µl EMM. 7 µl was spotted on ConA/polyK-coated (1:1 mixture of 2 mg/ml concanavalin A and 0.1% poly-L-lysine) glass slides covered with an 18 x 18 mm^2 cover slip. This mixture should effectively immobilize yeast cells on the glass slide due to the high amount of

polysaccharides and negatively charged proteins in the cell wall. Confocal images were obtained using LSM 710 confocal laser scanning microscope (Carl Zeiss AG, Oberkochen, Germany) equipped with a Plan-Apochromat 63×/1.4 Oil DIC M27 objective. Noise reduction and deconvolution of the images were performed with Huygens Essential (Scientific Volume Imaging B.V.).

***Localization of* ABCB6 in C. elegans** — Experiments were performed by J. Barna and D. Kovács and confocal images were made by N. Kucsma. Transgenic strains were grown in normal growth conditions at 20 °C. To test the subcellular co-localization of ABCB6 and CeHMT-1, the *phmt1::ABCB6::mCherry* (TTV677) strain was crossed with *phmt-1::HMT-1::GFP* (VF31) males and the F1 progeny co-expressing both transgenes was examined with a confocal microscope (Zeiss LSM 710, Plan-Apochromat 63×/1.4 NA Oil DIC M27objective). To prepare the sample, animals were plated on a 5% agar surface onto the slide in M9 physiological buffer (20 mM KH_2PO_4, 40 mM Na_2HPO_4, 85 mM NaCl, 1 mM $MgSO_4$, pH 7). Their motion was paralyzed by levamizole dropped onto agar, which acts as a nerve poison, being an agonist of the α-subunit of the L-subtype nicotinic acetylcholine receptor[136]. Lysosomal staining was performed as described. L4 larvae/young adult animals were placed on an OP50 grafted NGM plate containing 2 µM LysoTracker Red. Animals spent 12-48 hours in the absence of light then they were directly examined after removal from agar plates. To determine the subcellular localization of CeHMT-1::GFP and ABCB6::GFP, *phmt-1::hmt-1::gfp* (VF11) and *phmt-1::abcb6::gfp* (TTV634) were crossed with strains expressing different endosomal markers [137,138], resulting in *TTV700 unc-119(ed3)III; eluIs310[phmt-1::ABCB6::gfp + unc-119(+)]; TTV701 unc-119(ed3)III; eluIs310[phmt-1::ABCB6::gfp + unc-119(+)]; qxIs110(Pges-1mCHERRY::RAB-5), TTV702 unc-119(ed3)III; eluIs310[phmt-1::ABCB6::gfp + unc-119(+)];* qxIs111*(Pges-1mCHERRY::RAB-7), TTV703 unc-119(ed3)III; eluIs310[phmt-1::ABCB6::gfp + unc-119(+)]; qxIs213(Pges-1mCHERRY::RAB-10), TTV705 unc-119(ed3)III; gfIs1[phmt-1::hmt-1::gfp, unc-119(+)]; qxIs110(Pges-1mCHERRY::RAB-5), TTV706 unc-119(ed3)III; gfIs1[phmt-1::hmt-1::gfp, unc-119(+)];* qxIs111*(Pges-1mCHERRY::RAB-7), TTV707 unc-119 (ed3)III; gfIs1[phmt-1::hmt-1::gfp, unc-119(+)]; qxIs213(Pges-1mCHERRY::RAB-10).*

Localization of ABCB6 in human cells — Confocal images were made by Johannes M. Reisecker. HeLa, SNB-19 and MNT-1 cells expressing ABCB6 variants

were plated in an Eppendorf 8 well imaging coverglass (#0030742036). Hoechst 33342 was applied to the cells 20 min prior to fixation, subsequently cells were rinsed in PBS and fixed for 30 min in 4% PFA/PBS at RT. Fixed cells were quenched for 10 min in PBS/100 mM glycine (quenching buffer), washed with PBS and blocked and permeabilized in PBS containing 0.2 mg/ml BSA/0.1% Triton X-100/ 10% Normal Goat Serum (blocking buffer). The primary antibody was diluted in PBS containing 0.2 mg/ml BSA, 0.1% Triton X-100 and 3% Normal Goat Serum (incubation buffer, IB). Cells were incubated with the primary antibody overnight at 4 °C in a humidified chamber, washed five times in IB, and incubated with the corresponding secondary anti-human, anti-rabbit and anti-mouse antibodies conjugated to Alexa Fluor 488 or Alexa Fluor 647 diluted in IB for 90 min at RT. Samples were washed five times with PBS and subsequently imaged. Confocal images were obtained using LSM 700 or LSM 880 confocal laser scanning microscope (Carl Zeiss, Inc.) equipped with a Plan-Apochromat 63x/1.4 NA Oil DIC M27 objective. Images were acquired in three channels (blue (Hoechst 33342), green (Alexa Fluor 488), red (Alexa Fluor 647), blue emitting Hoechst 33342) was excited using the 405 nm laser line, green emitting Alexa Fluor 488 was excited using the 488 nm laser line and infrared emitting Alexa Fluor 647 was excited using the 633 nm laser line. Noise reduction and deconvolution of the images was performed with Huygens Essential (Scientific Volume Imaging B.V.). Colocalization analysis was performed with ImageJ (National Institute of Health) using the JACoP v2.0 plugin.

Antibodies and dyes — Monoclonal antibodies, dyes and their sources were as follows: ß-actin (A1978, Sigma-Aldrich, Saint Louis, MO, USA); anti-EGFP (ab184601 Abcam, Cambridge, UK), ABCB6-567[139], anti-HA antibody, (H6908 Sigma-Aldrich). HRP-dependent luminescence was detected using the enhanced chemiluminescence technique (ECL, Amersham). Rabbit monoclonal Anti-AIF [D39D2] antibody (#5318) to apoptosis inducing factor, rabbit monoclonal Anti-EEA1 [C45B10] antibody (#3288) to early endosome antigen 1, rabbit monoclonal Anti-LAMP1 [D2D11] antibody (#9091) to lysosome-associated membrane protein 1, secondary goat anti-mouse IgG (H+L) $F(ab')_2$ fragment conjugated to Alexa Fluor 647 (#4410) and secondary goat anti-rabbit IgG (H+L) $F(ab')_2$ fragment conjugated to Alexa Fluor 647 (#4414) were from Cell Signaling Technology. Secondary goat polyclonal antibody to human IgG conjugated to DyLight 488 (ab96907) was purchased from Abcam. Hoechst 33342 (R37605) nuclear

counterstain was from Thermo Fisher Scientific. The OSK43 antibody was a kind gift from Dr. Yoshihiko Tani (Japanese Red Cross Osaka Blood Center, Osaka, Japan).

Mouse monoclonal Anti-Melanoma Associated Antigen 100+/7 kDa [Nki/beteb] antibody (ab34165) and mouse monoclonal Anti-Melanoma [HMB45] antibody (ab787) to melanocyte protein (PMEL), mouse monoclonal Anti-TRP-1 [TA99] antibody (ab3312) to tyrosinase-related protein 1(TRP1), secondary goat polyclonal antibody to human IgG conjugated to DyLight 488 (ab96907) and horseradish peroxidase-conjugated goat polyclonal antibodies to rabbit IgG (ab6721) and to mouse IgG (ab6789) were from Abcam. Rabbit monoclonal Anti-AIF [D39D2] antibody (#5318) to apoptosis inducing factor, rabbit monoclonal Anti-Calnexin [C5C9] antibody (#2679) to Calnexin, rabbit monoclonal Anti-RCAS1 [D2B6N] to receptor binding cancer antigen expressed on SiSo cells (#12290), rabbit monoclonal Anti-EEA1 [C45B10] antibody (#3288) to early endosome antigen 1, rabbit monoclonal Anti-LAMP1 [D2D11] antibody (#9091) to lysosome-associated membrane protein 1, secondary goat anti-mouse IgG (H+L) $F(ab')_2$ fragment conjugated to Alexa Fluor 647 (#4410) and secondary goat anti-rabbit IgG (H+L) $F(ab')_2$ fragment conjugated to Alexa Fluor 647 (#4414) were from Cell Signaling Technology. Secondary goat anti-rabbit IgG (H+L) antibody conjugated to Alexa Fluor-488 (A-11034) and Hoechst 33342 (R37605) nuclear counterstain were from Thermo Fisher Scientific. The OSK43 antibody was a kind gift from Dr Yoshihiko Tani (Japanese Red Cross Osaka Blood Center, Osaka,Japan)[82]. ABCB6 ((61.5): sc-135726) mouse monoclonal antibody was from Santa Cruz Biotechnology.

Electron microscopic images and analysis were made by Guillaume van Niel, Ptissam Bergam and Graca Raposo.

3.9. Genome editing by CRISPR/Cas9

Fluorescent in situ hybridization (FISH) — ABCB6 specific FISH probe and Chromosome II control probe (Orange / Green SKU ABCB6-CHR2-20-ORGR, premixed) was purchased from Empire Genomics (Williamsville, NY, USA). The cytogenetic analysis and FISH hybridization protocol was implemented by Gergő Papp (1st Department of Pathology and Experimental Cancer Research, Semmelweis University, Budapest). Cells for cytogenetic analysis were stained by the modified Giemsa protocol (mixture of Sorensen buffer (0.133 M KH_2PO_4, 0.133 M $Na_2HPO4.H_2O$,

pH 7.2) and Giemsa dye for 5-10 minutes). For FISH analysis 40,000 cells were washed in PBS then transferred and dried on microscopic slide with cytospin centrifuge. After drying, samples were fixed in methanol-acetic acid. The probe and the cells were co-denatured at 73 °C, then 10 µl probe mixture was added to the slide (2 µl ABCB6 probe, 2 µl Chromosome II probe, 6 µl hybridization buffer) and hybridized at 37 °C for 16 hours. 10 µl DAPI was applied and the samples were visualized under fluorescent microscope. 200 cells in interphase per sample were analyzed for the FISH pattern. Nikon Eclipse E600 epi-fluorescent microscope (with DAPI, spectral-green and spectral-orange filter kits) and Lucia Cytogenetics (Laboratory Imaging) image analysis software were used.

CRISPR/Cas9 system — Clustered regularly interspaced short palindromic repeats (CRISPR)/Cas technology was used to modify the endogenous *ABCB6* gene in human MNT-1 cell line. Breaks in the targeted genomic position caused by SpCas9 involving one or both strands are effectively repaired by the cell using one of the two main repair pathways. The homology-directed repair (HDR) or the more error prone non-homologous end-joining (NHEJ). In the first cell lines we used HDR to modify ABCB6 alleles (ABCB6-GFP, ABCB6-SBP-GFP), while we used NHEJ to generate ABCB-KO cells.

Establishing the ABCB6-GFP, ABCB6-SBP-GFP, ABCB6-KO cell lines — To create ABCB6-GFP and ABCB6-SBP-GFP cells, $3x10^5$ MNT-1 cells were transfected using 6 µl Lipofectamine 2000/well (Thermo Fisher Scientific) in 6 well plates. Three types of plasmids were co-transfected: donor plasmid (pCDNA), SpCas9 expression plasmid (pX330) and gRNA (pColEI_U6) expression plasmid (Table 2, Table S2). In case of the negative controls, the pEGFP-N1 plasmid was used instead of the donor plasmid. Because of the moderate efficiency of the transfection in MNT-1 cells, to create ABCB6-KO cells, we used UO24 program of Nucleofector II (Amaxa-Lonza, Basel, Switzerland). $2x10^6$ cells were electroporated based on the protocol of Vriend and colleagues[140]. Transfected or electroporated cells were analyzed 8-days post-transfection (no background signal from plasmid was detected anymore) and cells were sorted by FACS Aria III Cell sorter (BD Biosciences) FACS and cloned on 96 well plates by serial dilution[141] or 0.5 cell/well dilution. To make the detection of single cells in the wells easier, Calcein AM assay was performed. Calcein AM is a cell-permeant dye that can be used to determine cell viability in most eukaryotic cells. In live cells the nonfluorescent Calcein AM is converted to a

green-fluorescent calcein after acetoxymethyl ester hydrolysis by intracellular esterase. Cells were incubated in medium containing 0.25 μM Ca-AM for 30 min at 37 °C with 5% CO_2. After incubation the 96 well plates were imaged by High-content analysis system (IXM XLS Fluid, Molecular Devices).

Table 2. ABCB6 constructs using CRISPR/Cas9

	ABCB6-GFP	**ABCB6-SBP-GFP**	**ABCB6-KO**
target site	At STOP codon: Target 1: CAGACCATGGAACGGTGACA Target 2: TGGAACGGTGACAAAAGTTT	At STOP codon: Target 1: CAGACCATGGAACGGTGACA Target 2: TGGAACGGTGACAAAAGTTT	In the first exon: target 1: GCTCGTGCCCTCGACGCGGA target 2: GGCGTTTGCAGCTGAGAACT
plasmids	• *pCDNA3*: GFP between homologous arms (933 ng) • *pX330*: WT SpCas9 coding plasmid (233 ng) • *pColEI_U6*: ABCB6 gRNA coding plasmids (167ng) molar ratio: 4;1;1	• *pCDNA3*: SBP–GFP between homologous arms (933 ng) • *pX330*: WT SpCas9 coding plasmid (233 ng) • *pColEI_U6*: ABCB6 gRNA coding plasmids (167 ng) molar ratio: 4;1;1	• *pCMV_BFP_U6*: ultimate target + BFP coding plasmid (1,9 μg) • *pX330:* WT SpCas9 + ABCB6 gRNA coding plasmids (1,9 μg) • *pColEI_U6:* ultimate spacer gRNA (1,2 μg) • molar ratio: 1;1.8;1.8
validation	FACS Sanger sequencing Immunoblot Confocal microscope	FACS Sanger sequencing Immunoblot Confocal microscope RT-PCR	FACS Sanger sequencing Immunoblot Confocal microscope

Single cell clones were grown in the mix of conditioned and fresh MNT-1 medium (1:1 ratio) for 7 days at 37 °C with 5% CO_2. Then the plates were imaged again after incubation with Calcein AM and clones originated from one single cell were selected. After several weeks clones were tested and selected by combination of the following methods: Sanger sequencing, Real Time-PCR, immunoblot, FACS and confocal microscopy. PCR reactions and sequencing were applied with the appropriate primer pairs (Table S1) to detect integration or indel (insertion/deletion) events at the adjacent location of the double strand break caused by SpCas9. In addition, we tested clones for integrated SpCas9 coding sequence in their genome by PCR and excluded those where integration occurred.

Retention Using Selective Hooks (RUSH) — To follow and understand the pathway of the protein in the cell, we tried to take advantages of a recently discovered method, the RUSH system. RUSH is a two-state assay based on the reversible interaction of a hook protein in a donor compartment and the protein of interest. Streptavidin binding peptide (SBP) sequence was cloned into earlier used pCDNA3 plasmid, upstream to GFP sequence. Cells were transfected according to Table 3. Thus, we create SBP-GFP tagged ABCB6 alleles. The other component of RUSH system, the hook in the ER will be a transiently expressed in future work. CD74 (HLA class II histocompatibility antigen gamma chain) protein fused to streptavidin (Sa) which contains an ER retention signal sequence will function as a transmembrane protein which will anchor the SBP-GFP tagged ABCB6. Biotin added to the media will bind to Sa, releasing ABCB6.

Genomic DNA (gDNA) extraction — Genomic DNAs were purified from genetically modified clones. $1x10^6$ cells were harvested, washed in PBS and centrifuged at 1000 g for 10 minutes. Genomic DNA was purified according to Puregene DNA Purification protocol (Gentra systems) and concentration was measured by NanoDrop OneC Microvolume UV-Vis Spectrophotometer.

RT-PCR — To determine the integrated EGFP copy number and thus the copy number of tagged ABCB6, we used a TaqMan assay. TaqMan Gene Expression Master Mix was applied (Thermo-Fischer Scientific 4369016) and K. Hupcsik helped us (HAS RCNS, EI). TaqMan Gene Expression Master Mix is an optimized 2x mix that contains all of the components, excluding the template and primers, for sensitive detection down to one copy of target. qPCRs were measured in triplicate and run on a StepOne Plus real-time device (Thermo-Fischer Scientific). We used standard temperature profile (95 °C 10 min, 40 cycles 95 °C 15 sec and 60 °C 1 min). The following primers and probes were used: Ribonuclease P RNA Component H1 (RPPH1, endogenous control) for 5’ – AGCTGAGTGCGTCCTGTCACT, rev 5’ – TCTGGCCCTAGTCTCAGACCTT, probe 5’ – CACTCCCATGTCCCTT; GFP for 5’- GAGCGCACCATCTTCTTCAAG, rev 5’ – TGTCGCCCTCGAACTTCAC, probe 5’ – ACGACGGCAACTACA. In 20 µl final volume 100 ng gDNA, 900 nM primer and 250 nM probe were added to the TaqMan master mix. For reference HEK293 cell clones were used bearing 1, 4 or 7 copies of RPPH1. [142] Data were analyzed by StepOne 2.1 software, after optimization ΔΔCt method was used ($p<0.05$).

DOI:10.14753/SE.2020.2354

4. Results

4.1. The relation of ABCB6 function to the HMT-1 proteins

Intracellular localization of ABCB6 has been a matter of debate, with conflicting reports suggesting mitochondrial or endolysosomal expression. ABCB6 shows significant sequence identity to HMT-1 (heavy metal tolerance factor 1) proteins, whose evolutionarily conserved role is to confer tolerance to heavy metals by the intracellular sequestration of metal complexes. We used the NCBI Blastp algorithm to quantify sequence similarity of ABCB6 and HMT-1 proteins (Table 3). We hypothesized that the cadmium-sensitive phenotype of HMT-1-defective *S. pombe* and *C. elegans* strains can be rescued by human ABCB6 protein.

Table 3. Clustal2.1 Percent Identity Matrix Sequence similarity was quantified using the NCBI Blastp algorithm (https://blast.ncbi.nlm.nih.gov/BlastAlign.cgi).

	SpHMT-1	**CeHMT-1**	**DmHMT-1**	**HsABCB6**
SpHMT-1	*100.00*	35.68	40.42	39.20
CeHMT-1	35.68	*100.00*	45.69	46.19
DmHMT-1	40.42	45.69	*100.00*	50.43
HsABCB6	39.20	46.19	50.43	*100.00*

4.1.1. Heterologous expression of SpHMT-1 and ABCB6 transporter in S. pombe model organism

S. pombe is a classic laboratory organism, and evolutionarily closer to animal cells than budding yeast (*S. cerevisiae*), thus it serves as an important model for elucidating conserved pathways and processes relevant to human diseases.

After verifying that the *hmt-1* deleted cells are significantly more sensitive to Cd than the wild type (WT) cells, we engineered plasmids enabling the heterologous expression of SpHMT-1 and ABCB6. The cDNA encoding *hmt-1* and C-terminal HA-tag was ordered from GenScript. HA-tag was necessary because an HMT-1 specific monoclonal antibody was not available in our lab. The cDNAs of SpHMT-1 and human ABCB6[129] were cloned into the pREP1 yeast expression vector yielding pREP1-HMT-1-

HA and pREP1-ABCB6. Plasmid was transformed into *hmt-1* deleted (*hmt-1*Δ) yeast cells. As a control, both strains (WT and *hmt-1*Δ) were transformed with empty pREP1 vector. Exogenously expressed HMT-1 was detected with an HA-specific antibody on immunoblot (Fig. 8A first lane). Human ABCB6 was detected by ABCB6-567 antibody was produced against an extracellular epitope of the protein[139]. Heterologous expression of a human glycosylated membrane transporter in an evolutionally lower, unicellular organism is not straightforward. But ABCB6 and ABCB6-KM was produced in relatively high amounts in yeast cells (Fig. 8A). The ABCB6 specific antibody also recognized SpHMT-1 protein (Fig. 8B). The cross reaction can be explained by the sequential similarity between the two proteins.

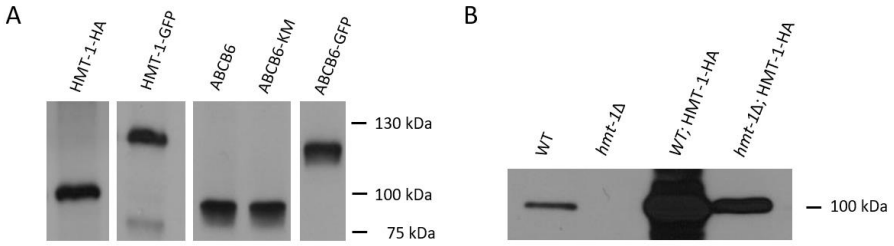

Figure 8. Immunoblot analysis of yeast cells. A *Hmt-1*-deleted cell expressing HMT-1-HA, HMT-1-GFP, ABCB6, ABCB6-KM or ABCB6-GFP. Expression of HMT-1 was revealed by using anti-HA antibody; ABCB6 was labeled by the ABCB6-567 antibody; EGFP tagged proteins were labeled by an anti-EGFP antibody. 50 µg total cell lysates were analyzed[132]. **B** ABCB6-567 antibody recognizes HMT-1 protein. No signal was detected in *hmt-1*Δ vector control cells, but specific bands were developed in WT vector control cells and HMT-1-HA expressing WT and *hmt-1*Δ cells. 50 µg total cell lysates were analyzed.

4.1.2. Heterologously expressed human ABCB6 localizes to the vacuolar membrane of S. pombe

HMT-1 is localized in the vacuolar membrane of the yeast cell. Addressing this purpose, GFP-tagged *hmt-1* and *ABCB6* DNA constructs were engineered and expressed in *S. pombe* (Fig 8A). After successful expression of the fusion proteins HMT-1-GFP and ABCB6-GFP, cells were stained with FM 4-64 which selectively stains the vacuolar membrane. A similar intracellular pattern was observed in both cases in confocal microscopic images, which indicated that the human ABCB6 protein was targeted to the yeast vacuoles (Fig. 9).

DOI:10.14753/SE.2020.2354

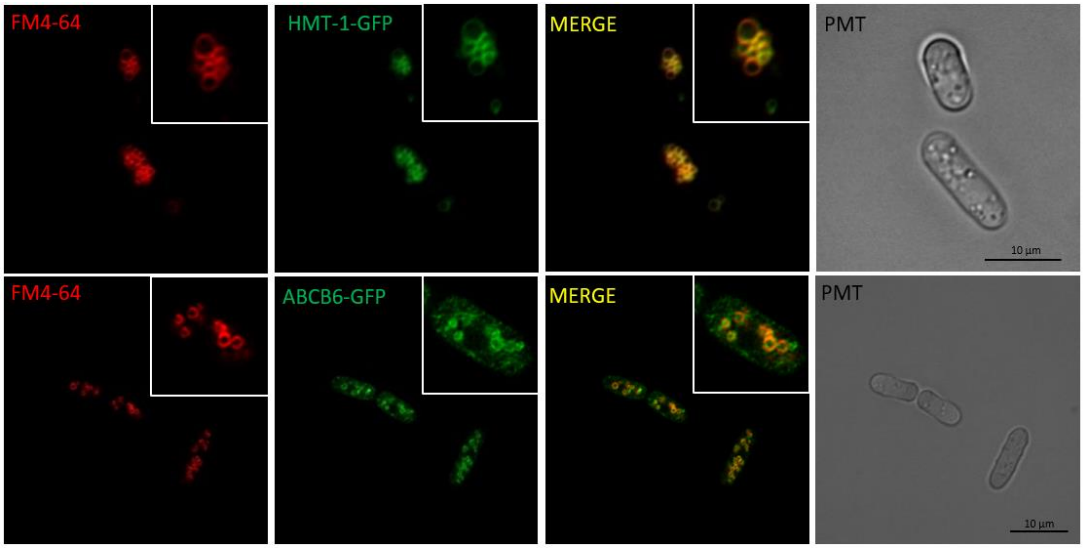

Figure 9. ABCB6-GFP localizes to vacuoles of *S. pombe*. *Hmt-1*-deleted *S. pombe* was transformed with pREP1-HMT-1-GFP or ABCB6-GFP (green); vacuoles were stained with FM 4-64 (red). Insets show individual cells. Scale bar 10 µm[132].

4.1.3. Heterologous expression of human ABCB6 restores cadmium tolerance of S. pombe *hmt-1Δ mutants*

Cd-sensitivity of the cells was examined by cytotoxicity assays in liquid culture and on solid medium. Cd-tolerance of *hmt-1*-deleted strains was increased when HMT-1-HA was expressed, suggesting that the protein could protect the *hmt-1*-deleted yeast strains from cadmium toxicity, i.e. the detoxifying function of the protein was not affected by the HA-tag. (Fig. 10A,B). To test whether ABCB6 can fulfil a detoxification function similar to HMT-1, we expressed the wild-type human ABCB6 protein and its catalytically inactive mutant variant (ABCB6-KM) in *hmt-1*-deleted strain. It was detected that expression of wild-type ABCB6 also restored cadmium tolerance, allowing transformed *S. pombe* colonies to grow in the presence of Cd (Fig. 10A). However, in the case of the inactive, Walker A mutant variant of ABCB6, the rescue effect could not be observed, suggesting that functional ABCB6 is needed to restore the tolerance. The cytotoxicity results in liquid culture supported this observation (Fig. 10B).

DOI:10.14753/SE.2020.2354

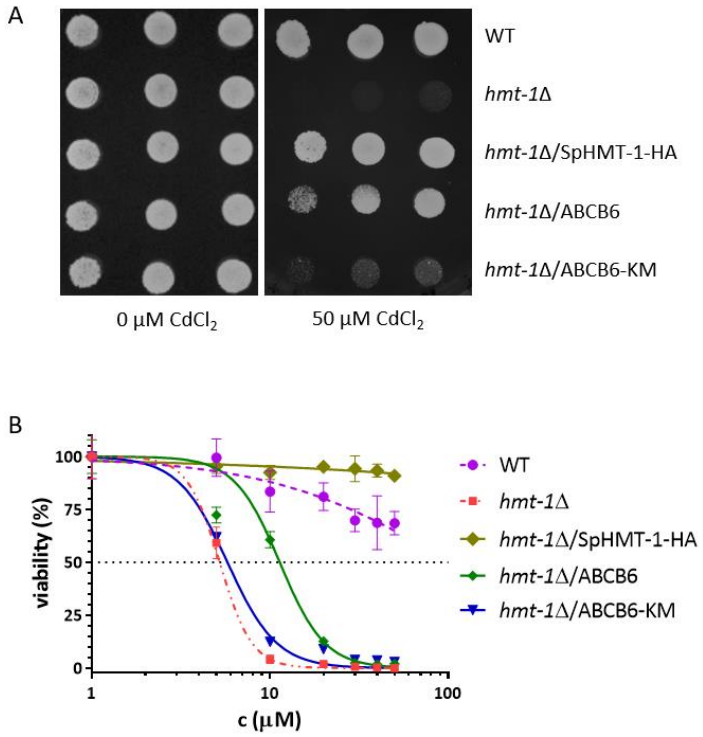

Figure 10. ABCB6 confers cadmium tolerance in *hmt-1*Δ mutant *S. pombe*. **A** Wild-type *S. pombe* cells transformed with empty pREP1 vector (WT); *hmt-1*Δ mutant cells transformed with empty pREP1 vector (*hmt-1*Δ), pREP1-HMT-1-HA (*hmt-1*Δ/SpHMT-1-HA), pREP1-ABCB6 (*hmt-1*Δ/ABCB6) or pREP1-ABCB6-KM (*hmt-1*Δ/ABCB6-KM) were grown overnight. Aliquots of the cell suspensions were then serially diluted (A_{600nm} of 0.7) and spotted onto solid EMM supplemented with adenine, uracil and the indicated concentrations of $CdCl_2$. Colonies were visualized after incubating the plates for 8 days at 30 °C. **B** Transformed yeast cells were grown overnight to an A_{600nm} of 0.8-1. 100 µl aliquots were inoculated into 2 mL of the same medium containing $CdCl_2$ at the indicated concentrations. A_{600nm} was measured after growth at 30 °C for 72 h. Values, expressed as viability (%), were normalized to untreated control (n=3)[132].

4.1.4. S. pombe functional assay

This functional assay gave us the opportunity to examine mutant variants of ABCB6. Mutant constructs (Table 4) were cloned into pREP1 plasmid, then expressed in fission yeast cells. Similarly to the wild type and the inactive (K629M) mutant variant of ABCB6, the tested mutants were successfully expressed in fission yeast cells (Fig. 11A). In cytotoxicity experiments cells were spotted on agar plates using OD=0.8 and OD=0.08 dilutions. Only two of the tested mutants failed to revert the Cd-tolerant phenotype. Cells expressing Lan mutants R192W and R276W (Table 4) could not grow on solid media containing 50 µM Cd (Fig. 11B red arrows). In contrast, disease associated mutants S170G (DUH) or A57T (ocular coloboma) and other Lan mutants (R192Q, G588S, R638C and V609M) successfully restored Cd tolerance (Fig. 11B).

Table 4. ABCB6 variants tested in *S. pombe* cytotoxicity experiments

Amino acid change	Nucleotide change	Phenotype	References
A57T	169G>A	Coloboma	[75]
S170G	508A>G	DUH	[30]
R192Q	575G>A	Lan	[29]
R192W	574C>T	Lan	[29,80,82]
R276W	826C>T	Lan	[29,80,82]
G588S	1762G>A	Lan	[29,80,82]
V609M	1825G>A	Lan	[85]
R638C	1912C>T	Lan	[85]

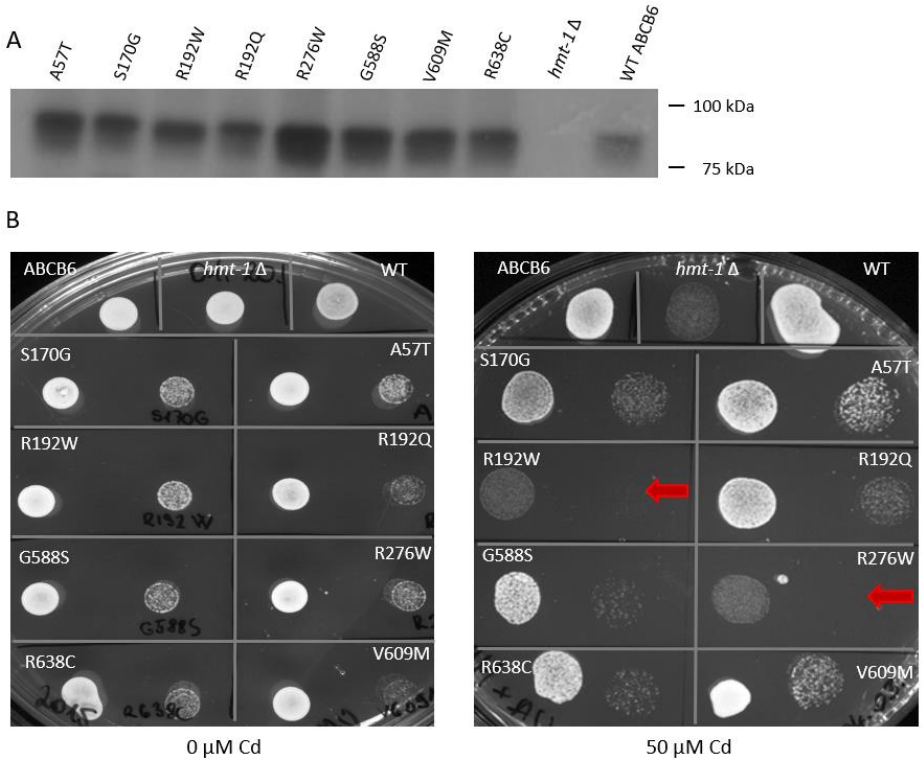

Figure 11. ABCB6 mutant variants were expressed and tested in *S. pombe* Cd-cytotoxicity assay. **A** Immunoblot analysis of mutant ABCB6 variants. *Hmt-1*Δ mutant cells were transformed with empty pREP1 vector (*hmt-1*Δ), or pREP1 vector containing ABCB6 variants. Expressions were revealed by the ABCB6-567 monoclonal antibody. 50 µg total cell lysates were analyzed. **B** Wild-type *S. pombe* cells were transformed with empty pREP1 vector (WT); *hmt-1*Δ mutant cells transformed with empty pREP1 vector (*hmt-1*Δ), or the mutant variant containing pREP1 plasmids. Cells were grown overnight and aliquots of the diluted cell suspensions (A_{600nm} of 0.8: 1x and 10x dilution) were then spotted onto solid EMM supplemented with adenine, uracil and the indicated concentrations of $CdCl_2$. Colonies were visualized after incubating the plates for 8 days at 30 °C (unpublished results).

We tested further metals in our rescue model system based on earlier finding, that CeHMT-1 can provide tolerance to cadmium, arsenic and copper[104]. In addition, experimental results supporting the role of ABCB6 in arsenic resistance were also reported[45,46,143]. Cytotoxicity assays revealed that the expression of ABCB6 in *hmt-1*Δ *S. pombe* cells conferred slight resistance to As(III) but not to As(V), Sb(V), Hg(II) or Zn(II) (Fig. 12). In case of Sb(III) and Cu(II) we could not detect toxic concentrations in EMM medium (data not shown).

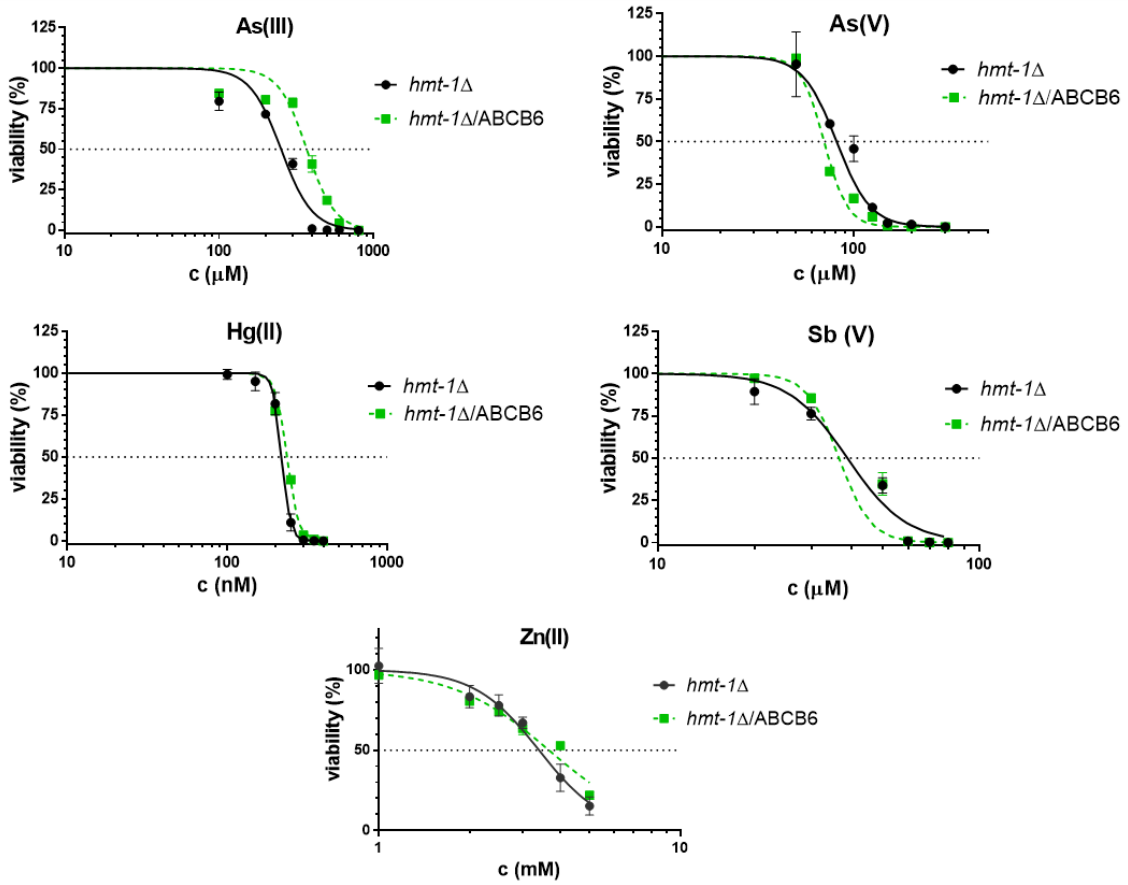

Figure 12. ABCB6 mediates resistance to As(III) in *hmt-1*Δ mutant *S. pombe*. Yeast cells were grown overnight to an A_{600nm} of 0.8-1. 100 µL aliquots were inoculated into 2 mL of the same medium containing the indicated concentrations of metal complexes. Absorbance was measured after growth at 30 °C for 48 h. Values, expressed as viability (%), were normalized to untreated control (n=2)[132].

4.1.5. Determination of vacuolar cadmium contents

Intracellular concentrations of cadmium are decreased by SpHMT-1, which transports Cd-PC complexes into the vacuole (sequestration)[102]. After these promising

results, we wanted to find further direct evidence proving the orthologous function. Intact vacuoles were isolated from Cd treated yeast cells and their Cd content was measured by graphite furnace atomic absorption spectrometry (GFAAS), performed by L. Bencs and N. Szoboszlai. Before the Cd measurement, integrity of the purified vacuoles was confirmed by the following method. First, isolated organelles were stained with Acridine-Orange (AO) labeling the acidic compartments, then vacuoles were lysed with the detergent TritonX. Detergent treatment destroyed the lipid bilayer of vacuoles, acidic pH was no longer sustainable thus the signal of AO decreased. The change of fluorescent signals was measured by Attune NxT flow cytometer, performed by Nóra Kucsma (Fig. 13).

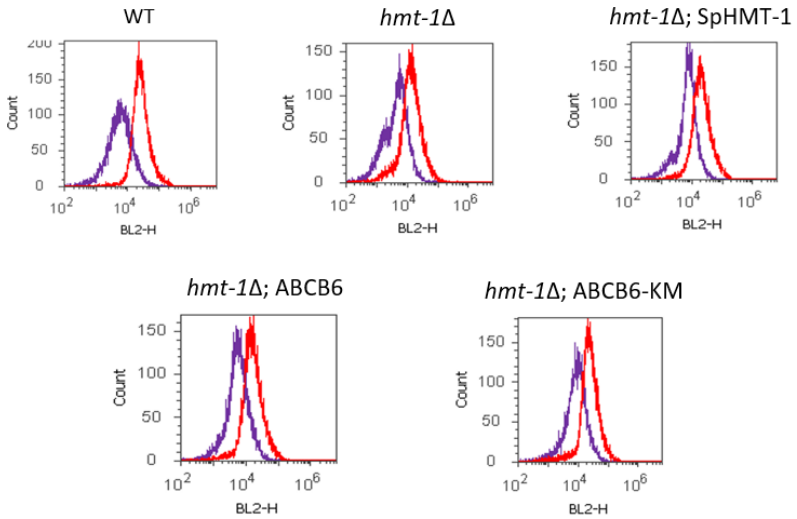

Figure 13. Assessment of vacuolar integrity. After incubation with 30 μM Acridine-Orange (AO) for 10 min integrity of the vacuoles was assessed by measuring fluorescence signal (red histograms). In control experiments (purple histograms), vacuoles were treated with 0,1% TritonX for 10 min after AO staining. Fluorescence was measured using an Attune Acoustic Focusing cytometer[132].

Compared to the wild-type, isolated vacuoles from *hmt-1*-deleted strains contained significantly less cadmium, in line with the absence of vacuolar sequestration. But vacuolar Cd content was restored when cells expressed SpHMT-1 or ABCB6 (Fig. 14). As it appeared in cytotoxicity assays, increased vacuolar accumulation of cadmium was dependent on the functionality of ABCB6, indicating that the rescue of *hmt-1*-deleted strains was due the ABCB6-mediated vacuolar sequestration of cadmium.

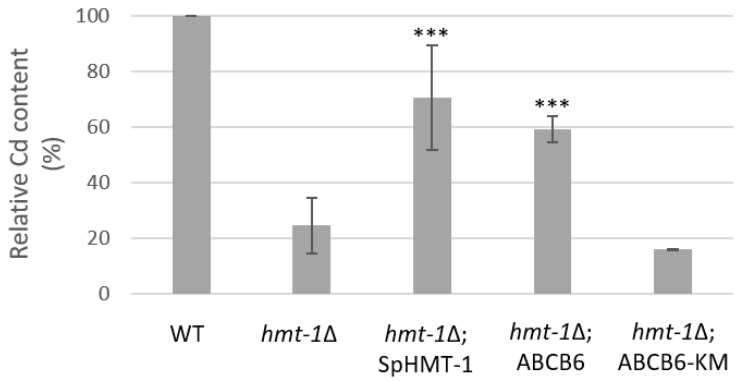

Figure 14. ABCB6 restores vacuolar Cd levels in *hmt-1*Δ mutant *S. pombe.* Yeast cells lacking SpHMT-1 (*hmt-1*Δ) were engineered to express ABCB6, ABCB6-KM or SpHMT-1. Transformed cells were cultured for 18 h in growth medium supplemented with 20 μM $CdCl_2$. Intact vacuoles were isolated by differential centrifugation; the Cd content of the isolated vacuoles was quantified by AAS (atomic absorption spectrophotometer). Data show average Cd levels relative to control calculated from independent experiments (n=3). All Cd concentration data were normalized to the protein content of the samples[132].

4.1.6. Human ABCB6 rescues the Cd Hypersensitivity of hmt-1-deleted C. elegans

Our next goal was to investigate the function of the heterologously expressed human ABCB6 protein in a multicellular organism. HMT-1 proteins of *S. pombe* and *C. elegans* have been shown to share an orthologous function[101]. We hypothesized that ABCB6 can also rescue the Cd-sensitive phenotype of HMT-1-deficient *C. elegans* worms like in the case of *S. pombe*. Experiments were implemented by J. Barna from research group of T. Vellai (Department of Genetics, Eötvös Loránd University). In adult worms, CeHMT-1 is expressed in coelomocytes, intestinal cells and in head and tail neurons. An adult nematode has six coelomocytes which have been suggested to serve an immune, scavenging and hepatic functions because of their ability to continuously endocytose and accumulate a variety of macromolecules from the body cavity fluid[105,144].

To express the human ABCB6 transporter in nematode, codon optimized ABCB6 cDNA was synthetized by GenScript and cloned into pPD95.75-GFP *C. elegans* expression plasmid. As a regulatory element for transcription, promoter of *hmt-1* gene of the nematode was used. After transformation, animals bearing the selection marker were chosen. Transgenic animals could be easily identified on immobile *Unc* phenotype background, because the wild allele of the co-transformed *unc-119* gene rescues motionless unc-119(ed3) mutant adult hermaphrodites. The transgenic strain expressing

HMT-1-GFP (VF31) was provided by the Vatamaniuk lab (Cornell University). Adult hermaphrodites were allowed to lay eggs onto NGM plates supplemented with the indicated concentrations of $CdCl_2$, and the progeny reaching adulthood was counted 3 days after hatching at 20 °C. As expected, wild type animals tolerated 10 µM $CdCl_2$, while the *hmt-1* (*gk161*) deletion mutant were sensitive to Cd, as no adult animal was observed after 4 days on Cd-containing plates. Expression of ABCB6 in the wild type background did not change Cd tolerance of the animals (not shown). This meant that integration of the transgene into the genome did not alter the heavy metal tolerance of the animals, and they developed normally on plates containing cadmium. In addition, integration of the transgene had no effect on the developmental rate of the worms. As described earlier[105], expression of CeHMT-1 rescued the Cd-sensitive phenotype of *hmt-1(-)* strain. Significantly, ABCB6 could also increase Cd tolerance of *hmt-1*-deleted strain (Fig. 15A,B)

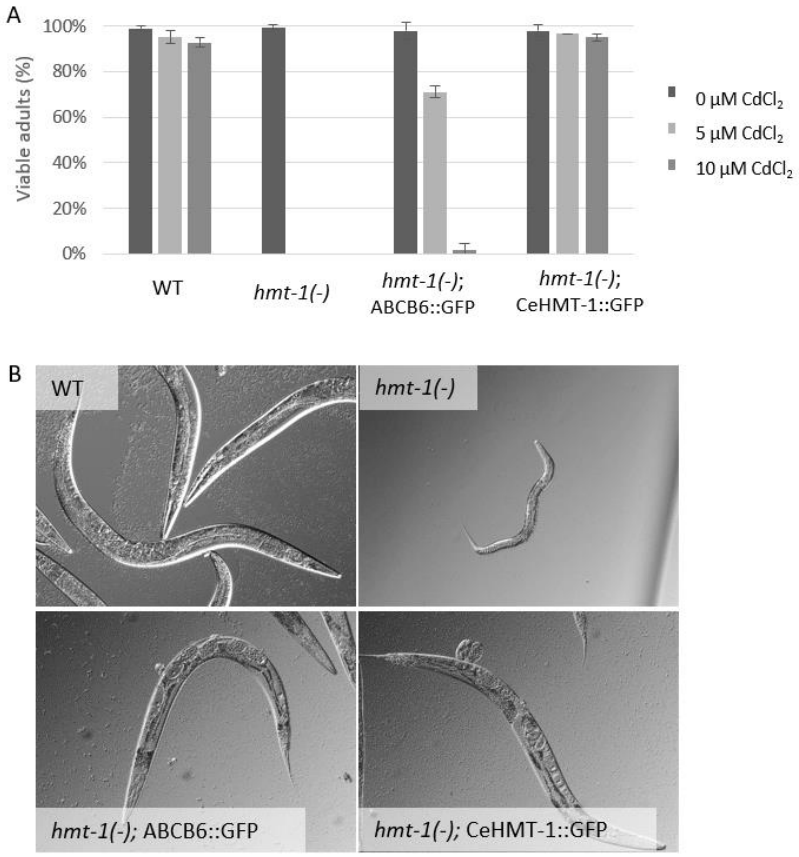

Figure 15. ABCB6 rescues the Cd-sensitive phenotype of HMT-1-deficient nematodes. A Wild-type (WT), *hmt-1*-deleted [*hmt-1(-)*], *hmt-1*-deleted expressing CeHMT-1::GFP [*hmt-1(-); hmt-1::gfp*] or ABCB6::GFP [*hmt-1(-); ABCB6::gfp*] adult hermaphrodites were placed

individually onto NGM plates supplemented with the indicated concentrations of Cd, and were allowed to lay eggs for 2 hours. Shown are the percentages of the progeny reaching adulthood 3 days after hatching (mean of 3 independent trials). ***: Student's T test, $p < 0{,}001$; bars represent ±SD). **B** Representative pictures of animals grown on plates containing 10 µM $CdCl_2$, 3 days after hatching at 20 °C. Heterologous expression of the human ABCB6 protein provided partial rescue, allowing the development of small sized adults, whereas *hmt-1*-deleted animals were arrested at the L2 – L3 larval stages[132].

We had to make sure that the rescue was not caused by the transgene integration into the genome, influenced the function of a gene that had any effect on animal's heavy metal tolerance. Therefore, J. Barna and D. Kovács performed an experiment on animals carrying *ABCB6::gfp* transgene on an extrachromosomal array. In the *hmt-1(-)* mutant, the extrachromosomal ABCB6 transgene also partially rescued the phenotype. While at 5 µM and 10 µM Cd exposure none of *hmt-1(-)* animals reached adulthood, the deletion mutant expressing ABCB6 was also partially rescued (Fig. 16). Compared to the integrated ABCB6, weaker effect can be explained by the mosaicism of the worms: not all of the cells contained ABCB6 transgene.

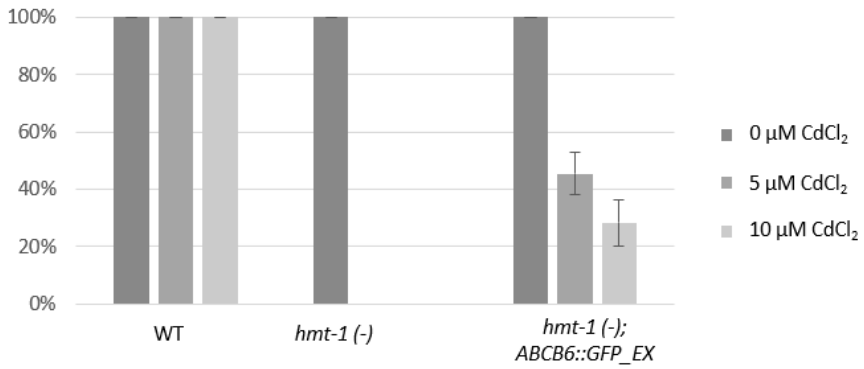

Figure 16. Animals carrying ABCB6::gfp transgene on an extrachromosomal array. Wild-type (WT), *hmt-1*-deleted [*hmt-1(-)*], *hmt-1*-deleted expressing ABCB6::GFP [*hmt-1(-); ABCB6::gfp_ex*] adult hermaphrodites were placed individually onto NGM plates supplemented with the indicated concentrations of Cd, and were allowed to lay eggs for 2 hours. Shown are the percentages of the progeny reaching adulthood 3 days after hatching (mean of 3 independent trials). ***: Student's T test, $p < 0{,}001$; bars represent ±SD) (unpublished data).

4.1.7. Heterologously expressed human ABCB6 localizes to endolysosomes of C. elegans.

After functional rescue was verified, localization of the transporters was also checked. ABCB6-mCherry fusion protein was constructed and expressed in a transgenic

strain. Crossing the strains expressing CeHMT-1-GFP and ABCB6-mCherry allowed the simultaneous evaluation of the distribution of both transporters in *C. elegans*. Images obtained by confocal microscopy indicated that ABCB6 is expressed in the same tissues as CeHMT-1 (Fig. 17).

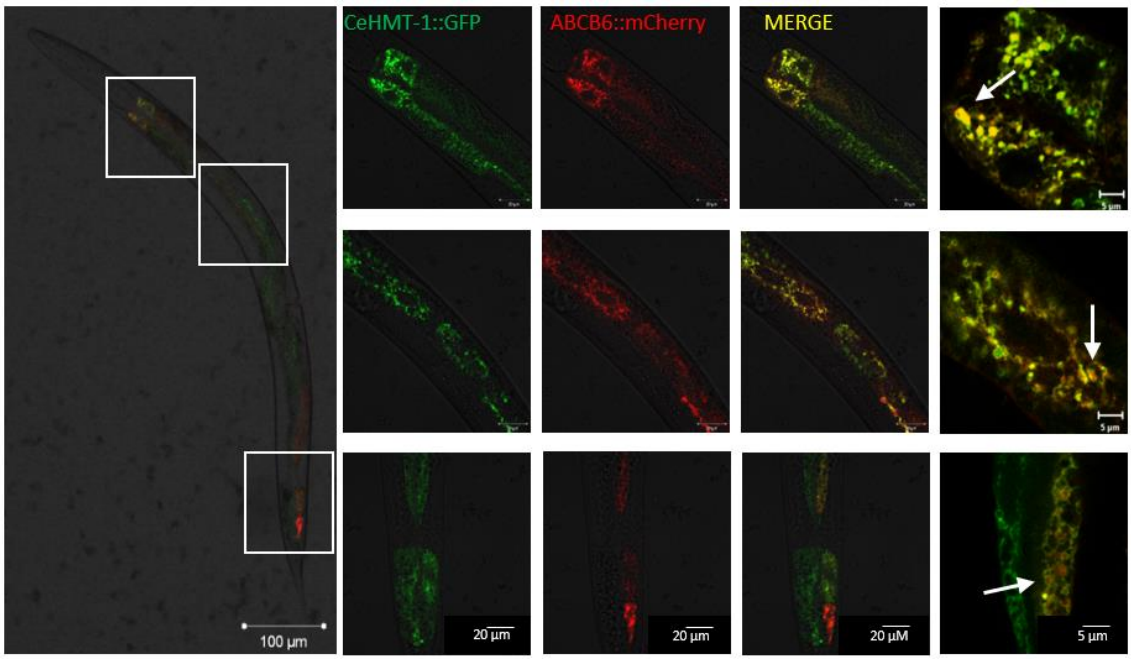

Figure 17. Confocal microscopy images of an adult nematode co-expressing ABCB6::mCherry and CeHMT-1::GFP. Crossing of strains expressing CeHMT-1:GFP and ABCB6::mCherry proved that the two transporters are expressed in identical subcellular compartments (scale bar: 100 µm). Boxed areas are shown at a higher magnification (scale bar 20 and 5 µm). Note that the ABCB6::mCherry strain carries the transgene extrachromosomally, resulting in a mosaic expression of ABCB6[132].

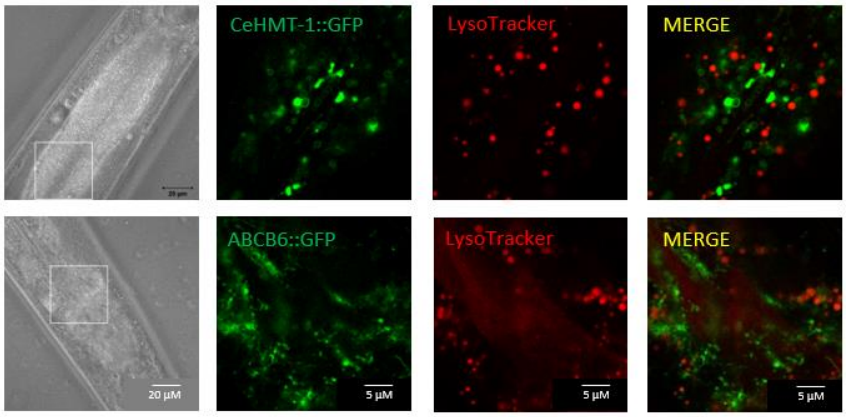

Figure 18. ABCB6 and CeHMT-1 does not colocalize with lysosomal marker in *C. elegans*. Lysosomal staining of animals expressing CeHMT-1::GFP or ABCB6::GFP was performed as

described[146]. The panels show the DIC images (left) the GFP (green) and the Lysotracker (red) signals and the overlay of the two (right). Scale bar: 20 μm[132].

Next, we investigated the subcellular localization of CeHMT-1 and ABCB6. Intracellular organelles corresponding to the sites of CeHMT-1-GFP or ABCB6-GFP expression proved to be distinct from Lysotracker Red-positive lysosomes[145] (Fig. 18). This was unexpected, because based on our previous results[67], we assumed that ABCB6 would colocalize with the lysosomal marker.

Further localization studies were done by applying transgenic strains that express fluorescently labeled endosomal proteins. Nematodes expressing fluorescent RAB proteins were provided by Dr. Xiaochen Wang. Phmt-1*::hmt-1::gfp* and phmt-1::*ABCB6::gfp* worms were crossed with *pges-1::mCherry::RAB-5, pges-1::mCherry::RAB-7, pges-1::mCherry::RAB-10* strains[147], which express the fluorescent mCherry protein in different endocytic compartments. Analysis of the transgenic strains showed that CeHMT-1 and ABCB6 partially colocalize with markers of the early, late and basolateral recycling endosomes (mCherry::RAB-5, mCherry::RAB-7 and mCherry::RAB-10, respectively) (Fig. 19A,B,C).

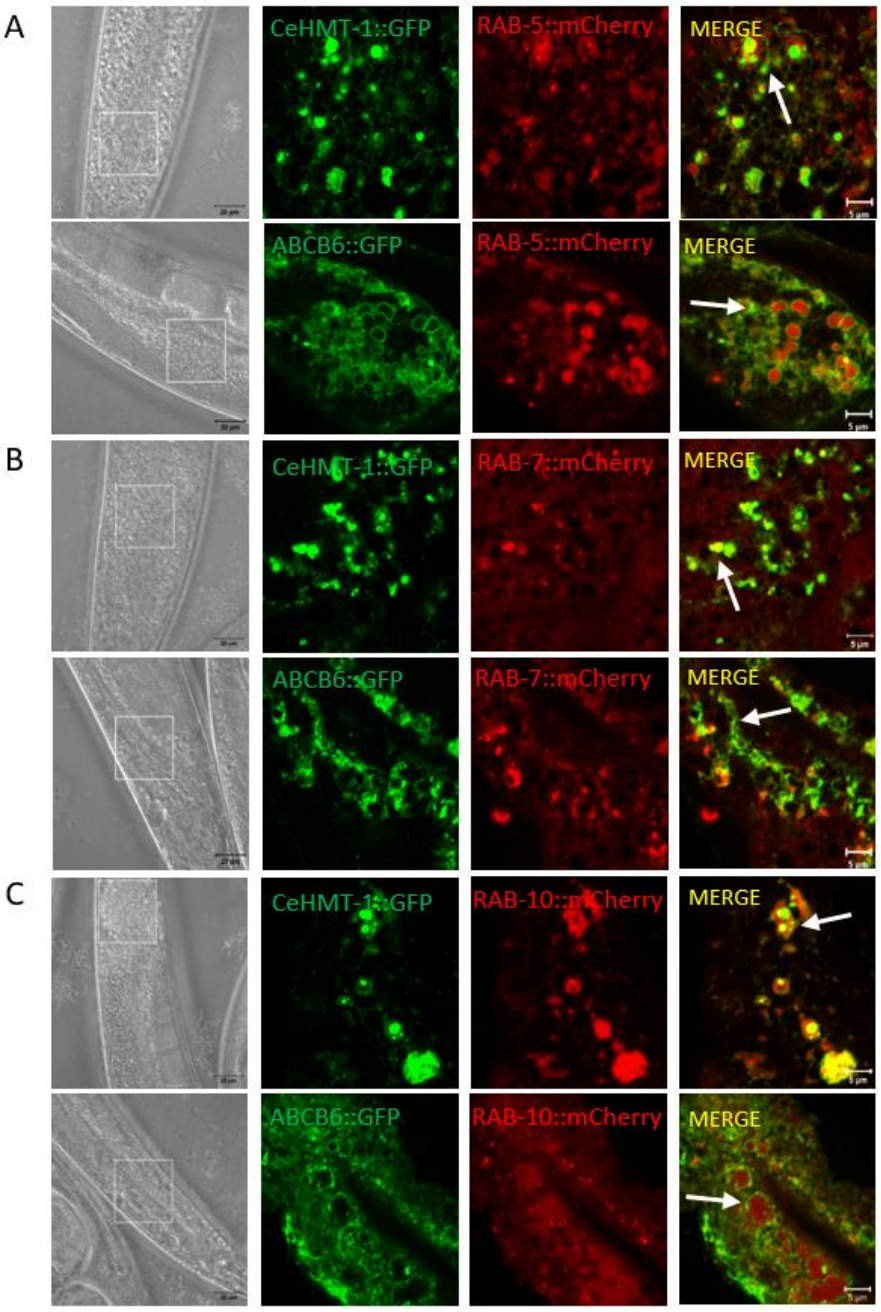

Figure 19. CeHMT-1 and ABCB6 show identical endosomal localization in nematodes. CeHMT-1 and ABCB6 partially colocalize with markers of the early, late and basolateral recycling endosomes. Subcellular localization of ABCB6 and CeHMT-1 was determined by confocal microscopy. Strains expressing CeHMT-1::GFP or ABCB6::GFP were crossed with worms expressing RAB-5::mCherry (early endosomal marker, **A**) or RAB-7::mCherry (late and early endosomal marker, **B**), or RAB-10::mCherry (basolateral recycling endosomes marker, **C)**. The panels show the DIC images (left) the GFP (green) and the mCherry (red) signals and the overlay of the two (right). Scale bar: 20 and 5µm[132].

DOI:10.14753/SE.2020.2354

4.1.8. Human ABCB6 confers Cd tolerance to SNB-19 glioblastoma cells

After exploring the function of ABCB6 in heterologous model systems, we wanted to investigate the relevance of ABCB6 in heavy metal detoxification in a human cell line as well. To generate ABCB6 overexpressed or silenced cell lines for human metal toxicity studies lentiviral expression system was used (N. Kucsma). Immunoblot analysis of the overexpressing cells showed 30-40-fold increase in ABCB6 protein level and in the case of RNA silenced cells amount of protein was one eighth (Fig. 20A).

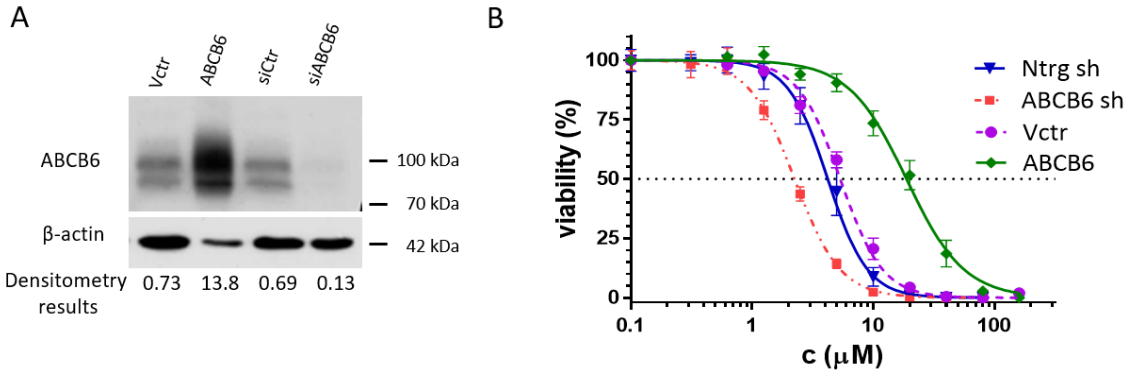

Figure 20. Overexpression or attenuation of ABCB6 modulates Cd sensitivity in SNB-19 cells. A Expression of ABCB6 from total cell lysates was monitored by immunoblot, using the anti-ABCB6 antibody ABCB6-567[139]. Whole cell lysates of SNB-19 cells (80 μg protein, lane 1), cells overexpressing ABCB6 (8 μg protein, lane 2), and cells transfected with a control (80 μg protein, lane 3) or an anti-ABCB6 shRNA vector (80 μg protein, lane 4). β-actin is shown for loading control[132]. **B** ABCB6 confers cadmium resistance in SNB-19 glioblastoma cells. SNB-19 cells were engineered to silence ABCB6 expression by ABCB6 shRNA (ABCB6 sh) or overexpress ABCB6 (ABCB6). As compared to cells expressing a non-target control shRNA (Ntrg sh) or a control (empty) vector (Vctr), overexpression of ABCB6 confers cadmium resistance, whereas attenuation of ABCB6 levels increases cadmium sensitivity. IC_{50} values represent means of triplicate measurements (see inset)[132].

Next, we investigated Cd-toxicity in these characterized constructions. Fit curve from cytotoxicity results demonstrated that overexpression of ABCB6 effectively increased Cd tolerance of SNB-19 cells, while attenuation of ABCB6 expression sensitized SNB-19 cells to Cd (Fig. 20B). We observed significant difference between IC_{50} values of ABCB6 attenuated and overexpressed cell lines. In the case of HeLa cells neither overexpression of ABCB6 nor attenuation of ABCB6 altered the Cd sensitivity (not shown).

4.1.9. Human ABCB6 localizes to lysosomes of SNB-19 glioblastoma cells

ABCB6 localization was examined in immunocytochemical experiments by using "Lan" OSK43 antibody recognizing an extracellular epitope of the transporter[28]. Analysis of SNB-19 cells by confocal microscopy confirmed the localization of the endogenous ABCB6 protein in the lysosomal compartment (labeled by LAMP1), and its absence in mitochondria (labeled by AIF). Overexpression of ABCB6 also resulted in endolysosomal expression that was clearly distinct from the mitochondrial pattern (Fig. 21).

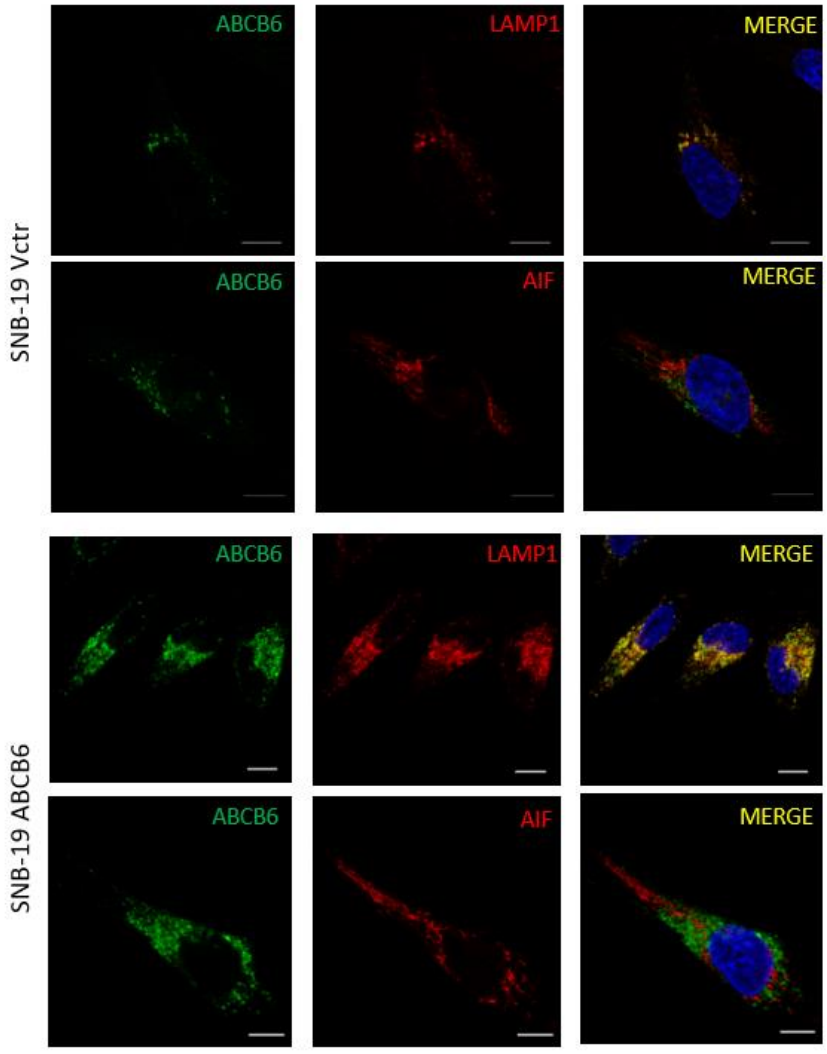

Figure 21. ABCB6 is localized in the endolysosomal compartment of SNB-19 cells. Subcellular localization of endogenous and overexpressed ABCB6 was revealed by immunofluorescence labelling and detected laser-scanning confocal microscopy. Endogenous (upper panels) and overexpressed (lower panels) ABCB6 was visualized by using the OSK43 ABCB6 antibody (green); nuclei were labelled with Hoechst 33342 (blue); organelles were labelled with specific markers (red): mitochondria (AIF), lysosomes (LAMP1). Scale bar: 10µm[132].

4.2. ABCB6 and melanogenesis

Several ABCB6 mutations are linked to the autosomal dominant pigmentary disorder DUH[30]. Initially, three mutations in the ABCB6 gene were described in DUH patients (L356P, S170G, G579E)[30]. Further variants of ABCB6 involved in DUH were identified: A453V, S322K[87], S322R, Y424H[88] and Q555K and deletion in exon 1, 776 delC[83,91]. At present, the mechanism how ABCB6 affects skin pigmentation is not known. Therefore in an attempt to understand the link between ABCB6 mutations and the DUH phenotype, we investigated the subcellular localization and function of ABCB6 in a human melanocytic cell line, MNT-1[148,149]. Most of the experimental work was relied on the expertise of G. van Niel and his colleagues.

4.2.1. ABCB6 localizes to early melanosomes and lysosomes in the human melanocytic cell line MNT-1

To investigate the localization of ABCB6 in MNT-1 cells, specific intracellular markers were used, while ABCB6 was labeled by the OSK43 antibody. Confocal microscopic analysis was made by N. Kucsma and J. M. Reisecker. Images confirmed that signal of mitochondria (AIF), ER (Calnexin) or Golgi (RCAS1) did not overlap with the signal of ABCB6 (Fig. 22A). But lysosomal compartments (LAMP1) and mainly early (stage II) melanosome markers (NKI-beteb and HMB45) showed colocalization with ABCB6. NKI-beteb and HMB45 antibodies recognize insoluble protofibrils and fibrils of PMEL. Earlier or even later forms of melanosomes did not contain appreciable ABCB6 levels. This suggests that ABCB6 is specifically associated with maturing melanosomes containing processed PMEL domain fragments and PMEL fibrils (Fig. 22A,B).

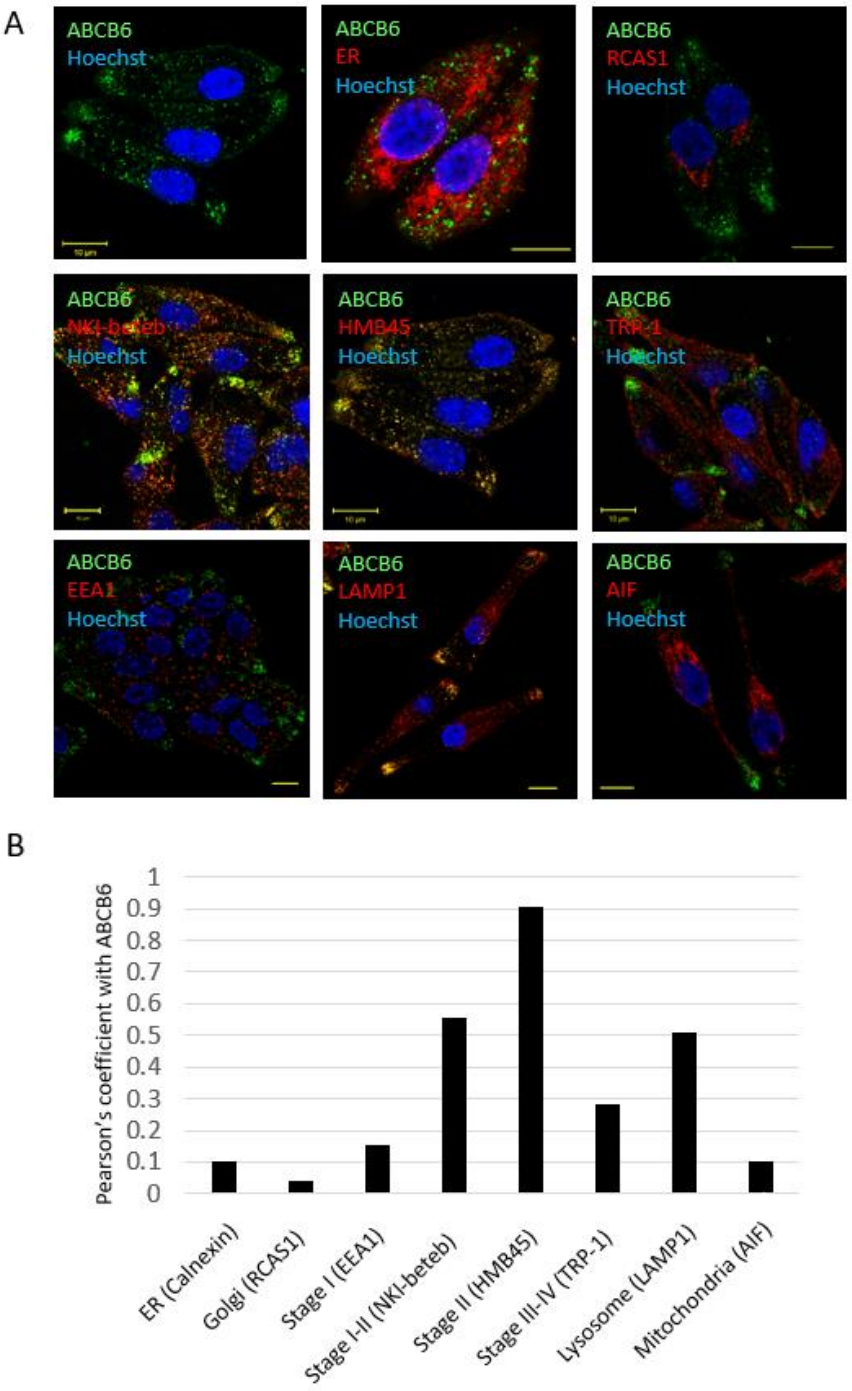

Figure 22. Determination of the subcellular localization of ABCB6 in MNT-1 cells. A Expression of the endogenous ABCB6 protein was visualized by the OSK43 ABCB6 antibody (green); nuclei were labeled with Hoechst 33342 (blue); and organelles were labeled with specific markers (red): ER (Calnexin), Golgi (RCAS1), mitochondria (AIF), early endosomes (EEA1), lysosomes (LAMP1). Non-pigmented melanosomes were labeled using an antibody directed against the luminal domain of PMEL (NKI-beteb) and HMB45; pigmented melanosomes were stained with TRP-1. Immunostaining and laser-scanning confocal microscope was used. The scale bar represents 10 µm. **B** Pearson's correlation coefficients for colocalization of ABCB6 with organelle-specific markers[130].

DOI:10.14753/SE.2020.2354

Intracellular distribution of ABCB6 was examined by using electron microscopy also. Imaging and analysis of EM images were made by P. Bergam in CRNS, Paris. Immunogold labeling of ultrathin cryosections of MNT-1 cells showed another evidence for enrichment of ABCB6 in stage II melanosomes. The transporter localized in tubulo-vesicular structures containing dense material that we identified as lysosomes (Fig. 23). These approaches have led us to conclude that endogenous ABCB6 is localized to lysosomes and early melanosomes. This expression pattern is exactly at the crossroad between the endo-lysosomal and the melanosomal biogenesis pathways where PMEL fibril formation is initiated[150].

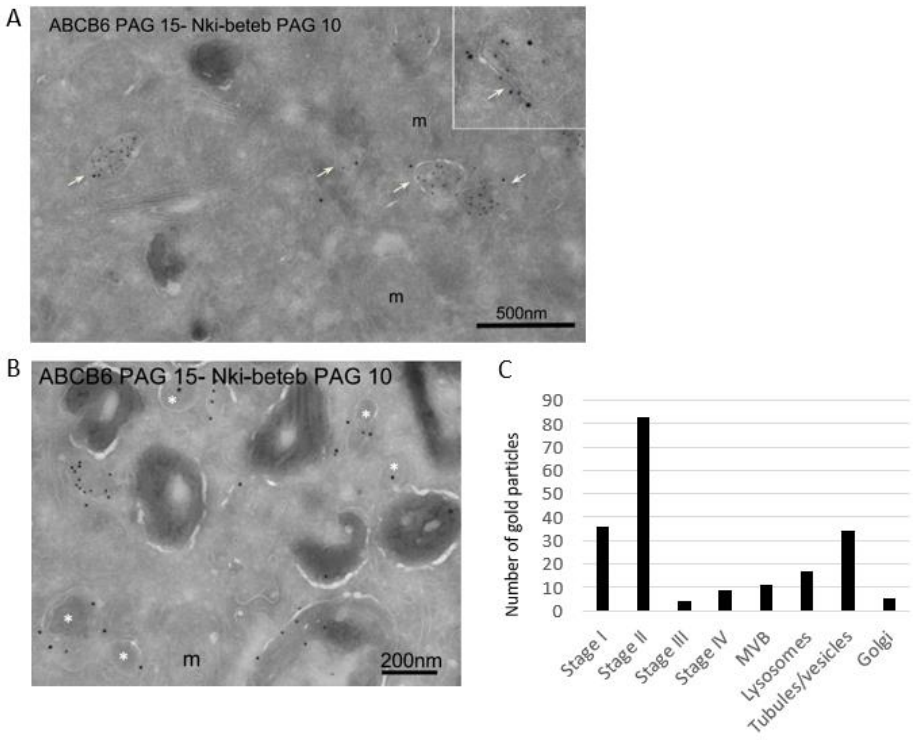

Figure 23. Localization of ABCB6 on ultrathin cryosections of MNT-1 cells. Cells were double immunogold labeled for PMEL luminal domain (NKI-beteb, PAG10 nm) and ABCB6 (PAG15 nm). **A** Arrows indicate colocalization of endogenous ABCB6 and PMEL in non-pigmented melanosomes. The scale bar represents 500 nm. **B** Asterisks show ABCB6 in lysosomal tubulovesicular structures. The scale bar represents 200 nm. Mitochondria are annotated with "m." **C** Quantification of immunogold labeling of endogenous ABCB6 inMNT-1 cells. Gold particles representing labeling for ABCB6 in the EM analysis were counted and assigned to the indicated compartments, which were identified based on morphology (MVB - multi vesicular bodies). The data are presented as the mean percentage of total gold particles in each compartment[130].

DOI:10.14753/SE.2020.2354

4.2.2. Downregulation of ABCB6 by siRNA perturbs early steps of PMEL amyloid formation without eliminating melanogenesis

In the next step we tried to unravel the functional relevance of ABCB6 in melanocytes. We were curious about how the elimination of ABCB6 will affect the pathway of melanogenesis. We didn't expect that the whole machinery will collapse without the transporter, since pigmentation disorders were not manifested even in *ABCB6* KO mice[45,72]. Additionally, Lan (-) patients did not show pathologic pigmentation symptoms[28,80]. First, specific siRNA constructs were tested for attenuation of ABCB6 (Fig. 24A). Melanin contents were measured in ABCB6 attenuated cells, but significant alteration was not detected (Fig. 24B).

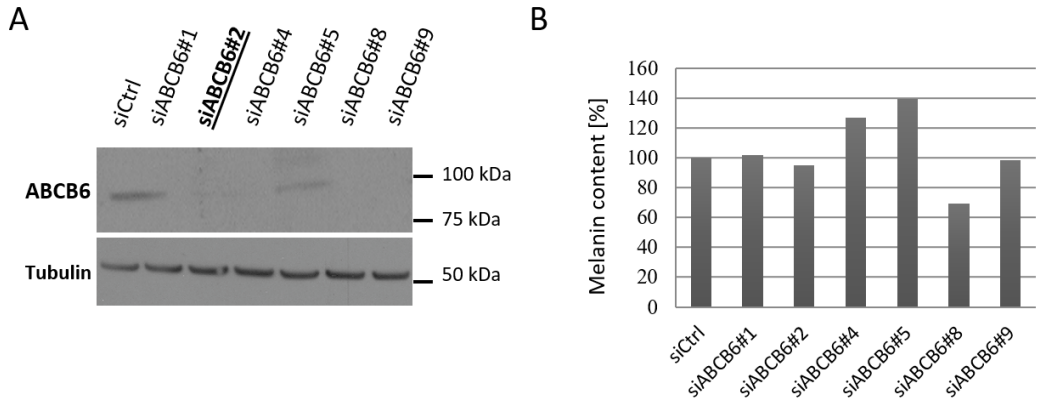

Figure 24. Effect of ABCB6 depletion on melanogenesis. A Downregulation of ABCB6 in MNT-1 cells. Immunoblot analysis of whole cell lysates isolated from MNT-1 cells treated with control or anti-ABCB6 siRNA constructs. Tubulin is shown for loading control. **B** Effect of ABCB6 depletion on the intracellular melanin content of MNT-1 cells. Values show averaged melanin levels obtained after treatment with 6 different siRNA constructs (MNT-1 siABCB6), relative to control (siCtrl)[130].

Confocal and electron microscopic results about the localization of ABCB6 suggested that the protein can affect the early steps of melanogenesis. Trafficking of melanosomal proteins (PMEL, TRP-1) into their respective melanosomal compartments were investigated, which is a crucial task during melanogenesis. During normal melanosomal maturation, PMEL is targeted to early melanosomes where it generates amyloid fibrils. Further steps include targeting of TRP-1 and other melanogenic enzymes to late stage melanosomes allowing the production of melanin that covers PMEL fibrils and hence PMEL epitopes. Despite efficient depletion of ABCB6 confocal microscopic

images showed separated PMEL-positive (NKI-beteb, red) and TRP-1-positive (TRP-1, green) compartments (Fig. 25).

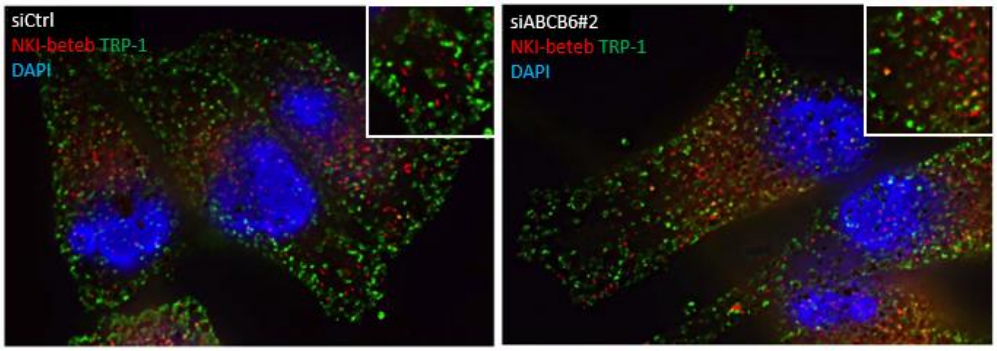

Figure 25. Downregulation of ABCB6 does not influence trafficking of melanosomal proteins. Subcellular localization of melanosomes was followed by confocal microscopy; using antibodies labeling early (NKI-beteb for PMEL, red) and late melanosomes (TRP-1, green). Nuclei are stained with DAPI (blue)[130].

Formation of PMEL-derived fibrils requires the sequential maturation of PMEL protein[115,117]. Analysis of PMEL amyloid matrix formation in MNT-1 cells by EM showed that abolishment of ABCB6 expression did not change the global ratio between pigmented and unpigmented melanosomes or the number of lysosomes (Fig. 26). However, loss of ABCB6 resulted in a significant decrease in the number of early melanosomes displaying normal PMEL fibril formation (Fig. 26B). Remarkable large aggregates filled the lumen of early and late melanosomes, identified by the presence of clathrin coats and melanized fibrils (Fig. 26A inset). These aggregates were slightly similar to lysosomal storage disorder structures such as ceroid lipofuscinosis[151] but with a more complex, hydrangea-like structure suggestive of lipid–protein complexes. These results showed that depletion of ABCB6 somehow modified PMEL fibril formation causing aberrant aggregates in the lumen of early melanosomes.

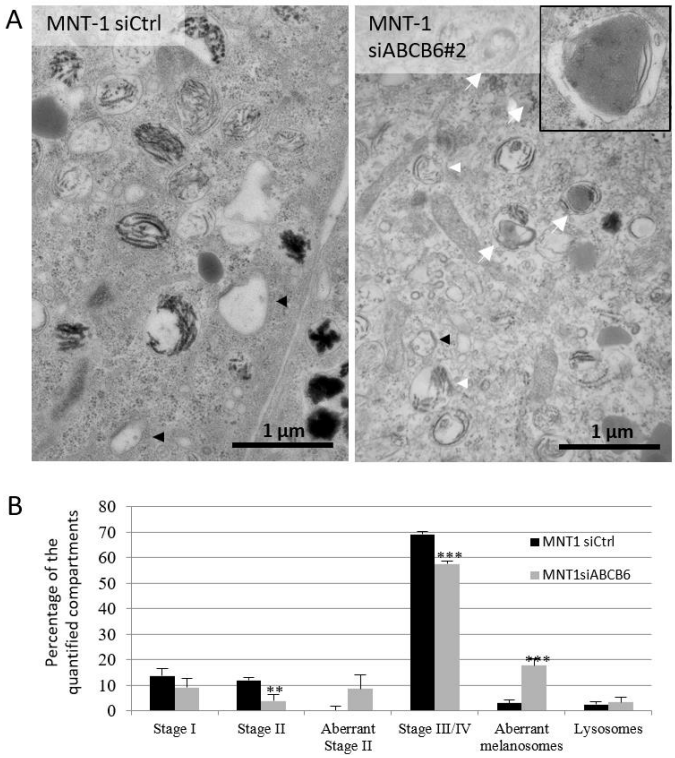

Figure 26. Representative ultrathin section images of control and ABCB6 depleted MNT-1 cells embedded in resin. A Black arrowheads indicate stage I melanosomes, and white arrowheads point to mature melanosomes containing PMEL fibrils covered by melanin. White arrows point to aberrant melanosomes containing a "hydrangea-like" structure (enlarged in the inset). The scale bar represents 1 µm. **B** Quantification of endosomal/melanosomal compartments, as defined by the morphology of the organelles in conventional EM of control or ABCB6-depleted MNT-1. Values represent the percentage of each compartment relative to all of the endosomal/melanosomal compartments identified in 20 cell profiles per condition. p Values: * $p<0.05$, ** $p<0.02$, *** $p<0.01$[130].

4.2.3. ABCB6 mutations prevent the rescue of normal amyloid fibril formation

In former experiments we saw that downregulation of ABCB6 caused perturbation at the early steps (stage II) of melanosome formation (Fig. 26) suggesting that some of the early step needed the function of ABCB6. So, we had the experimental setup in MNT-1 cells, where ABCB6 attenuation caused abnormal melanosomes. To enlighten the effect of ABCB6 in this process we attempted to rescue the abnormal phenotype with ABCB6 variants.

MNT-1 parental cells were transfected with ABCB6 variants: wild-type (WT), the inactive (K629M)[24] or a DUH mutant (G579E) variant[152]. Their localization was also investigated by confocal microscope. Non-pigmented melanosomes were labeled using

an antibody directed against the luminal domain of PMEL (NKI-beteb and HMB45), while pigmented melanosomes were stained with TRP-1. Overall, mutants (K629M, G579E) displayed a similar localization pattern to the endogenous ABCB6 protein, although the association of the DUH mutant variant with markers of the amyloidogenic luminal domain of PMEL and the PMEL fibrils was less pronounced (HMB45 and NKI-beteb) (Fig. 27, Fig. S2). Different staining pattern could indicate that PMEL luminal fragments were produced but their aggregation into fibrils might have been affected.

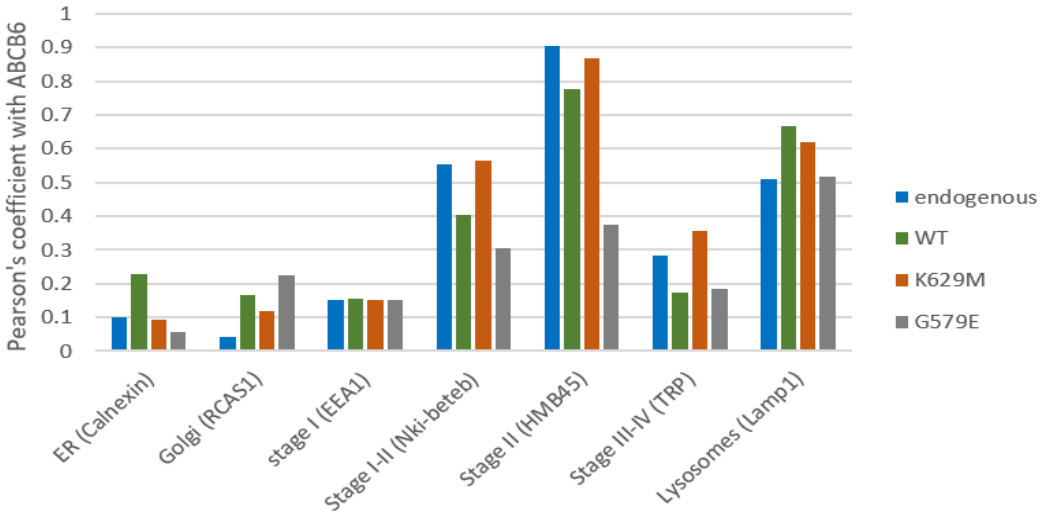

Figure 27. Localization of ABCB6 variants in MNT-1 cells. Pearson's correlation coefficients for colocalization of ABCB6 variants with the organelle-specific markers. (For confocal microscopic images see Fig. S2) Expression of WT (ABCB6 WT), and mutant ABCB6 variants (ABCB6 K629M and ABCB6 G579E) was visualized in MNT-1 cells using the OSK ABCB6 antibody, nuclei were labeled with Hoechst 33342; and organelles were labeled with specific markers: ER (Calnexin), Golgi (RCAS1), mitochondria (AIF), early endosomes (EEA1), lysosomes (LAMP1). Non-pigmented melanosomes were labeled using an antibody directed against the luminal domain of PMEL (NKI-beteb and HMB45); pigmented melanosomes were stained with TRP-1 (red). Colocalization analysis was performed with ImageJ (National Institute of Health) using the JACoP v2.0 plugin. The scale bar represents 10 μm[130].

In further experiments, melanoma cells stably expressing ABCB6 variants were depleted for endogenous ABCB6 using the siRNA construct targeting non-coding region of the gene (Fig. 24A siABCB6#2). Elimination of endogenous ABCB6 protein allowed the overexpression of the different ABCB6 variants thereby their effect could be tested (Fig. 28A). ABCB6 protein of parental cell line was also silenced by siRNA, like previously. Immunofluorescence assays using antibodies against PMEL (NKI-beteb) and

melanogenic enzyme TRP-1 revealed normal localization of both proteins (Fig. 28B), excluding impaired trafficking of PMEL and the melanogenic enzyme TRP-1 to early and late melanosomes.

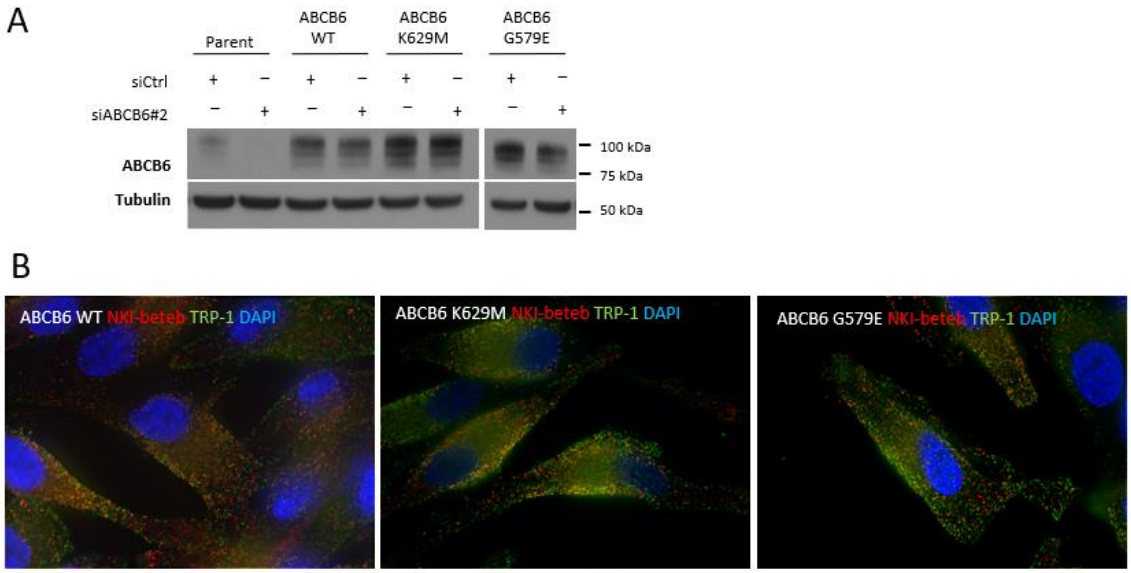

Figure 28. Overexpression of ABCB6 variants does not influence trafficking of melanosomal proteins. A Immunoblot analysis of whole cell lysates from parental MNT-1 cells (Parent), MNT-1 cells overexpressing WT ABCB6 (ABCB6 WT), a catalytically inactivate form of ABCB6 (ABCB6 K629M) or a DUH mutant variant (ABCB6 G579E). Cells were either treated with control or anti-ABCB6 siRNA (No. 2) constructs. Tubulin is shown for loading control. **B** Localization of ABCB6 variants and the melanosomal proteins. Subcellular localization of melanosomes was followed by confocal microscopy using antibodies labeling early (NKI-beteb, red) and late melanosomes (TRP-1, green). Nuclei are stained with DAPI (blue)[130].

In previous experiments, the collaborator group showed that depletion of ABCB6 by siRNA impaired PMEL amyloidogenesis in early melanosomes and induced aberrant accumulation of multilamellar aggregates in pigmented melanosomes. Ultrathin cryo-sections of MNT-1 cells immunogold labeled for ABCB6 and the PMEL amyloidogenic domain, showed enrichment of WT ABCB6 in early melanosomes, as shown for the endogenous protein (Fig. 29A left panel). Both mutants were localized to PMEL-positive endocytic structures and lysosomes confirming that these mutations did not affect their intracellular trafficking. In the case of (K629M), stage II melanosomes contained unstructured aggregates of various size, staining positive for PMEL luminal domain (Fig. 29A, middle panel). When the DUH mutant (G579E) was expressed, endosomal compartments contained intraluminal vesicles and unstructured aggregates staining

positive for the PMEL luminal domain (Fig. 29A, right panel). Morphological analysis of ultrathin sections of resin-embedded MNT-1 cells revealed that expression of WT ABCB6 restored the number and morphology of stage II melanosomes, suggesting the rescue of PMEL fibril formation (Fig. 29B left panel and C). At the same time, overexpression of WT ABCB6 resulted in a significant increase of the number of lysosomes (Fig. 29C). Notably, lamellar and multilamellar structures could be also observed in a minor fraction of early and mature melanosomes (Fig. 29B, left panel inset). In contrast, accumulation of aberrant early melanosomes and a decrease of pigmented melanosomes were observed on ultrathin cryosections of cells expressing mutant variants. Ultrathin sections of resin embedded MNT-1 cells overexpressing the K629M mutant confirmed a complete disorganization of PMEL fibrils in these melanosomes (Fig. 29B, middle panel, and Fig. 29C). K629M mutant induced the generation and accumulation of aberrant compartments, (Fig. 29B, middle panel inset) but devoid of the hydrangea-like structures observed in the siABCB6 condition. In the other case similar anomaly was observed. Expression of DUH mutant G579E also caused impaired fibril formation and showed accumulation of aberrant early and to a less extent late melanosomes. These melanosomes contained intraluminal multilamellar structures, as observed in cells overexpressing WT ABCB6, and hydrangea-like structures, as observed in ABCB6-depleted cells (Fig. 29B, right panel inset). These results clearly showed that in contrast to the WT protein, the mutant ABCB6 variants were unable to rescue PMEL fibril formation. Mutant variants failed to restore the number of normal early melanosomes depleted by the downregulation of ABCB6 and inducing instead an accumulation of aberrant stage II melanosomes showing signs of improper PMEL fibril formation.

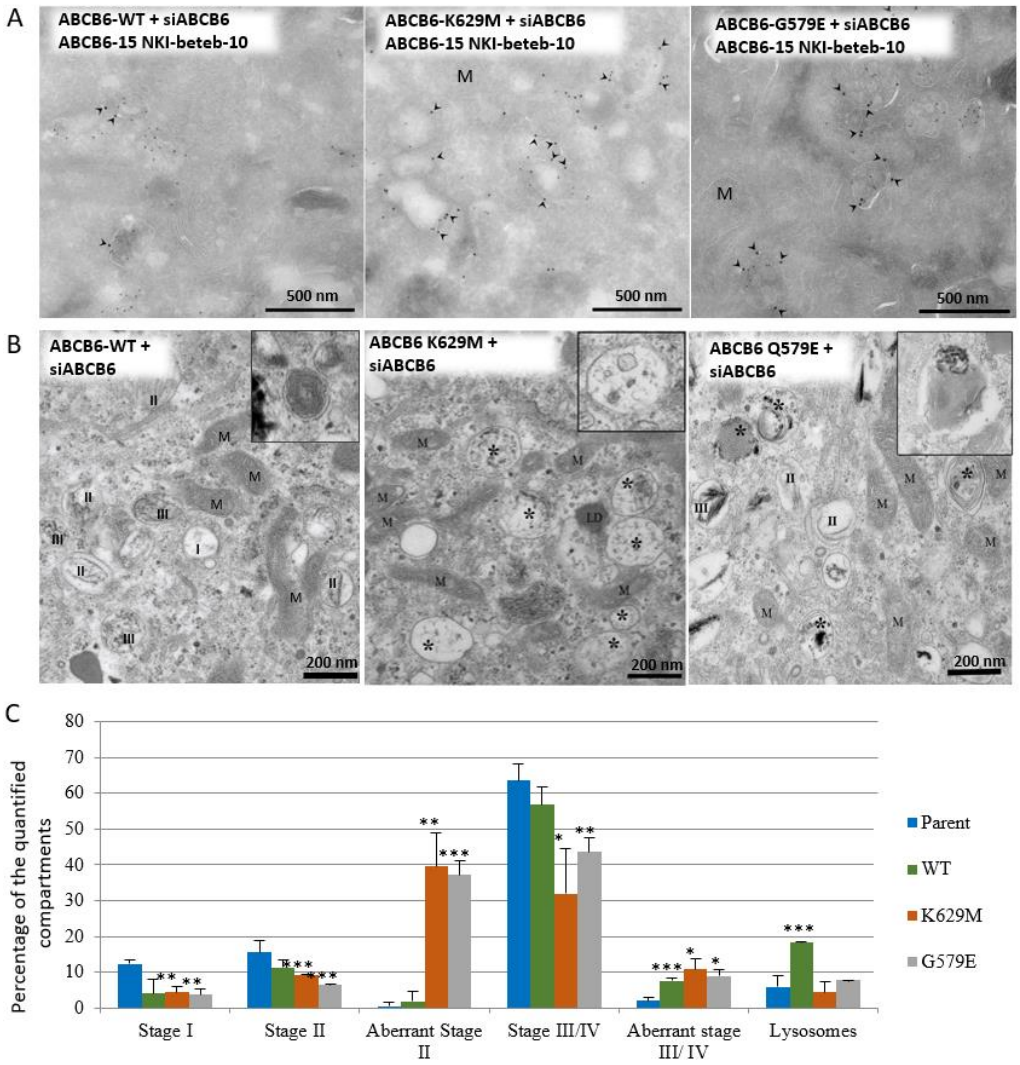

Figure 29. Overexpression of DUH mutant ABCB6 fails to rescue the ABCB6 depleted phenotype. A Ultrathin cryosections of MNT-1 cells overexpressing ABCB6 WT (left panel), inactive ABCB6 (middle panel) or the DUH variant (right panel) were double immunogold labeled for PMEL luminal domain (PAG 10 nm) and ABCB6 (PAG15 nm). Arrowheads indicate colocalization of ABCB6 and PMEL in non-pigmented melanosomes. Mitochondria are annotated with "m". The scale bar represents 500 nm. **B** Representative ultrathin section images of resin-embedded control and ABCB6-depleted MNT-1 cells and MNT-1 cells overexpressing WT ABCB6 (lower left panel), inactive ABCB6 (lower middle panel) or the DUH variant (lower right panel). Melanosome stages are annotated from I to IV; black flowers indicate aberrant pigmented melanosomes containing unstructured aggregates along with melanized fibers. White stars indicate aberrant lysosomal structures. LD, lipid droplet; V, vacuole; Lys, lysosome; M, mitochondria. Scale bar is 200 nm. **C** Quantification of endosomal/melanosomal compartments as defined by the morphology of the organelles in conventional EM of control or ABCB6-depleted MNT-1 with or without the overexpression of WT (ABCB6 WT) or mutant ABCB6 variants (ABCB6 K629M, ABCB6 G579E). Values represent the percentage of each compartment relative to all endosomal/melanosomal compartments identified in 20 cell profiles per condition. p Values: * $p<0.05$, ** $p<0.02$, *** $p<0.01$[130]. Imaging and analysis of EM images were made by P. Bergam in CRNS, Paris.

4.3. MNT-1 cell lines genome edited by CRISPR/Cas9

In case of a protein, especially in case of a membrane transporter, determination of its localization is indispensable. When the adequate membrane compartment is known, we can establish our hypothesis about its substrate. It is particularly true in the case of ABCB6 since its localization is still a matter of debate. Most studies were based on the overexpression of ABCB6, which is always prone to artefacts. That's why we wanted to detect the intracellular distribution of ABCB6 using the latest gene editing method.

4.3.1. Cytogenetic analysis of MNT-1 cells

Before starting genetic modification on a cell line, we have to be aware of the copy number of the gene of interest. Especially cancer cell lines have often abnormal, polyploid chromosome assemblies. Cytogenetic analysis was performed to determine chromosome assembly of MNT-1 cells. Analysis revealed that MNT-1 cells have complex karyotype (hyperdiploid), generally cells have 63-66 chromosomes. Fluorescent in situ hybridization (FISH) provides a powerful tool for identifying the location of a DNA sequence and quantitative differences, like copy number variations on metaphase chromosomes. Since *ABCB6* was mapped to chromosome 2q35, control FISH probe indicated chromosomes II (green centromeres). It appeared that red signals of *ABCB6* were observed on chromosomes II and one of the extra locuses was localized at the end of a chromosome and the other at the middle of another chromosome (Fig. 30A,B). These results indicated that MNT-1 cells have four *ABCB6* alleles. Analysis was performed by Gergő Papp (I, Pathology, Semmelweis University).

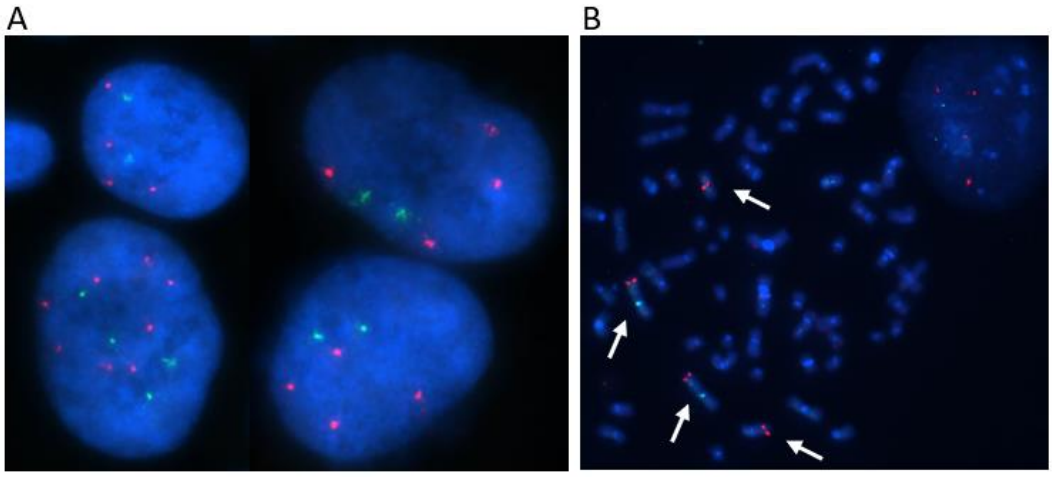

Figure 30. FISH analysis of DAPI stained nucleus of MNT-1 cells. A Inter- and **B** metaphase cells were imaged. Control probe labelled chromosomes II centromeres (green), ABCB6 specific probe labeled alleles containing *ABCB6* (red). There were two chromosomes II and *ABCB6* was located to them, plus there were two chromosomes, which were labeled *ABCB6*, but have no centromere II (unpublished data).

4.3.2. Endogenous ABCB6 is located to lysosomes

Using the latest and most efficient genome editing method, the CRISPR/Cas9, we aimed to modify *ABCB6* gene in MNT-1 cells. The work was done in cooperation with P. Kulcsár (EI RCNS, HAS). GFP label by genome editing can reveal the authentic location of a native protein, in contrast of examination of an artificially overexpressed and tagged protein. Thus, in our first engineered cell line, to monitor the physiological localization of the protein, the *ABCB6* gene was endogenously fused with GFP coding sequence. For this genetic modification 3 plasmids were used: the first contained the GFP coding sequence between the ABCB6 homologue arms (~1000 bp each), the second contained the SpCas9 expression cassette and the third contained the guide RNA sequence with the spacer, which targets *ABCB6* (Table S2). Cells successfully transfected with all the three plasmids and SpCas9 caused DSB, HDR could be used to modify the genome of MNT-1 cells. In every case of genetic modification, we chose several possible target sequences with the WGE web tool (https://www.sanger.ac.uk/science/tools/wge). Applying endogenous GFP tag we had to design the spacer sequences (Table S2), so that the GFP insertion is in frame with last exon of *ABCB6* (Fig 31A).

Transfected cells were analyzed 8-days post-transfection (no background signal from plasmid can be detected anymore) and cells were sorted by FACS for GFP and cloned on 96 well plates. We detected single cell clones using Calcein AM and a High Content Screening device. Single cell clones created by different spacer sequences were grown then tested and selected with the following methods. First, we confirmed the GFP positive population by flow cytometry. Integrated GFP sequence was validated by PCR on genomic DNA extract with two different primer pairs (Fig. 31A). Clones where integration happened, specific bands were detected at 1500 bp (Fig. 31B) or 1200 bp (Fig. 31C). PCR results suggested that on some alleles, the original sequence remained intact (Fig. 31B). Thus, we investigated non-tagged (original) and GFP-tagged (CRISPR) modified ABCB6 by immunoblot (Fig. 32D). Interestingly, clones generated by spacer sequence #1 did not express wild type ABCB6. Analyzing sequencing result validated

that the homologous arms mediated GFP insertion occurred. But it was revealed that in clones created with spacer #1, indel mutations caused frameshift in the coding sequence eliminating the STOP codon. We presumed that the translated mutant protein was unstable, and it was degraded by the proteasomal machinery and it could not be detected on immunoblot (Fig. 31D). But to sum up, we created endogenously GFP labeled melanoma cell lines.

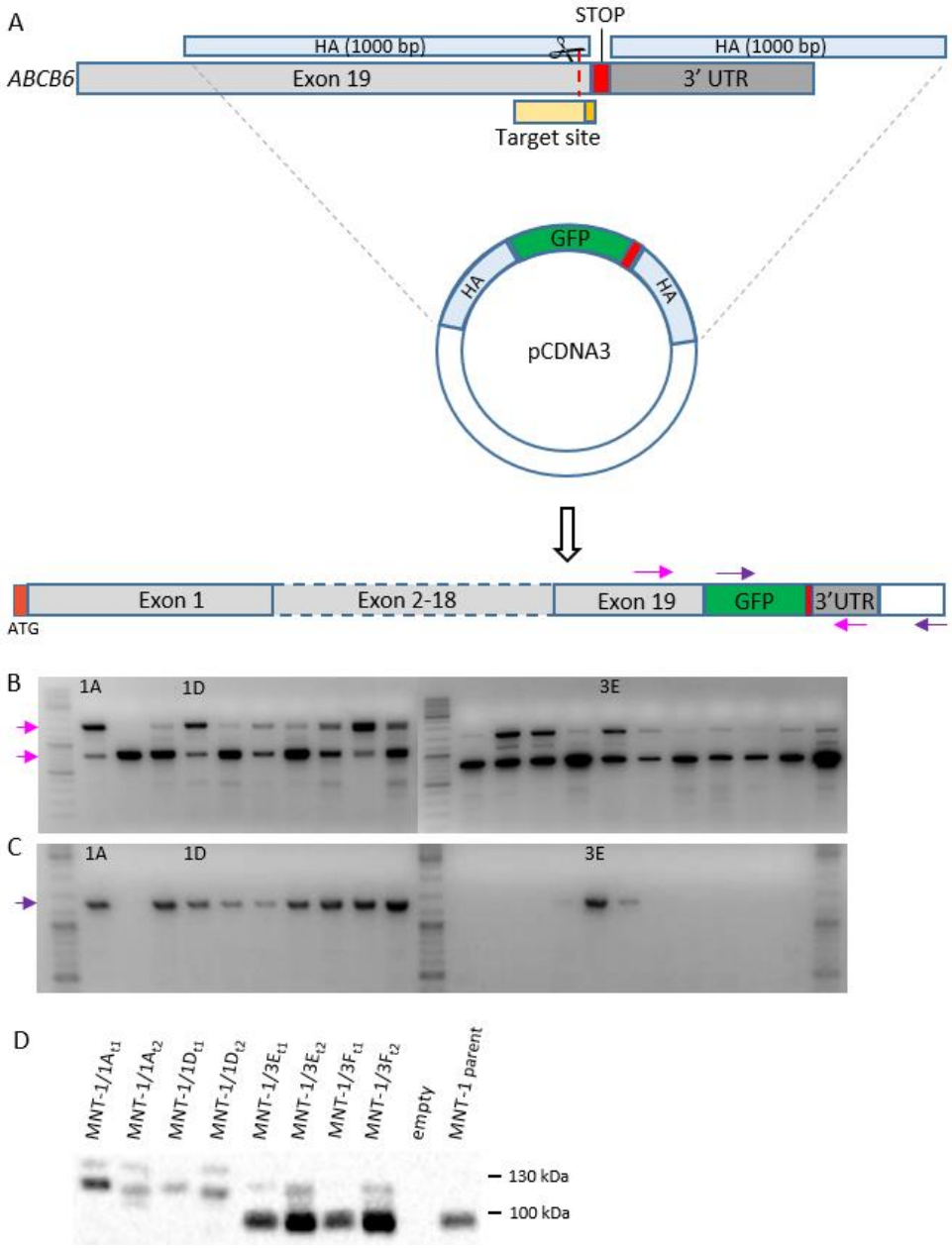

Figure 31. Single cell clones modified with CRISPR/Cas9 system were selected by different methods. A Schematic representation of ABCB6 gene modification by homology directed repair and CRISPR/Cas9 system. Dark orange - first methionine encoded by ATG, grey - exons of

ABCB6 gene, green - GFP sequence, light blue - homology arms (HA), red - stop codon, dark grey - 3' untranslated region (UTR), yellow - target site with PAM motif, scissor - double strand brake caused by Cas9 endonuclease. Two primer pairs were designed for PCR reactions (pink and purple arrows) **B** PCR reactions were run on extracted genomic DNA and PCR products were separated on agarose gel. Insertion of GFP coding sequence was detected with the first primer pair at 1500 bp, original genomic sequence was detected at 700 bp (pink arrows). **C** The position of the integrated GFP coding sequence was detected with the second primer pair (purple arrow) (unpublished data). **D** Immunoblot of three selected MNT-1 clones using anti-ABCB6 antibody ABCB6-567[139]. Samples were taken at two separate time points (t1 and t2). The molecular weight of wild type ABCB6 is 97 kDa, while the tagged transporter is about 125 kDa (unpublished data).

Figure 32 shows tagged ABCB6 localization in the selected clone MNT-1/1A. It is consistent with the overexpressing systems, ABCB6 colocalizes with the lysosomal marker (LysoTracker) and do not with mitochondrial marker. Images were obtained by J. M. Reisecker (MedUniWien).

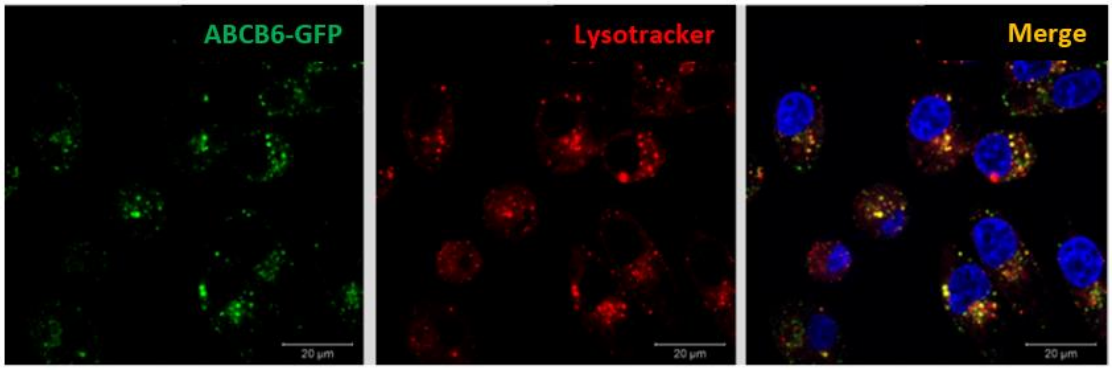

Figure 32. Endogenous ABCB6-GFP localizes to lysosomes in MNT-1 cells. ABCB6 signal (green) colocalized with red lysosomal marker (LysoTracker). Nucleuses were stained with DAPI. Scale bar 20 µm (unpublished data).

With this setup, we can only detect a steady-state condition of ABCB6. To expand our possibilities, in the next experiment, we used the RUSH system. RUSH is a two-state assay based on the reversible interaction of a hook protein in a donor compartment and the protein of interest. The hook protein is fused to streptavidin and stably anchored and the reporter protein is fused to streptavidin-binding peptide (SBP). Biotin addition causes a synchronous release of the reporter from the hook[153]. Another tag was cloned into the earlier used pCDNA3 plasmid. Between the HR arms, upstream to GFP, a Streptavidin-binding peptide (SBP) coding sequence was fused (Fig. 33A), which allows to arrest our transporter at the preferred intracellular compartment (i.e. ER). In the planned experiments, cells will be transiently transfected with the hook bearing a streptavidin tag.

DOI:10.14753/SE.2020.2354

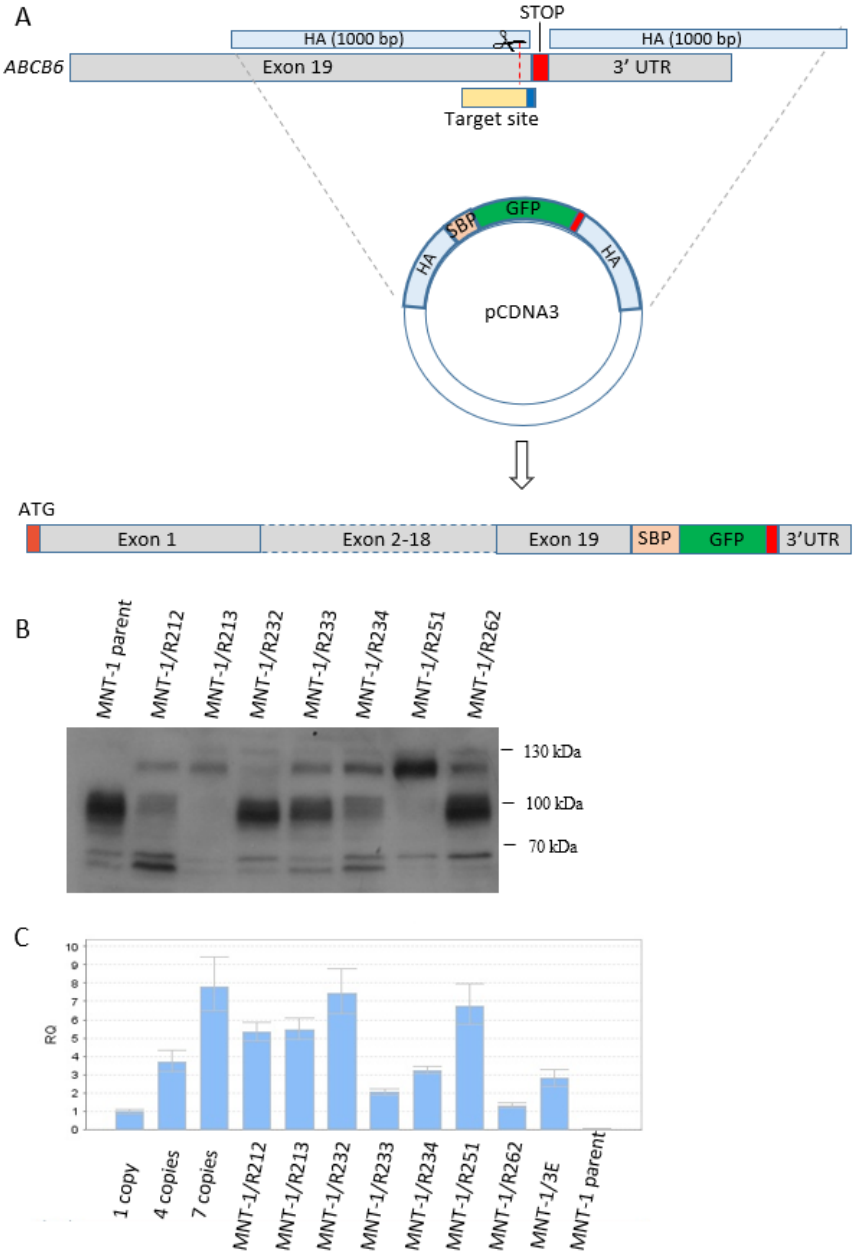

Figure 33. The selected clone, MNT-1/R251 carries four ABCB6-SBP-GFP alleles. A Schematic representation of ABCB6 gene modification by homology directed repair and CRISPR/Cas9 system. Dark orange - first methionine encoded by ATG, grey - exons of *ABCB6* gene, light orange - streptavidin binding protein (SBP), green - GFP sequence, light blue - homology arms (HA), red - stop codon, dark grey - 3' untranslated region (UTR), yellow - target site with PAM motif, scissor - double strand brake caused by Cas9 endonuclease. **B** Immunoblot analysis of modified MNT-1 clones using anti-ABCB6 antibody ABCB6-567[139]. The molecular weight of wild type ABCB6 is 97 kDa, while the tagged transporter is about 125 kDa.
C Real-time PCR quantification of GFP copy number in modified MNT-1 clones. For reference HEK293 cell clones were used bearing 1, 4 or 7 copies of RPPH1. Different RUSH-GFP clones named MNT-1/R. MNT-1/3E was a selected clone from the former experiment, expressing endogenously tagged ABCB6-GFP. Data were analyzed by the StepOne 2.1 software, using the ΔΔCt method ($p<0.05$) (unpublished data).

The “hook” CD74 protein fused to streptavidin contains an ER retention signal sequence will function as a transmembrane protein which will anchor the SBP-GFP tagged ABCB6. Biotin addition will release ABCB6 and we can monitor the intracellular route of the transporter. In preliminary experiments, without expressing the hook protein, ABCB6-SBP-GFP and the endogenous ABCB6-GFP or overexpressed constructs showed identical localization. Applying real-time PCR, immunoblot and Sanger sequencing we identified a clone (MNT-1/R251) which carries the designed modification in all alleles (Fig. 33B). From the former experiment MNT-1/3E cells (ABCB6-GFP) were also tested and we assumed that the clone has two GFP tagged and two unmodified alleles. Trafficking of ABCB6 after biotin addition will be examined by confocal microscopy.

4.3.3. ABCB6 KO cell line

Taking advantage of the fact that we had a cell line expressing GFP tagged ABCB6 in each chromosome, in the next step we wanted to create an *ABCB6* knockout (ABCB6 KO) cell line. It was straightforward to detect the abolishment of GFP signal by FACS. The first exon of ABCB6 was targeted and we chose several target sequences (Table S2). After DSB caused by RNA directed SpCas9, we wanted to integrate another selection marker, so we used NHEJ mechanism of the cells. Self-cleaving pCMV-tagBFP plasmid was co-transfected, which contained its own spacer sequence, thus the plasmid can cleave and linearize itself in the cell, thereby enhancing the integration of BFP selection cassette[154] (Fig. 34A).

After transfection, cells could be sorted by flow cytometry based on their fluorescence, selected cells were GFP negative, but BFP positive. Single cell cloning was evaluated as described in the Methods. Lack of ABCB6 expression was confirmed by immunoblot (Fig. 34B), confocal microscopy (Fig. 35) and results were verified in genomic level using PCR and Sanger sequencing. Based on immunoblotting results ABCB6 KO 32, 33 and 13 clones were not knockouts, but the rest of the clones did not express WT or SBP-GFP tagged ABCB6 (Fig. 35B, 36). To investigate the function of ABCB6 in pigmentation was a straightforward step to measure the melanin content of knockout clones. We chose several clones, but we detected variable melanin levels (Fig. 36). Interestingly during growing single cell clones KO 34 was one of the slowest clones,

but since then this kind of difference was not observed. These experiments did not reveal the physiological function as yet, further studies are needed. First, we intend to analyze morphology of ABCB6 KO cells by electron microscopy as ABCB6 attenuated cells.

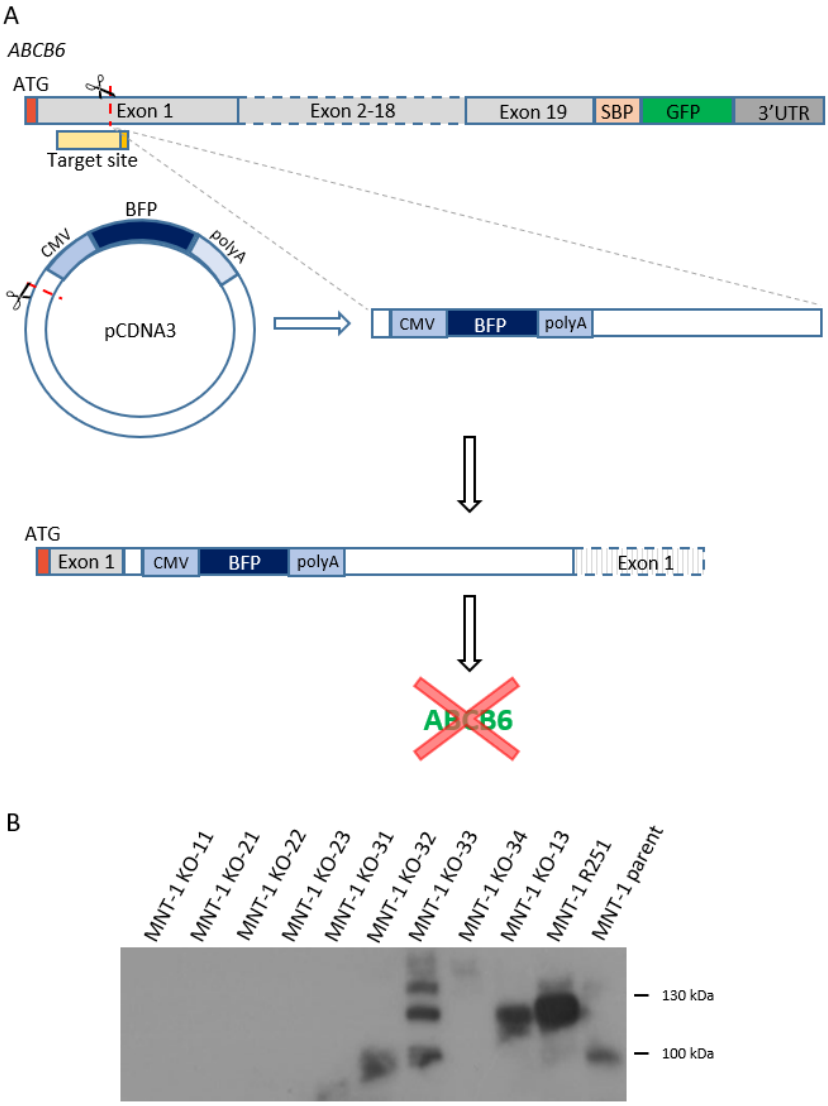

Figure 34. Creation of ABCB6 knockout cell line A Schematic figure of creation of ABCB6 KO cell line by CRISPR/Cas9. Dark orange - first methionine encoded by ATG, grey - exons of *ABCB6* gene, light orange - streptavidin binding protein (SBP), green - GFP sequence, red - stop codon, dark grey - 3' untranslated region (UTR), yellow - target site with PAM motif, scissor - double strand brake caused by Cas9 endonuclease, CMV-BFP-polyA shows the blue fluorescent protein expression cassette. **B** Immunoblot analysis of MNT-1 modified cell clones. Expression of ABCB6 from total MNT-1 cell lysates was monitored by immunoblotting, using the anti-ABCB6 antibody ABCB6-567[139]. Clones were made by different spacer sequences. Molecular weight of WT ABCB6 is 97 kDa (MNT-1 parent), while the tagged transporter was about 125 kDa (MNT-1/R251). (unpublished data).

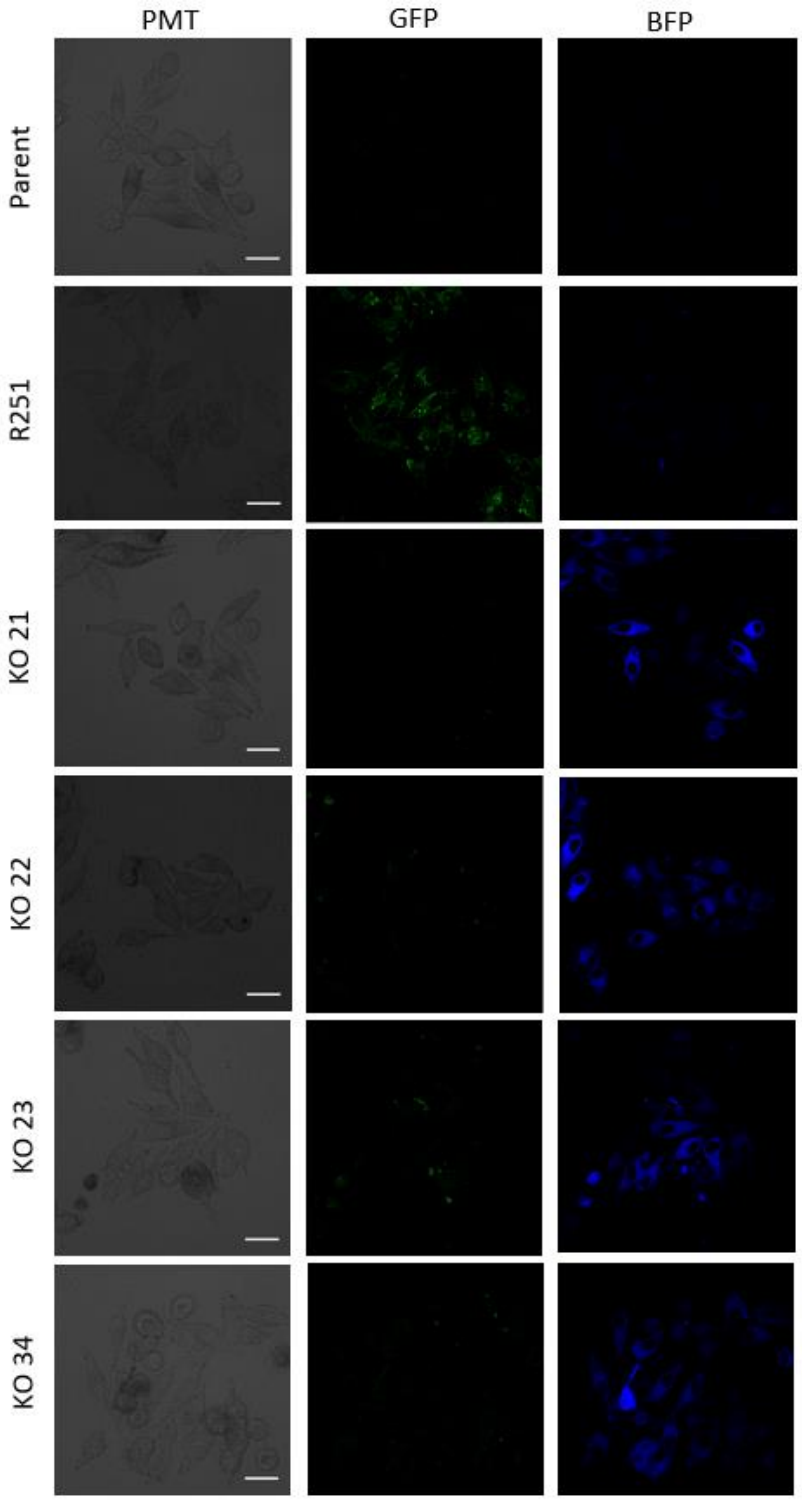

Figure 35. Confocal microscopy analysis of MNT-1 modified clones. After DSB in the first exon of ABCB6 caused by RNA directed SpCas9, a selection marker, BFP (blue), integrated in the genome. Parental cells do not express fluorescent protein, MNT-1/R251 cells are GFP positive and the selected ABCB6-KO clones are GFP negative but BFP positive (unpublished data).

DOI:10.14753/SE.2020.2354

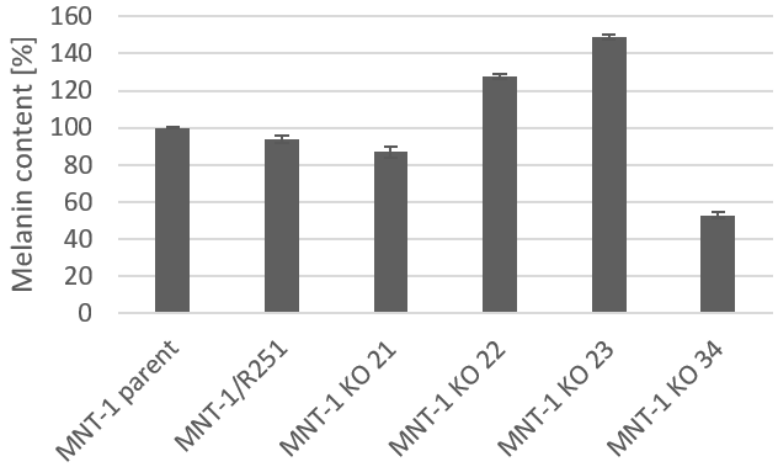

Figure 36. Effect of knockout of ABCB6 on the intracellular melanin content of MNT-1 cells. For determination of melanin content, cells were washed with PBS and dissolved in 250 µl of 1 N NaOH for 1 hour at 80 °C. Absorbance was measured at a wavelength of 405 nm (unpublished data).

DOI:10.14753/SE.2020.2354

5. Discussion

At present, the subcellular localization of ABCB6 remains a matter of debate. In 2006, ABCB6 was described as a mitochondrial porphyrin transporter, located to the outer mitochondrial membrane. Krishnamurthy and his colleagues concluded that the protein is a coproporphyrinogen III importer thus regulator of erythroid maturation and hem synthesis [25]. Subsequent studies have found ABCB6 to be dispensable for erythropoiesis, and located the protein to the surface of red blood cells [24,28], suggesting that mitochondrial porphyrin import may not depend on ABCB6. The research of K. Kiss fundamentally questioned statements in the literature and raised new insights about the physiological role of ABCB6. Results of our laboratory clearly corroborate the extramitochondrial localization of ABCB6 [24,67]. Further, ABCB6 was detected in the plasma membrane of cells [63], and throughout the endolysosomal continuum [56,64,155,156]. These findings challenged the paradigm linking the expression and function of ABCB6 to mitochondria. However, the physiological function of ABCB6 in the endolysosomal compartment has remained elusive. Therefore, in the presented work we investigated ABCB6 in different model systems to identify lysosome related functions.

5.1. The role of ABCB6 in Cd detoxification

S. pombe and *C. elegans* are important models for elucidating conserved pathways and processes relevant to human biology and disease. Even though this 'orthologue-function conjecture' has many known exceptions, it remains a valuable and widely used method for predicting gene functions based on sequence similarity. In particular, rescue of mutant phenotypes has established the function of several orthologous human proteins. It is assumed that such orthologous gene pairs share at least some aspects of their characteristics. Yeast and humans are separated by a billion years of evolution[157], yet there are thousands of recognizable orthologs between the two species. Moreover, there are hundreds of genes from one species that can functionally replace (complement) their orthologues in the other[158]. The high degree of sequence and topological similarity between the HMT-1 proteins and ABCB6 suggested an evolutionary conserved, orthologous function, implying ABCB6 in heavy metal resistance[32,104,132].

Organisms have evolved several mechanisms to detoxify or eliminate harmful heavy metals such as Cd[159]. Cadmium can mainly be found in the earth's crust; it always occurs in combination with zinc. Cadmium also consists in the industries as an inevitable by-product of zinc, lead and copper extraction and about three-fourths of cadmium production is used in Ni-Cd batteries[160]. It is also found in manures and pesticides, thus causing soil contamination[161]. Since it can accumulate in aquatic organisms and agricultural crops, animals are primarily exposed to cadmium through food or water[162–165]. In addition, humans are exposed to Cd pollution due to smoking tobacco products[166]. The major toxic form of Cd in eukaryotic cells is the Cd^{2+} ion. Although Cd^{2+} is not a Fenton metal and therefore is not capable of exerting redox reactions in biological systems, it may induce formation of reactive oxygen species (ROS) by depletion of endogenous redox scavengers, inhibition of antioxidative enzymes, inhibition of the mitochondrial electron transport chain, and/or displacement of redox active metals, such as Fe^{2+} or Cu^{2+}, from their carrier proteins and thereby cause mitochondrial damage and trigger apoptosis, to name few of the mechanisms underlying Cd^{2+} toxicity. Cd^{2+} can also substitute for Ca^{2+} in cellular signaling or for Zn^{2+} in many enzymes and transcription factors which may lead to cellular dysfunction. Organisms have evolved distinct mechanisms to detoxify and eliminate cadmium from the cells[167]. Animals and fungi produce metallothioneins (MTs), a class of low molecular weight (500–1400 Da), proteins located in Golgi apparatus[168]. These proteins are involved in responses to both xenobiotic heavy metals, such as mercury, cadmium, arsenic, as well as physiological ones, such as selenium (Se), copper, zinc, etc.[168]. Moreover, MTs were shown to be beneficial in controlling oxidative stress via capturing destructive free radicals[169]. Among the non-enzymatic antioxidants, glutathione (GSH; γ-glutamyl-cysteinyl-glycine) is a low molecular weight, water soluble thiol compound. Apart from the role in storage and transport of reduced sulfur, GSH is a common chelator involved in cellular response, transport and excretion of metal cations. In *Saccharomyces cerevisiae*, sequestration of cadmium–glutathione complexes is mediated by ScYCF1, which belongs to the ABCC subfamily[170]. Another major function of GSH is the formation of phytochelatins (PCs) that bind heavy metals for safe transport and sequestration in plant cells. Thus, GSH plays a vital role in detoxifying toxic metals/metalloids and xenobiotics[171]. In addition to plants, some Fungi and the nematode *C. elegans* produce PCs. Studies showed that HMT-1

proteins of *S. pombe* and *C. elegans* confer cadmium resistance by sequestrating Cd–phytochelatin complexes[102,105]. RNA interference analyses revealed, however, that *ce-hmt-1*-deficient worms were significantly more sensitive to cadmium than *ce-pcs*-deficient worms. In addition, morphological differences were observed between the two RNAi treated lines upon exposure to Cd. The intestinal cells of the progeny of *ce-pcs*-1-RNAi worms underwent necrosis, while the same cells in the progeny of *ce-hmt-1*-injected worms generated spherical refractive inclusions[106]. Further investigation of *hmt-1* and *pcs-1* revealed that these genes are expressed in different cell types but are co-expressed in coelomocytes of the worms. Cytotoxicity studies with knock out worms implied that CeHMT-1 also confers tolerance to As and Cu, and the transporter and PC synthase do not function in a simple linear pathway. Moreover, substrates of HMT-1 are not limited to Cd-PC complexes[104]. In addition, DmHMT-1 from the non-PC producing fruit fly was able to rescue the Cd-sensitivity of the *S. pombe hmt-1* mutant[101]. Conversely, SpHMT-1 conferred tolerance to Cd in *Escherichia coli* and *Saccharomyces cerevisiae*, organisms devoid of phytochelatins[103]. Furthermore, data showed that *S. pombe hmt-1* mutant accumulates significant levels of PCs in vacuoles[101], suggesting that other proteins may contribute to PC transport into the vacuoles. Mendoza-Cózatl and his colleagues performed systematic analysis of different *Abc* genes in fission yeast. Using the *hmt-1*-deleted background identified a full-size ABCC type transporter, SpAbc2, which was also a key factor of Cd tolerance. Complementation experiments were performed to identify the substrate specificity of the proteins. Testing different combination of mutants, authors noticed that both SpAbc2 and HMT-1 mediated the accumulation of PCs in the vacuoles. Furthermore treatment of mutant strains with a fluorescent glutathione conjugate showed that HMT-1 was also capable of transporting GSH complexes[172].

Investigating *S. pombe* model cells we showed that heterologous expression of ABCB6 rescues the Cd-sensitive phenotype of HMT-1 deficient strain (Fig. 10) and the protein was detected in the vacuolar membrane of *S. pombe* cells (Fig. 9). Measurement of vacuolar Cd content by GFAAS showed Cd accumulation in vacuoles of *hmt-1* deleted strain expressing ABCB6. This indicates that the rescue of HMT-1 deficient yeast cells was based on the vacuolar sequestration of cadmium. This cytotoxicity setup can be used to examine the relationships between mutations and rescuing function. Interestingly, the

absence of the protein in humans or mice does not lead any obvious phenotype. Although mutations cause abnormal phenotype or lower expression levels in patients (DUH, Coloboma, FP, Lan). The following set of mutant variants of ABCB6 were successfully expressed in *S. pombe* cells: A57T (Col), S170G (DUH), R192Q (Lan), R192W (Lan), R276W (Lan), G588S (Lan), V609M (Lan), R638C (Lan) (Fig. 11A). Only two of the mutations, R192W and R276W failed to cause Cd tolerance (Fig. 11B). In the other cases mutant ABCB6 behaved similar to wild type protein. In Hela cells R192Q and G588S mutations did not change the intracellular expression pattern of ABCB6, while R192W showed ER retention[29], which can explain the malfunction in yeast cells. In spite of this, R276W caused no alteration of expression or cellular localization of ABCB6 in HEK-293 cells. But measurement of cation flux demonstrated greater loss of potassium or rubidium ions from cells expressing R276W mutant protein.[173]. In all examined organisms, overexpression of SpHMT-1 conferred tolerance only to Cd[103], whereas substrates of CeHMT-1 also include As(III) and Cu(II)[106]. In fission yeast, ABCB6 conferred resistance to Cd(II), As(III), but not to As(V), Hg(II) or Cu(II) (Fig 12).

Encouraged by the results in fission yeast we performed cytotoxicity experiments with the nematode *C. elegans* to test the rescue effect of ABCB6 in a multicellular organism. Similar to *S. pombe*, human ABCB6 provided protection to *hmt-1* deleted animals against Cd toxicity. In *C. elegans*, ABCB6 was expressed under the control of endogenous CeHMT-1 promoter. This offered an opportunity to study ABCB6 localization in an intact organism without the burden of artifacts associated with overexpression. Co-expression of ABCB6 and CeHMT-1 showed colocalization, although maybe the same promoter led to the similar expression pattern (Fig. 17). Further experiments specifying intracellular organelles showed that CeHMT-1 is localized to the endosomal compartment, mainly to the apical recycling endosomes in the intestinal cells of the nematode (Fig. 19). This result was in complete agreement with a recent report[95], and importantly, ABCB6 was found in the same intracellular compartments (Fig. 19). Similar to ABCB6[67], CeHMT-1 lacking the NTE domain was targeted to the plasma membrane, and the truncated form of CeHMT-1 did not confer tolerance to Cd[95].

Determining the subcellular localization of a protein is a key step toward understanding its cellular function. Although we found that the endogenous ABCB6 protein is confined to the endolysosomal compartment of SNB-19 glioblastoma cells (Fig.

21), and it plays a role in Cd detoxification (Fig. 20), it is difficult to imagine that mammalian cells would be exposed to such high level of Cd contamination. Given the conservation of HMT-1 proteins, we suggest that the ABCB6-mediated increase of vacuolar cadmium levels shown in Fig. 14 can be explained by the direct transport of (Cd–GS2) complexes. It was shown that HMT-1s are able to detoxify Cd without PCs. SpHMT-1 overexpression in *E. coli* enhanced the Cd tolerance and DmHMT-1 overexpression in *S. pombe* suppressed the Cd sensitivity *hmt-1* mutants. Moreover, DmHMT-1 expressed in *S. pombe* cells was located to the vacuolar membrane but did not transport Cd-PC complexes[134]. We assume that it might be an evolutionary conserved mechanism and the real function is not revealed yet, may be transport of some other kind of metal-conjugates can be relevant in mammalian cells.

Overall, our laboratory showed that ABCB6 localizes to the same intracellular compartment as SpHMT-1 and CeHMT-1, performing an overlapping function linked to the intracellular sequestration of metal complexes. The finding that the monoclonal anti-ABCB6 antibody could recognize the yeast transporter (Fig. 8B) strengthened the similarity between HMT-1 and ABCB6. First, we showed that ABCB6 rescues the Cd-sensitive phenotype of HMT-1-deficient *S. pombe* and *C. elegans* strains (Fig. 10,15). Second, we revealed that ABCB6 function is required for the sequestration of cadmium into HMT-1-deficient yeast vacuoles (Fig. 14) by applying non-functional mutant of ABCB6. We mutated the universally conserved lysine residue in the Walker A sequence [24] which is crucial for nucleotide-binding[174]. Third, we provided evidence that ABCB6 localizes to lysosomes of human glioblastoma cells and modulates their cadmium sensitivity (Fig. 20). Taken together we had no functional essay before, but now we have a rescue model system for the characterization and study of ABCB6.

It also remains to be determined how the evolutionary conserved role in detoxification is manifested in pathological conditions. Genetic studies revealed that mutations in *ABCB6* can cause several hereditary diseases ranging from pseudohyperkalemia[81], coloboma[75], to dyschromatosis universalis hereditaria (DUH)[83,87,152]. The pathogenic role of ABCB6 in these conditions is not understood, as there is no obvious overlap between these phenotypes. Interestingly, the absence of the protein in humans or mice does not lead any obvious disorder. In case of ABCB6 knock out mice it is possible that the well-controlled laboratory environment lack of the adequate

stress factors where ABCB6 function can be clearly beneficial[175]. It is tempting to speculate that maybe impaired transport of glutathione adducts, thereby abnormal endolysosomal metal homeostasis can result these phenotypes. The relevance of endolysosomal compartment in the intracellular metal homeostasis is well-known[176]. The big question is that why the glioblastoma cells need the ABCB6 provided protection against Cd and how their (metal) metabolism differs from other cell lines.

5.2. The role of ABCB6 in pigmentation

Dyschromatosis Universalis Hereditaria (DUH) is a rare autosomal dominant genodermatosis characterized by asymptomatic hyper- and hypo-pigmented macules that appear in infancy or early childhood. Etiopathology of DUH is not known. Lesions show a focal increase or decrease in melanin and melanosome content of melanocytes and keratinocytes of the basal layer, which is believed to be the consequence of a defect in melanosome production and/or distribution, rather than a disorder of melanocyte numbers[177–179]. DUH patients with ABCB6 mutations do not exhibit any of the additional abnormalities.

Melanogenesis involves two sequential but independent processes, functional amyloid fibril formation and pigment synthesis. Melanosomes are cell type-specific lysosome-related organelles, they derive from early endosomes, which are called stage I melanosomes in pigment cells. During melanosome biogenesis, stage I melanosomes mature into stage II melanosomes which acquire specific identity and morphology separate from lysosomal organelles[87,111]. Stage I melanosomes are characterized by a clathrin coat and few intralumenal vesicles[180]. In their lumen amyloid fibril generation is initiated from cleavage products of PMEL, a transmembrane protein expressed in melanocytes[181]. During maturation into stage II melanosomes, the formation of these fibrils requires concomitant proteolytic processing of PMEL and differential sorting of PMEL cleavage products[118,121,182,183] (Fig. 37). PMEL amyloidogenesis is completed in ellipsoidal shaped stage II melanosomes where the assembled amyloid lumenal fibrils serve as a matrix for pigment deposition in later stage III and IV melanosomes, which have acquired melanogenic enzymes[180]. Interestingly, lysosomes are thought to contribute to PMEL fibril formation during early melanogenesis[184]. We hypothesized that

ABCB6 probably have a role in this lysosome related melanogenesis process and therefore we investigated melanisation in model cells.

Regarding melanogenesis, similar to our heterologous model systems (*S. pombe* and *C. elegans*) we aimed to set up a rescue system in which we can investigate the role of ABCB6. The widely used pigmentation model cell line, MNT-1 human melanoma cell culture was studied. It has the complete conserved apparatus to produce all melanosome stages continuously, from the generation of PMEL amyloid fibrils to the synthesis of eumelanin[180,185]. Several reports have used this cell line to reveal the role of key proteins involved in intracellular trafficking[118,186], proteolytic cleavage and signaling pathways[187] regulating melanogenesis. As a first step we characterized the localization of endogenous ABCB6 in melanoma cells. Consistent with our previous results we corroborated the localization of ABCB6 in the endolysosomal continuum[24,67]. Cell fractionation, confocal and electron microscopic analysis revealed that the protein was localized to lysosomes and early melanosomes of MNT-1 cells. While ABCB6 is present on exosomes of reticulocytes[67], it was not observed in the exosome fraction of MNT-1 cells, in line with known differences in the sorting mechanisms of melanocytes and reticulocytes[188].

In a first attempt to understand the role of ABCB6 in melanogenesis and why its mutations cause abnormal pigmentation, we eliminated the protein from MNT-1 cells. The fact that ABCB6 is located to lysosomes and early melanosomes indicated that the transporter may manipulate early steps of melanosome biogenesis. Stage I melanosomes have been proposed to be the crossroad where melanosomal and endolysosomal pathways segregate[180]. This expression pattern is where PMEL fibril formation is initiated (Fig. 37). Depletion of ABCB6 by different siRNA constructs was successful, but it did not change the melanin levels significantly. Interestingly, melanin content of the cells was highly variable when various siRNA constructs were used (Fig. 24). Nonetheless, it seemed that the traffic of melanosomal proteins was not disturbed, PMEL- and TRP-1-positive compartments showed separation (Fig. 25). PMEL is targeted to early melanosomes, while further steps include TRP-1 is targeted to late stage melanosomes[181]. However, our collaborators investigated the luminal amyloidogenic fragments of PMEL with HMB45 and I51 antibodies. ABCB6 depletion induced a variable decrease of the steady state levels of PMEL amyloid peptides (not shown)[130]. This suggested that depletion of

ABCB6 may affect the generation of amyloidogenic fragments or their aggregation into fibrils.

Modulation of amyloidogenic PMEL fragment levels has been associated with the defect of several steps in melanogenesis, including PMEL cleavage[180], PMEL sorting[118], the change of lysosomal protease activity[189], or the loss of melanosomal identity[190]. In all of these conditions, the decrease of amyloidogenic PMEL fragment levels was a result of disturbed PMEL fibril formation. Strikingly, morphological analysis at the ultrastructural level revealed a unique phenotype associated with ABCB6 depletion, confirming a defect in fibril formation (Fig. 26). Downregulation of ABCB6 resulted in decreased amyloid formation, and the appearance of large aggregates displaying a hydrangea-like morphology in early and mature melanosomes (Fig. 26). Based on their morphology, the aberrant structures are likely composed of proteo-lipid aggregates, corresponding to the unstructured aggregates containing PMEL luminal domain, as observed in electron microscopic cryosections (Fig. 26). We used MNT-1 cells with downregulated ABCB6 background to test the rescue effect of ABCB6 variants. Expression of the wild-type form of ABCB6 almost fully eliminated the aberrant structures and restored the normal PMEL fibril formation (Fig. 29). Although we observed increased generation of multilamellar lysosomal structures. In the next we investigated the effect of disease related mutations and non-functional ABCB6 mutant (Walker A K562M) in this model. (Mutation of the catalytic Walker A lysine residue is known to impair the function of ABC transporters[191]. Localization experiment in a mouse cell line showed that DUH mutation G579E affects a non-conserved amino acid in the cytoplasmic nucleotide binding domain, though it causes irregular phenotype[152]. In this report a mouse melanoma cell line was used (B16-F1) and the mutant protein showed accumulation in the Golgi. Importantly, in contrast to human skin, mice skin does not contain melanocytes, which are only present in hair follicles[192]. Therefore, mice pigmentation may not be relevant for the role of ABCB6 in human model MNT-1. In our set up both variants, G579E and K562M were targeted to melanosomes, but their association with markers of PMEL amyloidogenic luminal domain and PMEL fibrils was less unequivocal. Despite the appropriate intracellular localization (Fig. 28) neither the G579E nor the K562M mutant ABCB6 variant was able to restore normal biogenesis of PMEL fibrils. The DUH mutant displayed an accumulation of aberrant early, and to a less extent late melanosomes, similarly to

ABCB6-depleted cells (Fig. 29). In contrast, K562M mutant caused the accumulation of aberrant compartments full of protofibrils or small aggregates unable to form fully mature amyloid fibrils, but devoid of the abnormal structures observed in the case of ABCB6 depletion (Fig. 29). Overall, both mutations induced the accumulation of unpigmented aberrant melanosomes, showing signs of improper fibril formation. The depletion and mutation of ABCB6 prevented the normal maturation and organization of the amyloid matrix. The defect in amyloid formation observed in ABCB6-depleted MNT-1 cell line is contrary to the normal phenotype of ABCB6 knockout mice. We cannot rule out the possibility that the mutant transporter may be compensated by other mechanisms as in humans, as in mice. But because of the difference mentioned above between human and mice epidermis, pigmentation process in MNT-1 cell line and mice skin may not be identical. However, in our publication we showed that beneath the normal fur color of *ABCB6* −/− mice there are subtle but significant differences in the ultrastructure of the retinal pigment epithelium (not shown)[193]. In this special epithelial layer, formation of melanosomes is restricted to a brief developmental period[194]. We speculated that an early defect in melanosomal biogenesis impairs the formation or integrity of the organelles in ABCB6 knockouts. Similar phenotypes were described in conditions associated with a defect in PMEL fibril formation and the aggregation of aberrant and toxic PMEL amyloidogenic fragments damaging melanosome integrity[195]. In PMEL mutant mice models the RPE cells have round melanosomes, which indicate a defect in PMEL fibril assembly[183,196,197]. It has been known that characteristic ellipsoidal shape of melanosomes is formed by the fibrils[197,198]. Surprisingly the shape of the remaining melanosomes in the RPE of *ABCB6* knockout mice was not abnormal.

Based on the dominant inheritance of DUH[152] and the fact that ABCB6 functions in homodimers[24,25], we considered that the dominant negative effect can be a straightforward explanation and DUH mutations interfere with the wild-type allele. The DUH G579E mutation did not affect processing of PMEL, or the sorting of its luminal domain onto intraluminal vesicles. Rather, the defect seems to be associated with the last steps of fibrillation. The critical step may be when amyloidogenic PMEL fragments turn into mature fibrils, between stage I melanosomes and stage II melanosomes. At this phase PMEL luminal domain accumulate in multivesicular compartments. The aberrant structures in ABCB6 depleted cells resulting in the misaggregation of amyloid PMEL

luminal domains from the surface of intraluminal vesicles (Fig. 37). The localization of ABCB6 in early melanosomes, the variable melanin levels in ABCB6 attenuated cells and the morphological discrepancies observed by electron microscopy all point toward a defect in early melanogenesis involving PMEL amyloid fibril formation.

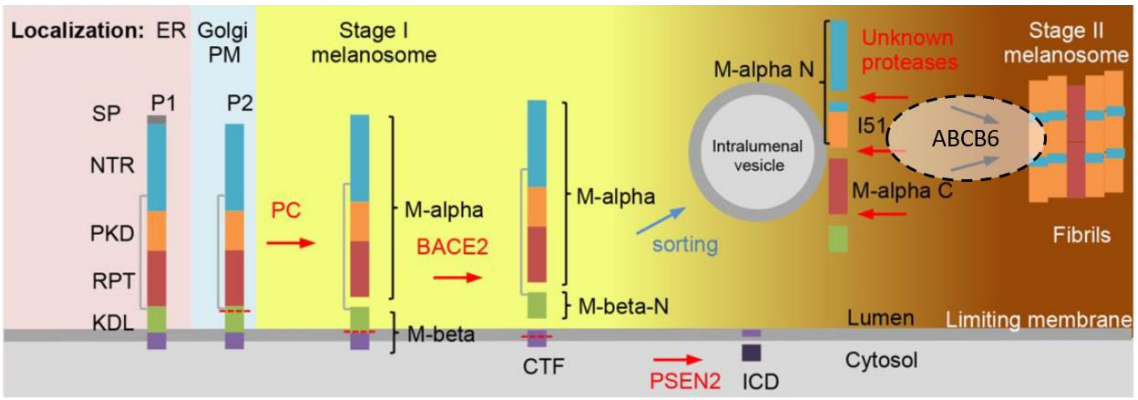

Figure 37. The putative position of ABCB6 function in PMEL fibril formation in stage I melanosomes. PMEL protein domains: signal peptide (SP), N-terminal region (NTR), polycystic kidney disease protein-1-like repeat domain (PKD), repeat domain (RPT), kringle-like domain (KDL), C-terminal fragment (CTF), intracellular domain (ICD). PMEL processing proteases are indicated in red: proprotein convertase (PC), β-site APP-cleaving enzyme 2 (BACE2) and presenilin 2 (PSEN2)[199].

Similarly to the *ABCB6*-null phenotype, complete depletion of PMEL has only a slight effect on the coat color of mice[197], while silver mice expressing a truncated version of PMEL are unable to produce a functional matrix[195], and BACE2 knock out mice that fail to process PMEL[183] display a grey coat color. The hypopigmented areas characteristic to DUH in humans may result from a defect in the maturation of early melanosomes or from the compromised integrity of pigmented melanosomes due to the accumulation of PMEL toxic oligomers[200].

In melanoma cells overexpressing wild type ABCB6 the number of lysosomes and the presence of lysosomal structures were increased (Fig. 30). It was tempting to speculate that ABCB6 may be involved in this process either by regulating lysosome activity or by influencing inter-organelle interactions between lysosomes and early melanosomes. A recent study strengthens our hypothesis, in which the authors observed that the substrate PMEL, localized to stage I melanosomes is processed by lysosomal proteases through transient fusions of stage I melanosomes and endolysosomes. These inter-organellar

"kiss-and-run" supports the role of stage I melanosomes as a crossroad between melanosomal and endolysosomal pathways[199].

DUH skin biopsies indicated a normal number of intact melanocytes in both hypo- and hyper-pigmented skin areas, a lower number of mature melanosomes in hypo-pigmented macules and an accumulation of pigmented melanosomes in melanocytes and in keratinocytes in hyper-pigmented macules[177].

At the same time, we cannot exclude the possibility that the DUH phenotype is due to a defect in the transfer of mature melanosomes to keratinocytes. To exclude this a different model system would be needed. Once transferred to keratinocytes, melanosomes are either stored in non-degradative compartments or degraded by lysosomal hydrolases. It is also possible that ABCB6 influences these events through its expression and function in lysosomes of keratinocytes[201–203].

5.3. MNT-1 cell lines genome edited by CRISPR/Cas9

A further new experimental model was established in this study where CRISPR genome editing method was used to assess the localization and function of endogenously regulated gene. Artificially overexpress a protein is not always expedient, especially in localization studies. It has a risk that a membrane transporter may appear in incorrect membrane structures, misleading the conclusion about the function. We should be aware that we may detect lysosomal localization due to overproduction and degradation. Because of this, we wanted to detect the intracellular distribution of ABCB6 using the latest gene editing method and suggest a functional model explaining the DUH phenotype. Frist, we performed FISH analysis to ascertain the copy number of the gene of interest. Results indicated that MNT-1 cells have four *ABCB6* alleles. Then, we created different cell lines modifying *ABCB6* at genomic level. At first, the lysosomal localization of the transporter was verified by a GFP tag fused to endogenous *ABCB6* gene by CRISPR method in MNT-1 cells. (Fig. 32). For more detailed analysis of ABCB6 trafficking between cellular compartments we applied RUSH system. By applying an additional SBP tag upstream to GFP sequence in genetic code of ABCB6 we could establish a RUSH system for analysis the process. We are currently in the preliminary stages of experimentation, when the hook peptide is not expressed in the cells. We confirmed that ABCB6-SBP-GFP and the endogenous ABCB6-GFP constructs showed identical,

lysosomal localization. These were in line with the previous results of the group. Investigating synchronized trafficking of ABCB6 remains a task for the future. Parallel with localization experiments, ABCB6 knock out cell line was generated for functional studies. We exploited the four SBP-GFP tagged alleles, as followed by ceasing of green fluorescent signal. Clones were validated at genomic and at protein level as well (Fig. 34). We hypothesized that elimination of ABCB6 from a highly pigmented melanoma cell line will alter the melanotic feature of the cells. But measuring the melanin levels of parental, ABCB6 overexpressed, and ABCB6-KO cell lines were hardly conclusive. The knockdown of ABCB6 did not clearly reduce the melanin content of MNT-1 cells (Fig. 36). This is consistent with results obtained by RNA silencing of ABCB6 (Fig. 24).

Although pigmentation problems associated with ABCB6 probably connected to melanosome function current experiments were unable to clearly identify the function of this transporter. Understanding the relevance of ABCB6 in melanogenesis will require a better understanding of the function of ABCB6 in the endolysosomal system. ABCB6 may be involved in regulating lysosomal activity or influencing inter-organelle interactions. We are speculating that based on our experiments in orthologue organisms we have to investigate more thoroughly the endolysosomal metal homeostasis to understand the role of ABCB6. Unfortunately, we still do not know the physiological substrate of ABCB6 in mammalian cells, but identification of possible substrates is an ongoing project that is clearly a main point in finding function.

DOI:10.14753/SE.2020.2354

6. Conclusion

The intracellular localization of ABCB6 has been a matter of debate, with conflicting reports suggesting mitochondrial or endolysosomal localization. ABCB6 shows significant sequence identity to HMT-1 (heavy metal tolerance factor 1) proteins, whose evolutionarily conserved role is to confer tolerance to heavy metals through the intracellular sequestration of metal complexes. We hypothesized that the cadmium-sensitive phenotype of *S. pombe* and *C. elegans* strains defective for HMT-1 can be rescued by the human ABCB6 protein. It may be argued that the precise intracellular localization can only be established with the discovery of a matching physiological function. First, we showed that ABCB6 localizes to the same intracellular compartment as HMT-1 in these models, performing an overlapping function linked to the intracellular sequestration of metal complexes. Second, we revealed that ABCB6 rescues the Cd-sensitive phenotype of HMT-1-deficient *S. pombe* and *C. elegans* strains. Third, we provided evidence that ABCB6 modulates the cadmium sensitivity of human glioblastoma cells. Determining the subcellular localization of a protein is a key step toward understanding its cellular function. Based on our previous results ABCB6 undoubtedly traffics through the ER, as it exists as an N-glycosylated protein[67]. Similar to ABCB6, HMT-1 lacking the NTE domain was targeted to the plasma membrane, and did not confer tolerance to Cd[95]. In addition to evidence based on imaging of ABCB6 in organisms, in our work we provided functional proof supporting the role of ABCB6 in the vacuolar/endosomal sequestration of cadmium[132].

In 2013, it was published, that there is a link between certain ABCB6 mutations and the pigmentary disorder DUH[30]. The disease shows autosomal dominant inheritance, but the mechanism how ABCB6 affects skin pigmentation is not known. Therefore, in an attempt to understand the link between ABCB6 mutations and the DUH phenotype, we investigated the subcellular localization and function of ABCB6 in a human melanocytic cell line MNT-1. Consistent with our other results we corroborated the localization of ABCB6 in the endolysosomal continuum[24,67,132]. Endogenous ABCB6 was localized to lysosomes and early melanosomes, which was validated by the examination of GFP labeled endogenous protein created by the latest genome editing method. ABCB6 depletion in melanoma cells resulted decreased amyloid formation, and the appearance of large aggregates in early and maturing melanosomes. The DUH mutant G579E or the

inactive K562M mutant variant also induced the accumulation of unpigmented aberrant melanosomes and could not restore normal biogenesis of PMEL fibrils. We speculated that ABCB6 affects the generation of amyloidogenic fragments or their aggregation into fibrils. Although we have found a slight but significant effect of ABCB6 in melanoma cell line in vivo data shows even less effect. It is known that total lack of ABCB6 in humans (Lan negative phenotype) does not cause any problem and ABCB6 knockout mice show no pathologic phenotype either in skin[68]. But there is a well-marked difference in the ultrastructure of the retinal pigment epithelium, where the density of melanosomes in *ABCB6*+/− and *ABCB6*−/− mice was significantly lower[193]. Given the rare occurrence of Cd in mammalian cells, we believe that ABCB6 is involved in certain metal-complex transport in the lysosomal system. Since stage I melanosomes are at the crossroad of melanosomal and endolysosomal pathways[199] ABCB6 may also play a role in melanin-forming activity of melanocytes linked to a cell specific endolysosomal function. Based on our research, we assume that the function of ABCB6 is not related to the mitochondria but to the endolysosomal compartment. However, further studies are needed to understand the physiological role of ABCB6.

DOI:10.14753/SE.2020.2354

7. Summary

In the human genome 48 different ABC (ATP binding cassette) proteins have been defined. In my PhD work I studied ABCB6, member of ABCB subfamily. Intracellular localization of ABCB6 has been a matter of debate. Our laboratory has provided evidence to support the endolysosomal localization of the protein, however, the physiological function of ABCB6 has remained elusive. My overall aim was to study the function and the pathophysiological role of ABCB6.

ABCB6 shows significant sequence identity to HMT-1 (heavy metal tolerance factor-1) proteins, whose role in lower organisms is to confer tolerance to heavy metals through intracellular sequestration of metal complexes. To examine the relation between ABCB6 and HMT-1 proteins, human ABCB6 was heterologously expressed in model organisms. We showed that ABCB6 rescues the Cd-sensitive phenotype of HMT-1-deficient *S. pombe* and *C. elegans* strains. In addition, ABCB6 is located in the lysosomes of human glioblastoma cells and increased cadmium tolerance of the cells.

However, absence of the protein does not lead to pathological changes, genetic studies revealed that mutations in *ABCB6* can cause distinct phenotypes: familial pseudohyperkalemia, ocular coloboma or DUH. DUH (Dyschromatosis universalis hereditaria) is a pigmentary genodermatosis with hyperpigmented and hypopigmented macules on the skin. To decipher the role of ABCB6 in melanogenesis, we expressed wild-type and mutant ABCB6 in MNT-1 melanoma cell line, which are widely used to model pigmentation processes. We showed that ABCB6 is localized to lysosomes and early melanosomes of MNT-1 cells. Early melanosomes are at the crossroad between melanosomal and endolysosomal pathways, where fibril formation is initiated. Downregulation of ABCB6 in MNT-1 cells resulted in decreased amyloid formation, and the appearance of proteo-lipid aggregates in early and mature melanosomes. In case of the expression of the mutant variants, similar aberrant structures were observed.

To summarize, we provided functional proof supporting the role of ABCB6 in the vacuolar/endosomal sequestration of cadmium. Furthermore, we showed that ABCB6 is expressed in lysosomes and early melanosomes of pigment cells and regulate early steps of melanogenesis. Our results provide functional evidence linking ABCB6 to endolysosomal compartment. This paves the way for further research to fully understand the pathophysiological role of this membrane transporter.

DOI:10.14753/SE.2020.2354

8. Összefoglalás

A humán genomban 48 ABC (ATP-kötő kazetta) fehérjét azonosítottak, melyek közül doktori munkám során a „B” alcsalád egy tagját, az ABCB6-ot tanulmányoztam. Az ABCB6 sejten belüli elhelyezkedése régóta vita tárgyát képezi. Az évek során kutatócsoportunk számos bizonyítékot szolgáltatott az ABCB6 endolizoszómális jelenlétére, azonban a fehérje élettani szerepe továbbra is kérdéses. Kutatásom során a célom az ABCB6 működésének és patofiziológiai szerepének tanulmányozása volt.

Filogenetikai elemzések alapján az ABCB6 jelentős szekvenciális hasonlóságot mutat a HMT-1 (nehézfém tolerancia faktor-1) fehérjecsaláddal, melyek alacsonyabb rendű élőlényekben nyújtanak védelmet a fémek intracelluláris transzportja révén. Az ABCB6 és a HMT-1 fehérjék kapcsolatának vizsgálatához a humán ABCB6-t heterológ módon termeltettük modell organizmusokban. Eredményeink alapján azt láttuk, hogy az ABCB6 képes menekíteni a HMT-1-hiányos *S. pombe* és *C. elegans* törzsek Cd-érzékeny fenotípusát. Ezen túlmenően az ABCB6 a humán glioblastoma sejtek lizoszómáiban lokalizálódott és képes volt fokozott Cd toleranciát biztosítani a sejteknek.

Annak ellenére, hogy a fehérje hiánya nem vezet kóros következményekhez, genetikai elemzések kimutatták, hogy az *ABCB6* mutációihoz többféle fenotípus is köthető: coloboma, familiáris pszeudohyperkalémia és a DUH. A DUH (Dyschromatosis universalis hereditaria) egy pigmentációs zavar, melynél a bőrön hiper- vagy hypopigmentált foltok figyelhetőek meg. Az ABCB6 melanogenezisben betöltött szerepének megfejtéséhez humán melanóma sejtben (MNT-1) vizsgáltuk a vad típusú és a mutáns ABCB6 változatokat. Megmutattuk, hogy az ABCB6 az MNT-1 sejtek lizoszómáiban és korai melanoszómáiban fordul elő. Az ABCB6 csendesítése során a sejtek korai és érett melanoszómáiban csökkent fibrillumképződést és fehérje-lipid aggregátumok megjelenését tapasztaltuk. A mutáns variánsok expressziója esetén hasonló aberráns struktúrák voltak megfigyelhetőek, tehát a mutáns fehérjék nem voltak képesek helyreállítani a normális fibrillum és melanoszóma képződést.

Kutatásaink alapján azt mondhatjuk, hogy az ABCB6 funkciója az endolizoszomális kompartmenthez kötődik, szerepet játszik a Cd intracelluláris detoxifikációjában, valamint melanoma sejtekben a lizoszómákban és korai melanoszómáiban található. Ahhoz viszont, hogy az ABCB6 patofiziológiai szerepét megértsük, még további kísérleteket kell végeznünk.

9. References

1. Dean M. (2001) The Human ATP-Binding Cassette (ABC) Transporter Superfamily. Genome Res 11:1156–1166.
2. Walker JE, Saraste M, Runswick MJ, Gay NJ. (1982) Distantly related sequences in the alpha- and beta-subunits of ATP synthase, myosin, kinases and other ATP-requiring enzymes and a common nucleotide binding fold. EMBO J 1:945–951.
3. Locher KP. (2009) Structure and mechanism of ATP-binding cassette transporters. Philos Trans R Soc B Biol Sci 364:239–245.
4. Locher KP. (2016) Mechanistic diversity in ATP-binding cassette (ABC) transporters. Nat Struct Mol Biol 23:487–493.
5. Oldham ML, Davidson AL, Chen J. (2008) Structural insights into ABC transporter mechanism. Curr Opin Struct Biol 18:726–733.
6. Ford RC, Beis K. (2019) Learning the ABCs one at a time: structure and mechanism of ABC transporters. Biochem Soc Trans BST20180147.
7. Higgins CF. (2007) Multiple molecular mechanisms for multidrug resistance transporters. Nature 446:749–757.
8. Robey RW, Pluchino KM, Hall MD, Fojo AT, Bates SE, Gottesman MM. (2018) Revisiting the role of ABC transporters in multidrug-resistant cancer. Nat Rev Cancer 18:452–464.
9. Cole SPC. (2014) Multidrug Resistance Protein 1 (MRP1, ABCC1), a "Multitasking" ATP-binding Cassette (ABC) Transporter. J Biol Chem 289:30880–30888.
10. Sarkadi B, Homolya L, Szakács G, Váradi A. (2006) Human Multidrug Resistance ABCB and ABCG Transporters: Participation in a Chemoimmunity Defense System. Physiol Rev 86:1179–1236.
11. Gottesman MM, Fojo T, Bates SE. (2002) Multidrug resistance in cancer: role of ATP–dependent transporters. Nat Rev Cancer 2:48–58.
12. Duarte AA, Gogola E, Sachs N, Barazas M, Annunziato S, R de Ruiter J, Velds A, Blatter S, Houthuijzen JM, van de Ven M, Clevers H, Borst P, Jonkers J, Rottenberg S. (2018) BRCA-deficient mouse mammary tumor organoids to study cancer-drug resistance. Nat Methods 15:134–140.

13. Domenichini A, Adamska A, Falasca M. (2019) ABC transporters as cancer drivers: Potential functions in cancer development. Biochim Biophys Acta BBA - Gen Subj 1863:52–60.
14. Cheng Y, Woolf TF, Gan J, He K. (2016) In vitro model systems to investigate bile salt export pump (BSEP) activity and drug interactions: A review. Chem Biol Interact 255:23–30.
15. Neumann J, Rose-Sperling D, Hellmich UA. (2017) Diverse relations between ABC transporters and lipids: An overview. Biochim Biophys Acta BBA - Biomembr 1859:605–618.
16. Thomas C, Tampé R. (2019) MHC I chaperone complexes shaping immunity. Curr Opin Immunol 58:9–15.
17. Csanády L, Vergani P, Gadsby DC. (2019) Structure, Gating, and Regulation of the CFTR Anion Channel. Physiol Rev 99:707–738.
18. Bull LN, Thompson RJ. (2018) Progressive Familial Intrahepatic Cholestasis. Clin Liver Dis 22:657–669.
19. Zollmann T, Bock C, Graab P, Abele R. (2015) Team work at its best – TAPL and its two domains. Biol Chem 396.
20. Schaedler TA, Faust B, Shintre CA, Carpenter EP, Srinivasan V, van Veen HW, Balk J. (2015) Structures and functions of mitochondrial ABC transporters. Biochem Soc Trans 43:943–951.
21. Chacinska A, Koehler CM, Milenkovic D, Lithgow T, Pfanner N. (2009) Importing Mitochondrial Proteins: Machineries and Mechanisms. Cell 138:628–644.
22. Maio N, Kim KS, Holmes-Hampton G, Singh A, Rouault TA. (2019) Dimeric ferrochelatase bridges ABCB7 and ABCB10 homodimers in an architecturally defined molecular complex required for heme biosynthesis. Haematologica haematol.2018.214320.
23. Ichikawa Y, Bayeva M, Ghanefar M, Potini V, Sun L, Mutharasan RK, Wu R, Khechaduri A, Jairaj Naik T, Ardehali H. (2012) Disruption of ATP-binding cassette B8 in mice leads to cardiomyopathy through a decrease in mitochondrial iron export. Proc Natl Acad Sci U S A 109:4152–4157.
24. Kiss K, Brozik A, Kucsma N, Toth A, Gera M, Berry L, Vallentin A, Vial H, Vidal M, Szakacs G. (2012) Shifting the Paradigm: The Putative Mitochondrial Protein

ABCB6 Resides in the Lysosomes of Cells and in the Plasma Membrane of Erythrocytes. PLoS ONE 7:e37378.

25. Krishnamurthy PC, Du G, Fukuda Y, Sun D, Sampath J, Mercer KE, Wang J, Sosa-Pineda B, Murti KG, Schuetz JD. (2006) Identification of a mammalian mitochondrial porphyrin transporter. Nature.
26. Chavan H, Taimur Khan MMd, Tegos G, Krishnamurthy P. (2013) Efficient Purification and Reconstitution of ATP Binding Cassette Transporter B6 (ABCB6) for Functional and Structural Studies. J Biol Chem 288:22658–22669.
27. Mitsuhashi N, Miki T, Senbongi H, Yokoi N, Yano H, Miyazaki M, Nakajima N, Iwanaga T, Yokoyama Y, Shibata T, Seino S. (2000) MTABC3, a Novel Mitochondrial ATP-binding Cassette Protein Involved in Iron Homeostasis*□S 7.
28. Helias V, Saison C, Ballif BA, Peyrard T, Takahashi J, Takahashi H, Tanaka M, Deybach J-C, Puy H, Le Gall M, Sureau C, Pham B-N, Le Pennec P-Y, Tani Y, Cartron J-P, Arnaud L. (2012) ABCB6 is dispensable for erythropoiesis and specifies the new blood group system Langereis. Nat Genet 44:170–173.
29. Koszarska M, Kucsma N, Kiss K, Varady G, Gera M, Antalffy G, Andrikovics H, Tordai A, Studzian M, Strapagiel D, Pulaski L, Tani Y, Sarkadi B, Szakacs G. (2014) Screening the Expression of ABCB6 in Erythrocytes Reveals an Unexpectedly High Frequency of Lan Mutations in Healthy Individuals. PLoS ONE 9:e111590.
30. Zhang C, Li D, Zhang J, Chen X, Huang M, Archacki S, Tian Y, Ren W, Mei A, Zhang Q, Fang M, Su Z, Yin Y, Liu D, Chen Y, Cui X, Li C, Yang H, Wang Q, Wang J, Liu M, Deng Y. (2013) Mutations in ABCB6 Cause Dyschromatosis Universalis Hereditaria. J Invest Dermatol 133:2221–2228.
31. Váradi A, Szakács G, Bakos É, Sarkadi B. (2008) P glycoprotein and the Mechanism of Multidrug Resistance, p. 54–68. *In* Bock, G, Goode, JA (eds.), Novartis Foundation Symposia. John Wiley & Sons, Ltd, Chichester, UK.
32. Furuya KN, Bradley G, Sun D, Schuetz EG, Schuetz JD. (1997) Identification of a New P-glycoprotein-like ATP-binding Cassette Transporter Gene That Is Overexpressed during Hepatocarcinogenesis. Cancer Res 57:3708–3716.

33. Savary S, Allikmets R, Denizot F, Luciani M-F, Mattei M-G, Dean M, Chimini G. (1997) Isolation and Chromosomal Mapping of a Novel ATP-Binding Cassette Transporter Conserved in Mouse and Human. Genomics 41:275–278.
34. Ortiz DF, Kreppel' L, Speiser DM, Scheel G, McDonald G, Ow DW. (1992) Heavy metal tolerance in the fission yeast requires an ATP-binding cassette-type vacuolar membrane 9.
35. Gebel TW, Leister M, Schumann W, Hirsch-Ernst K. (2002) Low-level self-tolerance to arsenite in human HepG2 cells is associated with a depressed induction of micronuclei. Mutat Res Toxicol Environ Mutagen 514:245–255.
36. Emadi-Konjin H-P, Zhang H, Anandan V, Sun D, Schuetz J, Furuya KN. (2002) Isolation of a genomic clone containing the promoter region of the human ATP binding cassette (ABC) transporter, ABCB6. Biochim Biophys Acta BBA - Gene Struct Expr 1574:117–130.
37. Piel RB, Dailey HA, Medlock AE. (2019) The mitochondrial heme metabolon: Insights into the complex(ity) of heme synthesis and distribution. Mol Genet Metab.
38. Krishnamurthy P, Xie T, Schuetz J. (2007) The role of transporters in cellular heme and porphyrin homeostasis. Pharmacol Ther 114:345–358.
39. Lynch J, Fukuda Y, Krishnamurthy P, Du G, Schuetz JD. (2009) Cell Survival under Stress Is Enhanced by a Mitochondrial ATP-Binding Cassette Transporter That Regulates Hemoproteins. Cancer Res 69:5560–5567.
40. Yasui K, Mihara S, Zhao C, Okamoto H, Saito-Ohara F, Tomida A, Funato T, Yokomizo A, Naito S, Imoto I, Tsuruo T, Inazawa J. (2004) Alteration in copy numbers of genes as a mechanism for acquired drug resistance. Cancer Res 64:1403–1410.
41. Park S, Shimizu C, Shimoyama T, Takeda M, Ando M, Kohno T, Katsumata N, Kang Y-K, Nishio K, Fujiwara Y. (2006) Gene expression profiling of ATP-binding cassette (ABC) transporters as a predictor of the pathologic response to neoadjuvant chemotherapy in breast cancer patients. Breast Cancer Res Treat 99:9–17.

42. Januchowski R, Zawierucha P, Andrzejewska M, Ruciński M, Zabel M. (2013) Microarray-based detection and expression analysis of ABC and SLC transporters in drug-resistant ovarian cancer cell lines. Biomed Pharmacother 67:240–245.
43. Heimerl S, Bosserhoff AK, Langmann T, Ecker J, Schmitz G. (2007) Mapping ATP-binding cassette transporter gene expression profiles in melanocytes and melanoma cells: Melanoma Res 17:265–273.
44. Hübner R-H, Schwartz JD, De BP, Ferris B, Omberg L, Mezey JG, Hackett NR, Crystal RG. (2009) Coordinate Control of Expression of Nrf2-Modulated Genes in the Human Small Airway Epithelium Is Highly Responsive to Cigarette Smoking 17.
45. Chavan H, Oruganti M, Krishnamurthy P. (2011) The ATP-Binding Cassette Transporter ABCB6 Is Induced by Arsenic and Protects against Arsenic Cytotoxicity. Toxicol Sci 120:519–528.
46. Zhang Y-K, Dai C, Yuan C, Wu H-C, Xiao Z, Lei Z-N, Yang D-H, Le XC, Fu L, Chen Z-S. (2017) Establishment and characterization of arsenic trioxide resistant KB/ATO cells. Acta Pharm Sin B 7:564–570.
47. Minami K, Kamijo Y, Nishizawa Y, Tabata S, Horikuchi F, Yamamoto M, Kawahara K, Shinsato Y, Tachiwada T, Chen Z-S, Tsujikawa K, Nakagawa M, Seki N, Akiyama S-I, Arima K, Takeda Y, Furukawa T. (2014) Expression of ABCB6 Is Related to Resistance to 5-FU, SN-38 and Vincristine. ANTICANCER Res 7.
48. Gómez MA, Navas A, Márquez R, Rojas LJ, Vargas DA, Blanco VM, Koren R, Zilberstein D, Saravia NG. (2014) Leishmania panamensis infection and antimonial drugs modulate expression of macrophage drug transporters and metabolizing enzymes: impact on intracellular parasite survival. J Antimicrob Chemother 69:139–149.
49. Joseph S, Nicolson TJ, Hammons G, Word B, Green-Knox B, Lyn-Cook B. (2015) Expression of drug transporters in human kidney: impact of sex, age, and ethnicity. Biol Sex Differ 6.
50. Sun N-K, Huang S-L, Lu H-P, Chang T-C, Chao CC-K. (2015) Integrative transcriptomics-based identification of cryptic drivers of taxol-resistance genes in ovarian carcinoma cells: Analysis of the androgen receptor. Oncotarget 6.

51. Karatas OF, Guzel E, Duz MB, Ittmann M, Ozen M. (2016) The role of ATP-binding cassette transporter genes in the progression of prostate cancer: ABC Transporters in Prostate Cancer Progression. The Prostate 76:434–444.
52. Zhao S-G, Chen X-F, Wang L-G, Yang G, Han D-Y, Teng L, Yang M-C, Wang D-Y, Shi C, Liu Y-H, Zheng B-J, Shi C-B, Gao X, Rainov NG. (2013) Increased Expression of ABCB6 Enhances Protoporphyrin IX Accumulation and Photodynamic Effect in Human Glioma. Ann Surg Oncol 20:4379–4388.
53. Nakayama T, Otsuka S, Kobayashi T, Okajima H, Matsumoto K, Hagiya Y, Inoue K, Shuin T, Nakajima M, Tanaka T, Ogura S. (2016) Dormant cancer cells accumulate high protoporphyrin IX levels and are sensitive to 5-aminolevulinic acid-based photodynamic therapy. Sci Rep 6.
54. Varatharajan S, Abraham A, Karathedath S, Ganesan S, Lakshmi KM, Arthur N, Srivastava VM, George B, Srivastava A, Mathews V, Balasubramanian P. (2017) ATP-binding casette transporter expression in acute myeloid leukemia: association with *in vitro* cytotoxicity and prognostic markers. Pharmacogenomics 18:235–244.
55. Sun H, Buchon N, Scott JG. (2017) Mdr65 decreases toxicity of multiple insecticides in Drosophila melanogaster. Insect Biochem Mol Biol 89:11–16.
56. Abdul Jalil Y, Ritz V, Jakimenko A, Schmitz-Salue C, Siebert H, Awuah D, Kotthaus A, Kietzmann T, Ziemann C, Hirsch-Ernst KI. (2008) Vesicular localization of the rat ATP-binding cassette half-transporter rAbcb6. Am J Physiol-Cell Physiol 294:C579–C590.
57. Campbell MR, Karaca M, Adamski KN, Chorley BN, Wang X, Bell DA. (2013) Novel Hematopoietic Target Genes in the NRF2-Mediated Transcriptional Pathway. Oxid Med Cell Longev 2013:1–12.
58. Ulrich DL, Lynch J, Wang Y, Fukuda Y, Nachagari D, Du G, Sun D, Fan Y, Tsurkan L, Potter PM, Rehg JE, Schuetz JD. (2012) ATP-dependent Mitochondrial Porphyrin Importer ABCB6 Protects against Phenylhydrazine Toxicity. J Biol Chem 287:12679–12690.
59. Aguiar JA, Tamminga A, Lobb B, Huff RD, Nguyen JP, Kim Y, Dvorkin-Gheva A, Stampfli MR, Doxey AC, Hirota JA. (2019) The impact of cigarette smoke exposure, COPD, or asthma status on ABC transporter gene expression in human airway epithelial cells. Sci Rep 9.

60. Kaisar MA, Sivandzade F, Bhalerao A, Cucullo L. (2018) Conventional and electronic cigarettes dysregulate the expression of iron transporters and detoxifying enzymes at the brain vascular endothelium: In vivo evidence of a gender-specific cellular response to chronic cigarette smoke exposure. Neurosci Lett 682:1–9.
61. Sarkar R, Kishida S, Kishida M, Nakamura N, Kibe T, Karmakar D, Chaudhuri CR, Barui A. (2019) Effect of cigarette smoke extract on mitochondrial heme-metabolism: An in vitro model of oral cancer progression. Toxicol In Vitro 60:336–346.
62. Egan ES, Weekes MP, Kanjee U, Manzo J, Srinivasan A, Lomas-Francis C, Westhoff C, Takahashi J, Tanaka M, Watanabe S, Brugnara C, Gygi SP, Tani Y, Duraisingh MT. (2018) Erythrocytes lacking the Langereis blood group protein ABCB6 are resistant to the malaria parasite Plasmodium falciparum. Commun Biol 1.
63. Paterson JK, Shukla S, Black CM, Tachiwada T, Garfield S, Wincovitch S, Ernst DN, Agadir A, Li X, Ambudkar SV, Szakacs G, Akiyama S, Gottesman MM. (2007) Human ABCB6 Localizes to Both the Outer Mitochondrial Membrane and the Plasma Membrane †. Biochemistry 46:9443–9452.
64. Tsuchida M, Emi Y, Kida Y, Sakaguchi M. (2008) Human ABC transporter isoform B6 (ABCB6) localizes primarily in the Golgi apparatus. Biochem Biophys Res Commun 369:369–375.
65. Krishnamurthy P, D. Schuetz J. (2011) The Role of ABCG2 and ABCB6 in Porphyrin Metabolism and Cell Survival. Curr Pharm Biotechnol 12:647–655.
66. Fukuda Y, Aguilar-Bryan L, Vaxillaire M, Dechaume A, Wang Y, Dean M, Moitra K, Bryan J, Schuetz JD. (2011) Conserved Intramolecular Disulfide Bond Is Critical to Trafficking and Fate of ATP-binding Cassette (ABC) Transporters ABCB6 and Sulfonylurea Receptor 1 (SUR1)/ABCC8. J Biol Chem 286:8481–8492.
67. Kiss K, Kucsma N, Brozik A, Tusnady GE, Bergam P, van Niel G, Szakacs G. (2015) Role of the N-terminal transmembrane domain in the endo-lysosomal targeting and function of the human ABCB6 protein. Biochem J 467:127–139.
68. Chavan H, Krishnamurthy P. (2012) Polycyclic Aromatic Hydrocarbons (PAHs) Mediate Transcriptional Activation of the ATP Binding Cassette Transporter

ABCB6 Gene via the Aryl Hydrocarbon Receptor (AhR). J Biol Chem 287:32054–32068.

69. Guengerich FP. (2017) Intersection of the Roles of Cytochrome P450 Enzymes with Xenobiotic and Endogenous Substrates: Relevance to Toxicity and Drug Interactions. Chem Res Toxicol 30:2–12.
70. Chavan H, Li F, Tessman R, Mickey K, Dorko K, Schmitt T, Kumer S, Gunewardena S, Gaikwad N, Krishnamurthy P. (2015) Functional Coupling of ATP-binding Cassette Transporter Abcb6 to Cytochrome P450 Expression and Activity in Liver. J Biol Chem 290:7871–7886.
71. Phillips JD. (2019) Heme biosynthesis and the porphyrias. Mol Genet Metab.
72. Fukuda Y, Cheong PL, Lynch J, Brighton C, Frase S, Kargas V, Rampersaud E, Wang Y, Sankaran VG, Yu B, Ney PA, Weiss MJ, Vogel P, Bond PJ, Ford RC, Trent RJ, Schuetz JD. (2016) The severity of hereditary porphyria is modulated by the porphyrin exporter and Lan antigen ABCB6. Nat Commun 7.
73. Polireddy K, Chavan H, Abdulkarim BA, Krishnamurthy P. (2011) Functional significance of the ATP-binding cassette transporter B6 in hepatocellular carcinoma. Mol Oncol 5:410–425.
74. Borel F, Han R, Visser A, Petry H, van Deventer SJH, Jansen PLM, Konstantinova P, with collaboration of the Réseau Centre de Ressources Biologiques Foie (French Liver Biobanks Network), France. (2012) Adenosine triphosphate-binding cassette transporter genes up-regulation in untreated hepatocellular carcinoma is mediated by cellular microRNAs. Hepatology 55:821–832.
75. Wang L, He F, Bu J, Liu X, Du W, Dong J, Cooney JD, Dubey SK, Shi Y, Gong B, Li J, McBride PF, Jia Y, Lu F, Soltis KA, Lin Y, Namburi P, Liang C, Sundaresan P, Paw BH, Li DY, Phillips JD, Yang Z. (2012) ABCB6 Mutations Cause Ocular Coloboma. Am J Hum Genet 90:40–48.
76. van der HART null, Moes M, van LOGHEM J, Enneking JH, Leeksma CH. (1961) A second example of red cell polyagglutinability caused by the Tn antigen. Vox Sang 6:358–361.
77. Smith DS, Stratton F, Johnson T, Brown R, Howell P, Riches R. (1969) Haemolytic disease of the newborn caused by anti-Lan antibody. Br Med J 3:90–92.

78. Okubo Y, Yamaguchi H, Seno T, Araki Y, Noguchi M, Shioda K, Takai M, Daniels GL. (1984) The rare red cell phenotype Lan negative in Japanese. Transfusion (Paris) 24:534–535.
79. Polireddy K, Khan MMdT, Chavan H, Young S, Ma X, Waller A, Garcia M, Perez D, Chavez S, Strouse JJ, Haynes MK, Bologa CG, Oprea TI, Tegos GP, Sklar LA, Krishnamurthy P. (2012) A Novel Flow Cytometric HTS Assay Reveals Functional Modulators of ATP Binding Cassette Transporter ABCB6. PLoS ONE 7:e40005.
80. Saison C, Helias V, Peyrard T, Merad L, Cartron J-P, Arnaud L. (2013) The ABCB6 mutation p.Arg192Trp is a recessive mutation causing the Lan− blood type: A missense mutation causing the Lan− blood type. Vox Sang 104:159–165.
81. Andolfo I, Alper SL, Delaunay J, Auriemma C, Russo R, Asci R, Esposito MR, Sharma AK, Shmukler BE, Brugnara C, De Franceschi L, Iolascon A. (2013) Missense mutations in the ABCB6 transporter cause dominant familialpseudohyperkalemia. Am J Hematol 88:66–72.
82. Reid ME, Hue-Roye K, Huang A, Velliquette RW, Tani Y, Westhoff CM, Lomas-Francis C, Zelinski T. (2013) Alleles of the LAN blood group system: molecular and serologic investigations: Alleles of the LAN Blood Group System. Transfusion (Paris) n/a-n/a.
83. Cui Y-X, Xia X-Y, Zhou Y, Gao L, Shang X-J, Ni T, Wang W-P, Fan X-B, Yin H-L, Jiang S-J, Yao B, Hu Y-A, Wang G, Li X-J. (2013) Novel Mutations of ABCB6 Associated with Autosomal Dominant Dyschromatosis Universalis Hereditaria. PLoS ONE 8:e79808.
84. Tanaka M, Yamamuro Y, Takahashi J, Ogasawara K, Osabe T, Tsuneyama H, Enomoto T, Watanabe S, Uchikawa M, Tadokoro K, Tani Y. (2014) Novel alleles of Lan− in Japanese populations: Removal of BRMs in PCs by columns. Transfusion (Paris) 54:1438–1439.
85. Haer-Wigman L, Ait Soussan A, Ligthart P, de Haas M, van der Schoot CE. (2014) Molecular analysis of immunized Jr(a-) or Lan- patients and validation of a high-throughput genotyping assay to screen blood donors for Jr(a-) and Lan- phenotypes: Genotyping of the Jr(a-) and Lan- Phenotype. Transfusion (Paris) 54:1836–1846.

86. Schoeman EM, Roulis EV, Liew Y-W, Martin JR, Powley T, Wilson B, Millard GM, McGowan EC, Lopez GH, O'Brien H, Condon JA, Flower RL, Hyland CA. (2018) Targeted exome sequencing defines novel and rare variants in complex blood group serology cases for a red blood cell reference laboratory setting: EXOME SEQUENCING FOR COMPLEX BLOOD GROUPS. Transfusion (Paris) 58:284–293.

87. Liu H, Li Y, Hung KKH, Wang N, Wang C, Chen X, Sheng D, Fu X, See K, Foo JN, Low H, Liany H, Irwan ID, Liu J, Yang B, Chen M, Yu Y, Yu G, Niu G, You J, Zhou Y, Ma S, Wang T, Yan X, Goh BK, Common JEA, Lane BE, Sun Y, Zhou G, Lu X, Wang Z, Tian H, Cao Y, Chen S, Liu Q, Liu J, Zhang F. (2014) Genome-Wide Linkage, Exome Sequencing and Functional Analyses Identify ABCB6 as the Pathogenic Gene of Dyschromatosis Universalis Hereditaria. PLoS ONE 9:e87250.

88. Lu C, Liu J, Liu F, Liu Y, Ma D, Zhang X. (2014) Novel missense mutations of ABCB6 in two chinese families with dyschromatosis universalis hereditaria. J Dermatol Sci 76:255–258.

89. Liu J-W, Asan, Sun J, Vano-Galvan S, Liu F-X, Wei X-X, Ma D-L. (2016) Differential Diagnosis of Two Chinese Families with Dyschromatoses by Targeted Gene Sequencing. Chin Med J (Engl) 129:33.

90. Jayanthi NS. (2016) A Case Report of Dyschromatosis Universalis Hereditaria (DUH) with Primary Ovarian Failure (POF). J Clin Diagn Res.

91. Zhong W, Pan Y, Shao Y, Yang Y, Yu B, Lin Z. (2018) Atypical presentation of dyschromatosis universalis hereditaria with a novel ABCB6 mutation. Clin Exp Dermatol.

92. Bawazir WM, Flatt JF, Wallis JP, Rendon A, Cardigan RA, New HV, Wiltshire M, Page L, Chapman CE, Stewart GW, Bruce LJ. (2014) Familial pseudohyperkalemia in blood donors: a novel mutation with implications for transfusion practice: Familial Pseudohyperkalemia in Blood Donors. Transfusion (Paris) 54:3043–3050.

93. Andolfo I, Russo R, Manna F, De Rosa G, Gambale A, Zouwail S, Detta N, Pardo CL, Alper SL, Brugnara C, Sharma AK, De Franceschi L, Iolascon A. (2016)

Functional characterization of novel ABCB6 mutations and their clinical implications in familial pseudohyperkalemia. Haematologica 101:909–917.

94. Williamson KA, FitzPatrick DR. (2014) The genetic architecture of microphthalmia, anophthalmia and coloboma. Eur J Med Genet 57:369–380.
95. Kim S, Sharma AK, Vatamaniuk OK. (2018) N-Terminal Extension and C-Terminal Domains Are Required for ABCB6/HMT-1 Protein Interactions, Function in Cadmium Detoxification, and Localization to the Endosomal-Recycling System in Caenorhabditis elegans. Front Physiol 9.
96. Tchounwou PB, Yedjou CG, Patlolla AK, Sutton DJ. (2012) Heavy Metal Toxicity and the Environment, p. 133–164. *In* Luch, A (ed.), Molecular, Clinical and Environmental Toxicology. Springer Basel, Basel.
97. Hamer DH. (1986) Metallothionein. Annu Rev Biochem 55:913–951.
98. Grill E, Winnacker E-L, Zenk MH. (1985) Phytochelatins: The Principal Heavy-Metal Complexing Peptides of Higher Plants. Science 230:674–676.
99. Grill E, Loffler S, WINNACKERt E-L, Zenk MH. (1989) Phytochelatins, the heavy-metal-binding peptides of plants, are synthesized from glutathione by a specific y-glutamylcysteine dipeptidyl transpeptidase (phytochelatin synthase). Proc Natl Acad Sci USA 5.
100. Mutoh N, Hayashi Y. (1988) Isolation of mutants of Schizosaccharomyces pombe unable to synthesize cadystin, small cadmium-binding peptides. Biochem Biophys Res Commun 151:32–39.
101. Sooksa-nguan T, Yakubov B, Kozlovskyy VI, Barkume CM, Howe KJ, Thannhauser TW, Rutzke MA, Hart JJ, Kochian LV, Rea PA, Vatamaniuk OK. (2009) Drosophila ABC Transporter, DmHMT-1, Confers Tolerance to Cadmium: DmHMT-1 and its yeast homolog, SpHMT-1, are not essential for vacuolar phytochelatin sequestration. J Biol Chem 284:354–362.
102. Ortiz DF, Ruscitti T, McCue KF, Ow DW. (1995) Transport of metal-binding peptides by HMT1, a fission yeast ABC-type vacuolar membrane protein. J Biol Chem 270:4721–4728.
103. Prévéral S, Gayet L, Moldes C, Hoffmann J, Mounicou S, Gruet A, Reynaud F, Lobinski R, Verbavatz J-M, Vavasseur A, Forestier C. (2009) A Common Highly Conserved Cadmium Detoxification Mechanism from Bacteria to Humans: Heavy

metal tolerance conferred by the ATP-binding cassette (ABC) transporter SpHMT1 requires glutathione but not metal-chelating phytochelatin peptides. J Biol Chem 284:4936–4943.

104. Schwartz MS, Benci JL, Selote DS, Sharma AK, Chen AGY, Dang H, Fares H, Vatamaniuk OK. (2010) Detoxification of Multiple Heavy Metals by a Half-Molecule ABC Transporter, HMT-1, and Coelomocytes of Caenorhabditis elegans. PLoS ONE 5:e9564.
105. Vatamaniuk OK, Bucher EA, Sundaram MV, Rea PA. (2005) CeHMT-1, a Putative Phytochelatin Transporter, Is Required for Cadmium Tolerance in Caenorhabditis elegans. J Biol Chem 280:23684–23690.
106. Vatamaniuk OK, Bucher E a, Sundaram M V, Rea P a. (2005) CeHMT-1, a putative phytochelatin transporter, is required for cadmium tolerance in Caenorhabditis elegans. J Biol Chem 280:23684–90.
107. Liu J-W, Asan, Sun J, Vano-Galvan S, Liu F-X, Wei X-X, Ma D-L. (2016) Differential Diagnosis of Two Chinese Families with Dyschromatoses by Targeted Gene Sequencing: Chin Med J (Engl) 129:33–38.
108. Ozeki H. (1996) Spectrophotometric Characterization of Eumelanin and Pheomelanin in Hair. Pigment Cell Res - Wiley Online Libr.
109. Solano F. (2014) Melanins: Skin Pigments and Much More—Types, Structural Models, Biological Functions, and Formation Routes. New J Sci 2014:1–28.
110. Meredith P, Sarna T. (2006) The physical and chemical properties of eumelanin. Pigment Cell Res 19:572–594.
111. Passeron T, Mantoux F, Ortonne J-P. (2005) Genetic disorders of pigmentation. Clin Dermatol 23:56–67.
112. Bonifacino JS. (2004) Insights into the Biogenesis of Lysosome-Related Organelles from the Study of the Hermansky-Pudlak Syndrome. Ann N Y Acad Sci 1038:103–114.
113. Dell'Angelica EC. (2004) The building BLOC(k)s of lysosomes and related organelles. Curr Opin Cell Biol 16:458–464.
114. Marks MS, Heijnen HF, Raposo G. (2013) Lysosome-related organelles: unusual compartments become mainstream. Curr Opin Cell Biol 25:495–505.

115. Bissig C, Rochin L, van Niel G. (2016) PMEL Amyloid Fibril Formation: The Bright Steps of Pigmentation. Int J Mol Sci 17:1438.
116. Berson JF, Theos AC, Harper DC, Tenza D, Raposo G, Marks MS. (2003) Proprotein convertase cleavage liberates a fibrillogenic fragment of a resident glycoprotein to initiate melanosome biogenesis. J Cell Biol 161:521–533.
117. Rochin L, Hurbain I, Serneels L, Fort C, Watt B, Leblanc P, Marks MS, De Strooper B, Raposo G, van Niel G. (2013) BACE2 processes PMEL to form the melanosome amyloid matrix in pigment cells. Proc Natl Acad Sci 110:10658–10663.
118. van Niel G, Charrin S, Simoes S, Romao M, Rochin L, Saftig P, Marks MS, Rubinstein E, Raposo G. (2011) The Tetraspanin CD63 Regulates ESCRT-Independent and -Dependent Endosomal Sorting during Melanogenesis. Dev Cell 21:708–721.
119. Sannerud R, Esselens C, Ejsmont P, Mattera R, Rochin L, Tharkeshwar AK, De Baets G, De Wever V, Habets R, Baert V, Vermeire W, Michiels C, Groot AJ, Wouters R, Dillen K, Vints K, Baatsen P, Munck S, Derua R, Waelkens E, Basi GS, Mercken M, Vooijs M, Bollen M, Schymkowitz J, Rousseau F, Bonifacino JS, Van Niel G, De Strooper B, Annaert W. (2016) Restricted Location of PSEN2/γ-Secretase Determines Substrate Specificity and Generates an Intracellular Aβ Pool. Cell 166:193–208.
120. Hurbain I, Geerts WJC, Boudier T, Marco S, Verkleij AJ, Marks MS, Raposo G. (2008) Electron tomography of early melanosomes: Implications for melanogenesis and the generation of fibrillar amyloid sheets. Proc Natl Acad Sci 105:19726–19731.
121. van Niel G, Bergam P, Di Cicco A, Hurbain I, Lo Cicero A, Dingli F, Palmulli R, Fort C, Potier MC, Schurgers LJ, Loew D, Levy D, Raposo G. (2015) Apolipoprotein E Regulates Amyloid Formation within Endosomes of Pigment Cells. Cell Rep 13:43–51.
122. Watt B, Tenza D, Lemmon MA, Kerje S, Raposo G, Andersson L, Marks MS. (2011) Mutations in or near the Transmembrane Domain Alter PMEL Amyloid Formation from Functional to Pathogenic. PLoS Genet 7:e1002286.

123. Hellström AR, Watt B, Fard SS, Tenza D, Mannström P, Narfström K, Ekesten B, Ito S, Wakamatsu K, Larsson J, Ulfendahl M, Kullander K, Raposo G, Kerje S, Hallböök F, Marks MS, Andersson L. (2011) Inactivation of Pmel Alters Melanosome Shape But Has Only a Subtle Effect on Visible Pigmentation. PLoS Genet 7:e1002285.
124. Raposo G, Tenza D, Murphy DM, Berson JF, Marks MS. (2001) Distinct Protein Sorting and Localization to Premelanosomes, Melanosomes, and Lysosomes in Pigmented Melanocytic Cells. J Cell Biol 152:809–823.
125. Ho T, Watt B, Spruce LA, Seeholzer SH, Marks MS. (2016) The Kringle-like Domain Facilitates Post-endoplasmic Reticulum Changes to Premelanosome Protein (PMEL) Oligomerization and Disulfide Bond Configuration and Promotes Amyloid Formation. J Biol Chem 291:3595–3612.
126. Kawaguchi M, Hozumi Y, Suzuki T. (2015) ADAM protease inhibitors reduce melanogenesis by regulating PMEL17 processing in human melanocytes. J Dermatol Sci 78:133–142.
127. Leonhardt RM, Vigneron N, Hee JS, Graham M, Cresswell P. (2013) Critical residues in the PMEL/Pmel17 N-terminus direct the hierarchical assembly of melanosomal fibrils. Mol Biol Cell 24:964–981.
128. Brenner S. (1974) The genetics of Caenorhabditis elegans. Genetics 77:71–94.
129. Kiss K, Brozik A, Kucsma N, Toth A, Gera M, Berry L, Vallentin A, Vial H, Vidal M, Szakacs G. (2012) Shifting the paradigm: The putative mitochondrial protein ABCB6 resides in the lysosomes of cells and in the plasma membrane of erythrocytes. PLoS ONE 7.
130. Bergam P, Reisecker JM, Rakvács Z, Kucsma N, Raposo G, Szakacs G, van Niel G. (2018) ABCB6 Resides in Melanosomes and Regulates Early Steps of Melanogenesis Required for PMEL Amyloid Matrix Formation. J Mol Biol 430:3802–3818.
131. Yeastmaker™ Yeast Transformation System 2 User Manual 9.
132. Rakvács Z, Kucsma N, Gera M, Igriczi B, Kiss K, Barna J, Kovács D, Vellai T, Bencs L, Reisecker JM, Szoboszlai N, Szakács G. (2019) The human ABCB6 protein is the functional homologue of HMT-1 proteins mediating cadmium detoxification. Cell Mol Life Sci.

133. Watt B, van Niel G, Fowler DM, Hurbain I, Luk KC, Stayrook SE, Lemmon MA, Raposo G, Shorter J, Kelly JW, Marks MS. (2009) N-terminal Domains Elicit Formation of Functional Pmel17 Amyloid Fibrils. J Biol Chem 284:35543–35555.
134. Sooksa-Nguan T, Yakubov B, Kozlovskyy VI, Barkume CM, Howe KJ, Thannhauser TW, Rutzke M a, Hart JJ, Kochian L V, Rea P a, Vatamaniuk OK. (2009) Drosophila ABC transporter, DmHMT-1, confers tolerance to cadmium. DmHMT-1 and its yeast homolog, SpHMT-1, are not essential for vacuolar phytochelatin sequestration. J Biol Chem 284:354–62.
135. Rodrigues J, Silva RD, Noronha H, Pedras A, Gerós H, Côrte-Real M. (2013) Flow cytometry as a novel tool for structural and functional characterization of isolated yeast vacuoles. Microbiol U K 159:848–856.
136. Fay D. (2006) Genetic mapping and manipulation: Chapter 1-Introduction and basics. WormBook.
137. Chen B, Jiang Y, Zeng S, Yan J, Li X, Zhang Y, Zou W, Wang X. (2010) Endocytic Sorting and Recycling Require Membrane Phosphatidylserine Asymmetry Maintained by TAT-1 / 6.
138. Liu B, Du H, Rutkowski R, Gartner A. (2013) Europe PMC Funders Group LAAT-1 is the Lysosomal Lysine / Arginine Transporter that Maintains Amino Acid Homeostasis 337:351–354.
139. Paterson JK, Shukla S, Black CM, Tachiwada T, Garfield S, Wincovitch S, Ernst DN, Agadir A, Li X, Ambudkar S V., Szakacs G, Akiyama SI, Gottesman MM. (2007) Human ABCB6 localizes to both the outer mitochondrial membrane and the plasma membrane. Biochemistry 46:9443–9452.
140. Vriend LEM, Jasin M, Krawczyk PM. (2014) Assaying break and nick-induced homologous recombination in mammalian cells using the DR-GFP reporter and Cas9 nucleases. Methods Enzymol 546:175–191.
141. Genecopoeia. (2016) CRISPR/TALEN Insertion or Deletion Detection System | Genecopoeia.
142. Kolacsek O, Krízsik V, Schamberger A, Erdei Z, Apáti Á, Várady G, Mátés L, Izsvák Z, Ivics Z, Sarkadi B, Orbán TI. (2011) Reliable transgene-independent method for determining Sleeping Beauty transposon copy numbers. Mob DNA 2:5.

143. Córdova EJ, Martínez-Hernández A, Uribe-Figueroa L, Centeno F, Morales-Marín M, Koneru H, Coleman MA, Orozco L. (2014) The NRF2-KEAP1 Pathway Is an Early Responsive Gene Network in Arsenic Exposed Lymphoblastoid Cells. PLoS ONE 9:e88069.
144. Fares H, Greenwald I. (2001) Genetic analysis of endocytosis in Caenorhabditis elegans: coelomocyte uptake defective mutants. Genetics 159:133–145.
145. O'Rourke EJ, Soukas AA, Carr CE, Ruvkun G. (2009) C. elegans Major Fats Are Stored in Vesicles Distinct from Lysosome-Related Organelles. Cell Metab 10:430–435.
146. O'Rourke EJ, Soukas AA, Carr CE, Ruvkun G. (2009) C. elegans Major Fats Are Stored in Vesicles Distinct from Lysosome-Related Organelles. Cell Metab 10:430–435.
147. Chen B, Jiang Y, Zeng S, Yan J, Li X, Zhang Y, Zou W, Wang X. (2010) Endocytic Sorting and Recycling Require Membrane Phosphatidylserine Asymmetry Maintained by TAT-1/CHAT-1. PLoS Genet 6:e1001235.
148. Raposo G, Tenza D, Murphy DM, Berson JF, Marks MS. (2001) Distinct protein sorting and localization to premelanosomes, melanosomes, and lysosomes in pigmented melanocytic cells. J Cell Biol 152:809–823.
149. Kushimoto T, Basrur V, Valencia J, Matsunaga J, Vieira WD, Ferrans VJ, Muller J, Appella E, Hearing VJ. (2001) A model for melanosome biogenesis based on the purification and analysis of early melanosomes. Proc Natl Acad Sci 98:10698–10703.
150. Raposo G, Marks MS. (2007) Melanosomes — dark organelles enlighten endosomal membrane transport. Nat Rev Mol Cell Biol 8:786–797.
151. Smith KR, Dahl H-HM, Canafoglia L, Andermann E, Damiano J, Morbin M, Bruni AC, Giaccone G, Cossette P, Saftig P, Grotzinger J, Schwake M, Andermann F, Staropoli JF, Sims KB, Mole SE, Franceschetti S, Alexander NA, Cooper JD, Chapman HA, Carpenter S, Berkovic SF, Bahlo M. (2013) Cathepsin F mutations cause Type B Kufs disease, an adult-onset neuronal ceroid lipofuscinosis. Hum Mol Genet 22:1417–1423.
152. Zhang C, Li D, Zhang J, Chen X, Huang M, Archacki S, Tian Y, Ren W, Mei A, Zhang Q, Fang M, Su Z, Yin Y, Liu D, Chen Y, Cui X, Li C, Yang H, Wang Q,

Wang J, Liu M, Deng Y. (2013) Mutations in ABCB6 Cause Dyschromatosis Universalis Hereditaria. J Invest Dermatol.

153. Boncompain G, Divoux S, Gareil N, de Forges H, Lescure A, Latreche L, Mercanti V, Jollivet F, Raposo G, Perez F. (2012) Synchronization of secretory protein traffic in populations of cells. Nat Methods 9:493–498.
154. Tálas A, Kulcsár PI, Weinhardt N, Borsy A, Tóth E, Szebényi K, Krausz SL, Huszár K, Vida I, Sturm Á, Gordos B, Hoffmann OI, Bencsura P, Nyeste A, Ligeti Z, Fodor E, Welker E. (2017) A convenient method to pre-screen candidate guide RNAs for CRISPR/Cas9 gene editing by NHEJ-mediated integration of a 'self-cleaving' GFP-expression plasmid. DNA Res 24:609–621.
155. Bagshaw RD, Mahuran DJ, Callahan JW. (2004) A Proteomic Analysis of Lysosomal Integral Membrane Proteins Reveals the Diverse Composition of the Organelle*□S 11.
156. Valle MCD, Sleat DE, Zheng H, Moore DF, Jadot M. (2011) Classification of Subcellular Location by Comparative Proteomic Analysis of Native and Density-shifted Lysosomes*□S 14.
157. Douzery EJP, Snell EA, Bapteste E, Delsuc F, Philippe H. (2004) The timing of eukaryotic evolution: Does a relaxed molecular clock reconcile proteins and fossils? Proc Natl Acad Sci U S A 101:15386–15391.
158. Kachroo AH, Laurent JM, Yellman CM, Meyer AG, Wilke CO, Marcotte EM. (2015) Systematic humanization of yeast genes reveals conserved functions and genetic modularity. Science 348:921–925.
159. Ballatori N. (2002) Transport of toxic metals by molecular mimicry. Environ Health Perspect 110:689–694.
160. Mezynska M, Brzóska MM. (2018) Environmental exposure to cadmium-a risk for health of the general population in industrialized countries and preventive strategies. Environ Sci Pollut Res Int 25:3211–3232.
161. Tabelin CB, Igarashi T, Villacorte-Tabelin M, Park I, Opiso EM, Ito M, Hiroyoshi N. (2018) Arsenic, selenium, boron, lead, cadmium, copper, and zinc in naturally contaminated rocks: A review of their sources, modes of enrichment, mechanisms of release, and mitigation strategies. Sci Total Environ 645:1522–1553.
162. Satarug S. (2018) Dietary Cadmium Intake and Its Effects on Kidneys. Toxics 6.

163. Rizwan M, Ali S, Rehman MZU, Maqbool A. (2019) A critical review on the effects of zinc at toxic levels of cadmium in plants. Environ Sci Pollut Res Int 26:6279–6289.
164. Kumar V, Parihar RD, Sharma A, Bakshi P, Singh Sidhu GP, Bali AS, Karaouzas I, Bhardwaj R, Thukral AK, Gyasi-Agyei Y, Rodrigo-Comino J. (2019) Global evaluation of heavy metal content in surface water bodies: A meta-analysis using heavy metal pollution indices and multivariate statistical analyses. Chemosphere 236:124364.
165. Huang Y, He C, Shen C, Guo J, Mubeen S, Yuan J, Yang Z. (2017) Toxicity of cadmium and its health risks from leafy vegetable consumption. Food Funct 8:1373–1401.
166. Ganguly K, Levänen B, Palmberg L, Åkesson A, Lindén A. (2018) Cadmium in tobacco smokers: a neglected link to lung disease? Eur Respir Rev Off J Eur Respir Soc 27.
167. Thévenod F. (2010) Catch me if you can! Novel aspects of cadmium transport in mammalian cells. BioMetals 23:857–875.
168. Ziller A, Fraissinet-Tachet L. (2018) Metallothionein diversity and distribution in the tree of life: a multifunctional protein. Met Integr Biometal Sci 10:1549–1559.
169. Fu Y, Bruce KE, Wu H, Giedroc DP. (2016) Metallothionein diversity and distribution 1 in the tree of life: a multifunctional protein. Metallomics 8:61–70.
170. Li Z-S, Lu Y-P, Zhen R-G, Szczypka M, Thiele DJ, Rea PA. (1997) A new pathway for vacuolar cadmium sequestration in Saccharomyces cerevisiae: YCF1-catalyzed transport of bis(glutathionato)cadmium. Proc Natl Acad Sci 94:42–47.
171. Hasanuzzaman M, Nahar K, Anee TI, Fujita M. (2017) Glutathione in plants: biosynthesis and physiological role in environmental stress tolerance. Physiol Mol Biol Plants 23:249–268.
172. Mendoza-Cózatl DG, Zhai Z, Jobe TO, Akmakjian GZ, Song W-Y, Limbo O, Russell MR, Kozlovskyy VI, Martinoia E, Vatamaniuk OK, Russell P, Schroeder JI. (2010) Tonoplast-localized Abc2 Transporter Mediates Phytochelatin Accumulation in Vacuoles and Confers Cadmium Tolerance. J Biol Chem 285:40416–40426.

173. Andolfo I, Russo R, Manna F, De Rosa G, Gambale A, Zouwail S, Detta N, Pardo CL, Alper SL, Brugnara C, Sharma AK, De Franceschi L, Iolascon A. (2016) Functional characterization of novel ABCB6 mutations and their clinical implications in familial pseudohyperkalemia. Haematologica 101:909–917.
174. Hanson PI, Whiteheart SW. (2005) AAA+ proteins: have engine, will work. Nat Rev Mol Cell Biol 6:519–529.
175. Sarkadi B, Homolya L, Szakács G, Váradi A. (2006) Human multidrug resistance ABCB and ABCG transporters: participation in a chemoimmunity defense system. Physiol Rev 86:1179–1236.
176. Polishchuk EV, Polishchuk RS. (2016) The emerging role of lysosomes in copper homeostasis. Metallomics 8:853–862.
177. Cui Y-X, Xia X-Y, Zhou Y, Gao L, Shang X-J, Ni T, Wang W-P, Fan X-B, Yin H-L, Jiang S-J, Yao B, Hu Y-A, Wang G, Li X-J. (2013) Novel Mutations of ABCB6 Associated with Autosomal Dominant Dyschromatosis Universalis Hereditaria. PLoS ONE 8:e79808.
178. Kim NS, Im S, Kim SC. (1997) Dyschromatosis universalis hereditaria: an electron microscopic examination. J Dermatol 24:161–164.
179. Al Hawsawi K, Al Aboud K, Ramesh V, Al Aboud D. (2002) Dyschromatosis universalis hereditaria: report of a case and review of the literature. Pediatr Dermatol 19:523–526.
180. Raposo G, Tenza D, Murphy DM, Berson JF, Marks MS. (2001) Distinct Protein Sorting and Localization to Premelanosomes, Melanosomes, and Lysosomes in Pigmented Melanocytic Cells. J Cell Biol 152:809–823.
181. Bissig C, Rochin L, van Niel G. (2016) PMEL Amyloid Fibril Formation: The Bright Steps of Pigmentation. Int J Mol Sci 17:1438.
182. Hurbain I, Geerts WJC, Boudier T, Marco S, Verkleij AJ, Marks MS, Raposo G. (2008) Electron tomography of early melanosomes: Implications for melanogenesis and the generation of fibrillar amyloid sheets. Proc Natl Acad Sci 105:19726–19731.
183. Rochin L, Hurbain I, Serneels L, Fort C, Watt B, Leblanc P, Marks MS, De Strooper B, Raposo G, van Niel G. (2013) BACE2 processes PMEL to form the

melanosome amyloid matrix in pigment cells. Proc Natl Acad Sci 110:10658–10663.

184. Ho T, Watt B, Spruce LA, Seeholzer SH, Marks MS. (2016) The Kringle-like Domain Facilitates Post-endoplasmic Reticulum Changes to Premelanosome Protein (PMEL) Oligomerization and Disulfide Bond Configuration and Promotes Amyloid Formation. J Biol Chem 291:3595–3612.
185. Raposo G, Marks MS. (2007) Melanosomes — dark organelles enlighten endosomal membrane transport. Nat Rev Mol Cell Biol 8:786–797.
186. Delevoye C, Hurbain I, Tenza D, Sibarita J-B, Uzan-Gafsou S, Ohno H, Geerts WJC, Verkleij AJ, Salamero J, Marks MS, Raposo G. (2009) AP-1 and KIF13A coordinate endosomal sorting and positioning during melanosome biogenesis. J Cell Biol 187:247–264.
187. Lo Cicero A, Delevoye C, Gilles-Marsens F, Loew D, Dingli F, Guéré C, André N, Vié K, van Niel G, Raposo G. (2015) Exosomes released by keratinocytes modulate melanocyte pigmentation. Nat Commun 6:7506.
188. van Niel G, D'Angelo G, Raposo G. (2018) Shedding light on the cell biology of extracellular vesicles. Nat Rev Mol Cell Biol 19:213–228.
189. Sannerud R, Esselens C, Ejsmont P, Mattera R, Rochin L, Tharkeshwar AK, De Baets G, De Wever V, Habets R, Baert V, Vermeire W, Michiels C, Groot AJ, Wouters R, Dillen K, Vints K, Baatsen P, Munck S, Derua R, Waelkens E, Basi GS, Mercken M, Vooijs M, Bollen M, Schymkowitz J, Rousseau F, Bonifacino JS, Van Niel G, De Strooper B, Annaert W. (2016) Restricted Location of PSEN2/γ-Secretase Determines Substrate Specificity and Generates an Intracellular Aβ Pool. Cell 166:193–208.
190. Giordano F, Bonetti C, Surace EM, Marigo V, Raposo G. (2009) The ocular albinism type 1 (OA1) G-protein-coupled receptor functions with MART-1 at early stages of melanogenesis to control melanosome identity and composition. Hum Mol Genet 18:4530–4545.
191. Bársony O, Szalóki G, Türk D, Tarapcsák S, Gutay-Tóth Z, Bacsó Z, Holb IJ, Székvölgyi L, Szabó G, Csanády L, Szakács G, Goda K. (2016) A single active catalytic site is sufficient to promote transport in P-glycoprotein. Sci Rep 6:24810.

192. Slominski A, Wortsman J, Plonka PM, Schallreuter KU, Paus R, Tobin DJ. (2005) Hair Follicle Pigmentation. J Invest Dermatol 124:13–21.
193. Bergam P, Reisecker JM, Rakvács Z, Kucsma N, Raposo G, Szakacs G, van Niel G. (2018) ABCB6 Resides in Melanosomes and Regulates Early Steps of Melanogenesis Required for PMEL Amyloid Matrix Formation. J Mol Biol 430:3802–3818.
194. Lopes VS, Wasmeier C, Seabra MC, Futter CE. (2007) Melanosome Maturation Defect in Rab38-deficient Retinal Pigment Epithelium Results in Instability of Immature Melanosomes during Transient Melanogenesis. Mol Biol Cell 18:3914–3927.
195. Watt B, Tenza D, Lemmon MA, Kerje S, Raposo G, Andersson L, Marks MS. (2011) Mutations in or near the Transmembrane Domain Alter PMEL Amyloid Formation from Functional to Pathogenic. PLoS Genet 7:e1002286.
196. Brunberg E, Andersson L, Cothran G, Sandberg K, Mikko S, Lindgren G. (2006) A missense mutation in PMEL17 is associated with the Silver coat color in the horse. BMC Genet 7:46.
197. Hellström AR, Watt B, Fard SS, Tenza D, Mannström P, Narfström K, Ekesten B, Ito S, Wakamatsu K, Larsson J, Ulfendahl M, Kullander K, Raposo G, Kerje S, Hallböök F, Marks MS, Andersson L. (2011) Inactivation of Pmel Alters Melanosome Shape But Has Only a Subtle Effect on Visible Pigmentation. PLoS Genet 7:e1002285.
198. Theos AC. (2006) Dual Loss of ER Export and Endocytic Signals with Altered Melanosome Morphology in the silver Mutation of Pmel17 | Molecular Biology of the Cell.
199. Bissig C, Croisé P, Heiligenstein X, Hurbain I, Lenk GM, Kaufman E, Sannerud R, Annaert W, Meisler MH, Weisman LS, Raposo G, Niel G van. (2019) The PIKfyve complex regulates the early melanosome homeostasis required for physiological amyloid formation. J Cell Sci 132:jcs229500.
200. Watt B, van Niel G, Fowler DM, Hurbain I, Luk KC, Stayrook SE, Lemmon MA, Raposo G, Shorter J, Kelly JW, Marks MS. (2009) N-terminal Domains Elicit Formation of Functional Pmel17 Amyloid Fibrils. J Biol Chem 284:35543–35555.

201. Correia MS, Moreiras H, Pereira FJC, Neto MV, Festas TC, Tarafder AK, Ramalho JS, Seabra MC, Barral DC. (2018) Melanin Transferred to Keratinocytes Resides in Nondegradative Endocytic Compartments. J Invest Dermatol 138:637–646.
202. Murase D, Hachiya A, Takano K, Hicks R, Visscher MO, Kitahara T, Hase T, Takema Y, Yoshimori T. (2013) Autophagy Has a Significant Role in Determining Skin Color by Regulating Melanosome Degradation in Keratinocytes. J Invest Dermatol 133:2416–2424.
203. Diment S, Eidelman M, Rodriguez GM, Orlow SJ. (1995) Lysosomal Hydrolases Are Present in Melanosomes and Are Elevated in Melanizing Cells. J Biol Chem 270:4213–4215.

10. List of publications

Publications related to the thesis

Rakvács Z, Kucsma N, Gera M, Igriczi B, Kiss K, Barna J, Kovács D, Vellai T, Bencs L, Reisecker JM, Szoboszlai N, Szakács G.
The human ABCB6 protein is the functional homologue of HMT-1 proteins mediating cadmium detoxification.
Cell Mol Life Sci. 2019 May 3. doi: 10.1007/s00018-019-03105-5.
PMID: 31053883

Bergam P, Reisecker JM, Rakvács Z, Kucsma N, Raposo G, Szakacs G, van Niel G.
ABCB6 Resides in Melanosomes and Regulates Early Steps of Melanogenesis Required for PMEL Amyloid Matrix Formation.
J Mol Biol. 2018 Oct 12;430(20):3802-3818. doi: 10.1016/j.jmb.2018.06.033. Epub 2018 Jun 22.
PMID: 29940187

DOI:10.14753/SE.2020.2354

11. Acknowledgement

Above all, I am thankful to my supervisor, Gergely Szakács, who directed my masters and PhD years and supported my professional progress. I am really grateful to my colleague Nóra Kucsma, her knowledge and skills was indispensable over the years and she has provided invaluable help in the lab. She was always available for a discussion about how to plan my experiments. Thanks to Melinda Gera for the ABCB6 mutant constructs and being a pleasant neighbor in the office. I am thankful to all of my colleagues, the elders who trod the way and the younger ones for sharing the difficulties of doctorate course at any time. I am thankful for my 'student' Barbara Igriczi, she helped me a lot in yeast and mammalian cytotoxicity experiments and now I know that teaching was a good way also to learn. I am also thankful to Kriszta Mohos to manage the everyday life of the lab, thus keeping us away from boring formalities.

I wish to express appreciation also to my colleagues in the Institute of Enzymology, whom I met and worked with during my thesis years, especially to Ervin Welker who provided the opportunity to learn and use the best gene editing method. I am also thankful to György Várady for FACS, Kornélia Némethy for RT-PCR and Tamás Orbán, I used their photometer every day during the yeast project. To measure cadmium content in fission yeast cells the professionalism and technical background of Norbert Szoboszlai and László Bencs were needed. Experiments with nematode *C. elegans* could not have been done without the laboratory of Tibor Vellai, namely János Barna and Dániel Kovács.

My kind appreciation is expressed to our collaborators in MNT-1 project, they did a huge effort to characterize ABCB6 in melanoma cells: Guillaume van Niel, Graca Raposo and Ptissma Bergam. I am thankful to Johannes M. Reisecker in Vienna for precise confocal microscopic images in both projects.

I appreciate critical comments of my father-in-law, mother in law, my polite Canadian friend Wes Lindinger and my pre-reviewer Ágnes Telbisz, my dissertation has been improved for miles.

Special thanks to my genome engineer husband with whom we created my first cell lines together. Beside this, he supported me in many ways to facilitate to accomplish the present thesis, he was really encouraging and empathetic and always stood beside me. I'm delighted that we went along this journey together. And last but not least I am grateful to my whole family who supported me throughout this endeavor.

DOI:10.14753/SE.2020.2354

12. Supplementary Data

Supplementary Table 1. Primers

		Primer name	Sequence
Common ABCB6 sequencing primers		B6-long-A	gtcttggaacagcccacagt
		B6-long-B	gttacgtcttcctcaagttcctc
		B6-long-C	tttactaaatcagacccagaacctg
		B6-long-D	ctgtttcgcttctacgacatcag
		B6-long-E	gtcagcgctggatacatctaatga
		B6-long-rev-A	ccagaagtagatagcttggcagtg
		B6-long-rev-B	cttcatgaacctgcaatgtatagg
		B6-long-rev-C	gaacttgaggaagacgtaactggta
		B6-seq-A-F	tgactgtgggcaactactgc
		B6-seq-A-R	gccacatgtcagcatacacc
		B6-seq-B-F	ctggatcaagttcaggcaca
		B6-seq-B-R	cagcctccacctcatcattc
		B6-seq-out-F	cagcagggacaggaagaaac
		B6-seq-out-R	gcagtagttgcccacagtca
		C6-seq-C-F	cctcctgagtggctacctgt
		C6-seq-C-R	aaccaattgaggggcatgta
S. pombe	Mutagenic primers	ABCB6-A57T-F	gagcggcccaccggtgctgatt
		ABCB6-A57T-R	tggactccctcgaggccacagggt
		ABCB6-S170G-F	cctggtgtcttggaacggcccacagtggtggtg
		ABCB6-S170G-R	caccaccactgtgggccgttccaagacaccagg
		ABCB6-R192Q-F	ctgtgggtgctgcagtatgtggtctct
		ABCB6-R192Q-R	agagaccacatactgcagcacccacag
		ABCB6-R192W-F	cctgtgggtgctgtggtatgtggtctctgg
		ABCB6-R192W-R	ccagagaccacataccacagcacccacagg
		ABCB6-R276W-F	gggctcatgggtttggaatgggcactcaatgtgttgg
		ABCB6-R276W-R	ccaacacattgagtgcccattccaaacccatgagccc
		ABCB6-G588S-F	ccccttcgctttcagaagagccgtattgagtttgag
		ABCB6-G588S-R	ctcaaactcaatacggctcttctgaaagcgaaggggg
		ABCB6-V609M-F	cgggagactctgcaggacatgtctttcactgtgatg
		ABCB6-V609M-R	catcacagtgaaagacatgtcctgcagagtctcccg
		ABCB6-R638C-F	cgcctgctgttttgcttctacgacatcagctctggc
		ABCB6-R638C-R	gccagagctgatgtcgtagaagcaaaacagcaggcg
C. elegans	Cloning primers	hmt1-F-2	aaactagttttttaaattaataaatt
		hmt1-R-2	cggatttttggcctgaaaatctataa
	Sequencing primers	B6 seq 1	gcatggtgactgtcggaaac
		B6 seq 2	gcgagattttggtcgtaagttg
		B6 seq 3	cttggacttttggccggatc
		Seq B6 rev out	cgacagtccatcctgcatcc
		Seq mCh fw	cggaagatactaagccacagac
		Seq mCh rev	cgaggacaattctcatcgttcg

		pRH21-daf7_FW	cgactgcccggttcagcccgcttgaagttc
		ABCB6 Ce seq1	cccatcgtctctctccactgtt
		ABCB6 Ce seq2	tcaaggatggatgcattgtg
CRISPR	Mutagenic primers	ABCB6-G579E-F	gtgaaggaccttcctgaagcagggccccttcgc
		ABCB6-G579E-R	gcgaaggggccctgcttcaggaaggtccttcac
	Linkers for spacer sequences	ABCB6 stop target 1 oligo 1	cacctgtcaccgttccatggtctg
		ABCB6 stop target 1 oligo 2	aaacagaccatggaacggtgaca
		ABCB6 stop target 2 oligo 1	caccatggaacggtgacaaaagtt
		ABCB6 stop target 2 oligo 2	aaacaacttttgtcaccgttccat
		ABCB6 stop target 3 oligo 1	caccaaacttttgtcaccgttcca
		ABCB6 stop target 3 oligo 2	aaactggaacggtgacaaaagttt
		ABCB6 stop target 4 oligo 1	caccgttagtctttgagagggaag
		ABCB6 stop target 4 oligo 2	aaaccttccctctcaaagactaac
		ABCB6 KO target 1 oligo1	caccgcacggcagcgtctggcaat
		ABCB6 KO target 1 oligo2	aaacattgccagacgctgccgtgc
		ABCB6 KO target 2 oligo1	caccgcctcgacgcggatggctctg
		ABCB6 KO target 2 oligo2	aaaccagagccatccgcgtcgaggc
		ABCB6 KO target 3 oligo1	caccgctcgtgccctcgacgcgga
		ABCB6 KO target 3 oligo2	aaactccgcgtcgagggcacgagc
		ABCB6 KO target 4 oligo1	caccggcgtttgcagctgagaact
		ABCB6 KO target 4 oligo2	aaacagttctcagctgcaaacgcc
	Sequencing primers	B6 HRkar-genomi-fw-1	cgtcagcgctggatacatct
		B6 HRkar-genomi-rev-1	agccgtgtcaagaatgctca
		B6 HRkar-genomi-fw-2	tggagaggggacggtaagag
		B6 HRkar-genomi-rev-2	gcagtaccccatcccacaaa
		B6 HR-GFP-genomi-fw-1	aggtcttctgaattgggggc
		B6 HR-GFP-genomi-rev-1	ccgtttacgtcgccgtcc
		B6 HR-GFP-genomi-fw-2	agatccgccacaacatcgag
		B6 HR-GFP-genomi-rev-2	agccgtgtcaagaatgctca
		ABCB6-HRout1	acccaccttgtagtgttgct
		ABCB6-HRout2	gcccaacacacacagatcaga
		Abcb6 seq fw 1.0	catggtgactgtgggcaact
		AmpStop fw zsofi	gtcaggcaactatggatgaacg
		TagBFP rev zsofi	ccaccttgattctcatggtctgg
		CMV rev zsofi	gtgggcagtttaccgtaaatactc
		Ori rev zsofi	ctacagcgtgagctatgagaaagc
		ABCB6 seq target 156 rev	ggggactggtgtcatgaacac
		B6-long-rev-A	ccagaagtagatagcttggcagtg
		B6-seq-A-F	tgactgtgggcaactactgc

DOI:10.14753/SE.2020.2354

Supplementary Table 2. Plasmid constructs

		Name
Cloning	Addgene	pEGFP-N1
	Genscript	pUC57-HMT1-HA
	Genscript	pUC57-B6-opt (C. elegans)
Expression	*S. pombe*	pREP1-HMT1-HA
		pREP1-HMT1-GFP
		pREP1-ABCB6
		pREP1-ABCB6-GFP
		pREP1-ABCB6-KM
		pREP1-ABCB6-A57T
		pREP1-ABCB6-S170G
		pREP1-ABCB6-R192W
		pREP1-ABCB6-R192Q
		pREP1-ABCB6-R276W
		pREP1-ABCB6-G588S
		pREP1-ABCB6-V609M
		pREP1-ABCB6-G638C
	C. elegans	pPD95.75-Hmt1 promoter-B6-opt
		pRH21-Hmt1 promoter-B6-opt
		pPD95.75-Hmt1 promoter-B6-opt-mCherry
	Lentiviral	pSEW-EF1-ABCB6-PGK-Puromycin
		psPax2
		pMD2.G
CRISPR	ultimate target + BFP coding plasmid	pCMV-tagBFP_U6
	GFP between homologous arms	pCDNA3-HR kar-GFP-HR kar
	ABCB6 gRNA coding plasmid	pColEI_U6-ABCB6 stop spacer 1-gRNA_CBH-mCh
	ABCB6 gRNA coding plasmid	pColEI_U6-ABCB6 stop spacer 2-gRNA_CBH-mCh
	ABCB6 gRNA coding plasmid	pColEI_U6-ABCB6 stop spacer 3-gRNA_CBH-mCh
	ABCB6 gRNA coding plasmid	pColEI_U6-ABCB6 stop spacer 4-gRNA_CBH-mCh
	SBP–GFP between homologous arms	pCDNA3-HR kar-SBP-GFP-HR kar
	wt SpCas9 coding plasmid	px330_BglII
	ultimate spacer gRNA	U6-utarget7-spacer-gRNA_Cherry

	wt SpCas9 + ABCB6-KO gRNA coding plasmid	px330_ABCB6 KO target 1
	wt SpCas9 + ABCB6-KO gRNA coding plasmid	px330_ABCB6 KO target 2
	wt SpCas9 + ABCB6-KO gRNA coding plasmid	px330_ABCB6 KO target 3
	wt SpCas9 + ABCB6-KO gRNA coding plasmid	px330_ABCB6 KO target 4

DOI:10.14753/SE.2020.2354

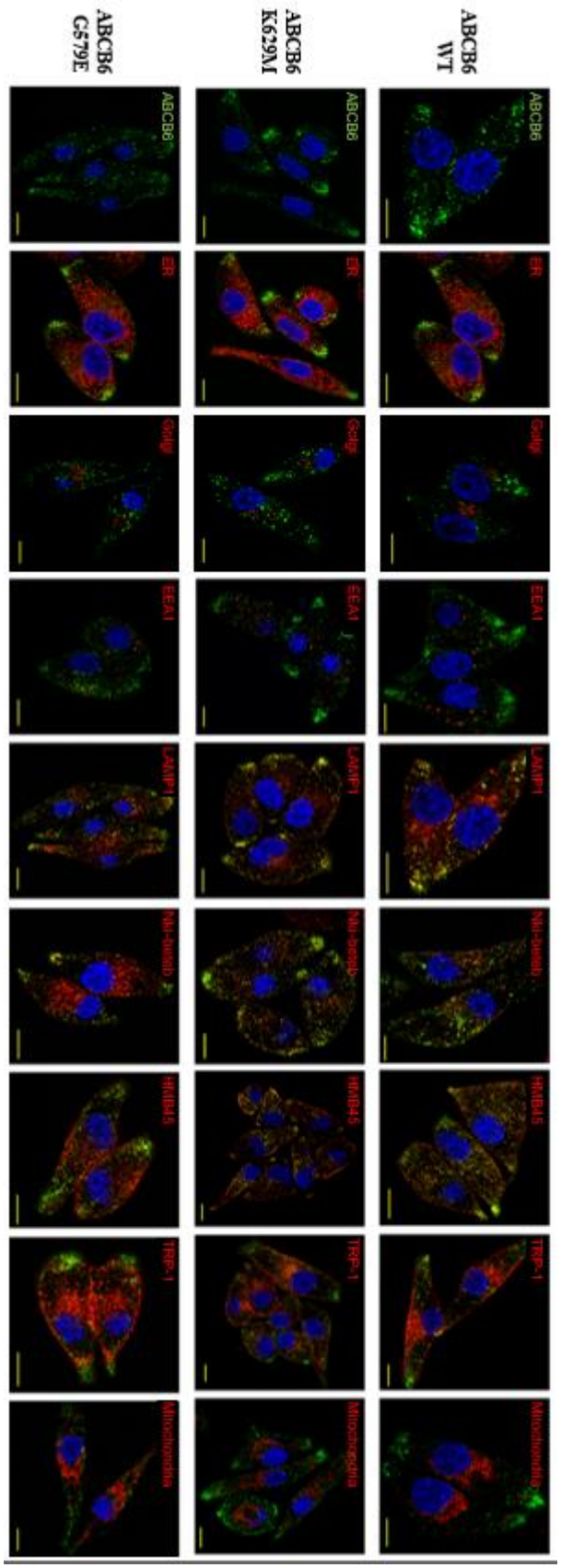

Supplementary figure 1. Determination of the subcellular localization of ABCB6 by immunofluorescence labeling and laser-scanning confocal microscopy. Expression of WT (ABCB6 WT), and mutant ABCB6 variants (ABCB6 K629M and ABCB6 G579E) was visualized in MNT-1 cells using the OSK ABCB6 antibody (green); nuclei were labeled with Hoechst 33342 (blue); and organelles were labeled with specific markers (red): ER (Calnexin), Golgi (RCAS1), mitochondria (AIF), early endosomes (EEA1), lysosomes (LAMP1). Non-pigmented melanosomes were labeled using an antibody directed against the luminal domain of PMEL (Nki-beteb and HMB45); pigmented melanosomes were stained with TRP-1 (red). The scale bar represents 10 μm